Taiwan Big Snow Mountain Summer Camp 1997

The Life of a Star

Notes of lectures given by

Achim Weiss

Max-Planck-Institut für Astrophysik, Garching, Germany

e-mail: weiss@mpa-garching.mpg.de

Note:
These notes are a summary of the lectures that will be given during the summer camp 1997. They are not complete in the sense that explanatory material and some figures might be missing, that will be included in the actual lecture. However, these notes should be sufficient for a preparation of the students and as an aid to follow the lectures

Contents

Chapter 1

Principles of stellar structure theory

The canonical theory of stellar structure and evolution assumes spherical sphericity (i.e. the absence of rotation and magnetic fields) and hydrostatic equilibrium. Under these assumptions a star can be described by the run of four structure variables – r, T, P, L_r – with the Lagrangian coordinate m. We will derive the corresponding four partial differential equations. From the discussion of those several important aspects of stellar structure can be derived, such as timescales, estimates for typical solar values and homology relations.
This first lecture will provide the student with an overview of the physics important for most stars. It is oriented closely at the following excellent text books:

- Kippenhahn R. & Weigert A.: Stellar structure and evolution, Springer, 1990 (hereafter abbreviated by KW)
- Hansen C.J. & Kawaler S.D.: Stellar interiors, Springer, 1994 (hereafter abbreviated by HK)

In the second lecture the missing micro-physics will be discussed. These are nuclear reaction rates, plasma neutrino emission, opacity sources and equation of state. Each topic will consist of fundamental processes and considerations and up-to-date data used.
Finally, an overview of numerical methods used to solve the complete problem will be given.
For this lecture, in addition of the two textbooks, the following literature contains very instructive material:

- Schwarzschild M.: Structure and evolution of the stars, Dover, 1965
- Clayton D.D.: Principles of stellar evolution and nucleosynthesis, Univ. of Chicago Press, 1983
- Kippenhahn, Weigert, Hofmeister: Methods in Computational Physics, vol. 7, 129 (1967); the original paper about the standard numerical method; a description is also contained in the KW textbook
- de Loore B., Doom, C.: Structure and Evolution of Single and Binary Stars, Kluwer, 1992, contains a basic introduction and a discussion about alternative numerical methods (hereafter abbreviated by dLD)

1.1 Some observational facts

Stars appear as white point-like objects in the night sky. You see them through the *filter* of your eye. Astronomical observations make use of several broad-band filters to measure the flux of a star in different wavelength-bands. (This is called *photometry*; a much better way is *spectroscopy*, but this needs bright objects.) There are several filter systems, the best-known is the UBV system. The V (for *visual*; filter is similar to the human eye).

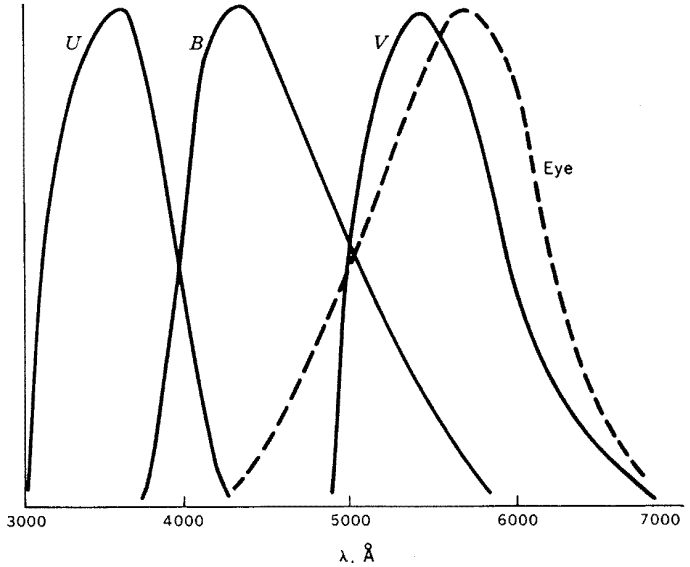

Illustration of the UBV-filter response functions (from Clayton, 1983)

Measuring the flux in several bands allows to draw conclusions about the stellar temperature. Stars are, as known from the Sun, almost perfect *Black Body* radiators, whose spectrum is characterized by its temperature T only. Measurements at two wavelengths, therefore, provide T, even if the distance – and thus the total flux – is not known.

$$I_\lambda = \frac{2c^2h}{\lambda^5} \exp\left(\frac{hc}{\lambda kT} - 1\right)^{-1} \quad \left(\frac{\text{erg}}{\text{cm}^3\text{s}}\right) \tag{1.1}$$

$$\pi F = \int_0^\infty d\lambda I_\lambda = \sigma T^4 \quad \left(\frac{\text{erg}}{\text{cm}^2\text{s}}\right) \tag{1.2}$$

$$\frac{2\pi^5 k^4}{15c^2h^3} = \frac{ac}{4} = \sigma = 5.67 \cdot 10^{-5} \quad \frac{\text{erg}}{\text{cm}^2\,\text{s}\,\text{K}^4} \tag{1.3}$$

Photometric observations of interest for this lecture yield

- $V \equiv M_v$: brightness
- $B - V$: colour (temperature)
- (sometimes $V - I$)

Luminosity, magnitudes, etc.:

In the case of the Sun, if $F := \int F_\lambda \mathrm{d}\lambda$ is the net flux at all wavelenghts through a sphere at the solar radius $R_\odot$, we define

$$L_\odot = 4R_\odot^2(\pi F) \tag{1.4}$$

as the solar luminosity. The flux on earth, $S = 1.36 \cdot 10^6 \frac{\mathrm{erg}}{\mathrm{cm^2 s}}$ (called the *solar constant*) relates to F as $S = F(\pi R_\odot^2/d^2)$, which gives $F = 2 \cdot 10^{10}$ and

$$L_\odot = 3.82 \cdot 10^{33} \mathrm{erg/s}$$

and therefore, with

$$L_\odot = 4\pi\sigma R_\odot^2 T_{\mathrm{eff}}^4 \tag{1.5}$$

$$T_{\mathrm{eff}} = 5770\,\mathrm{K}. \tag{1.6}$$

L, T_{eff}, mass M (or g, R) are the basic global stellar parameters.

In the **Hertzsprung-Russell-Diagram** (HRD), L is plotted against T_{eff} (decreasing to right). The observational counterpart is the **Colour-Magnitude-Diagram** (CMD), which shows V vs. $(B-V)$ (more general: brightness vs. colour index).
Magnitudes are a historical, unreasonable measure of stellar brightness in a $\log L$-system.

$$m_2 - m_1 = 2.5 \log b_1/b_2 \tag{1.7}$$

(b stands here for the measured apparent brightness, which depends on collector area, response function and flux). Five magnitudes (or classes) correspond to a factor of 100 in L. Lowercase m denote *apparent* magnitudes, i.e. the distance difference is included as well. Smaller m = higher b (brightness).
Absolute magnitude M is defined as

$$M - m \equiv 5 - 5 \log d \tag{1.8}$$

where d is the distance in parsec ($3.08 \cdot 10^{18}$ cm); M correponds to the brightness at 10 pc. $m - M$ is also called *distance modulus*; $0.2(m-M) + 1 = \log d$.
Magnitudes measured in a wavelength band are denoted by their indices, e.g. M_V or m_B. If the total or *bolometric* luminosity or brightness is meant, it is M_b. The difference to M_V is called the *bolometric correction* B.C., which includes all energy emitted at frequencies outside the filter range.
For the sun, at $d = 10$ pc, $M_b = 4.72$ and therefore

$$M_b = -2.5 \log \frac{L}{L_\odot} + 4.72 \tag{1.9}$$

A further convention is that for a star of spectral class A0 V (e.g. α Lyr = Vega), $M_V = M_B = M_U$. This defines the bolometric corrections for U and B bands.

We now have a first look at an **observed CMD**:

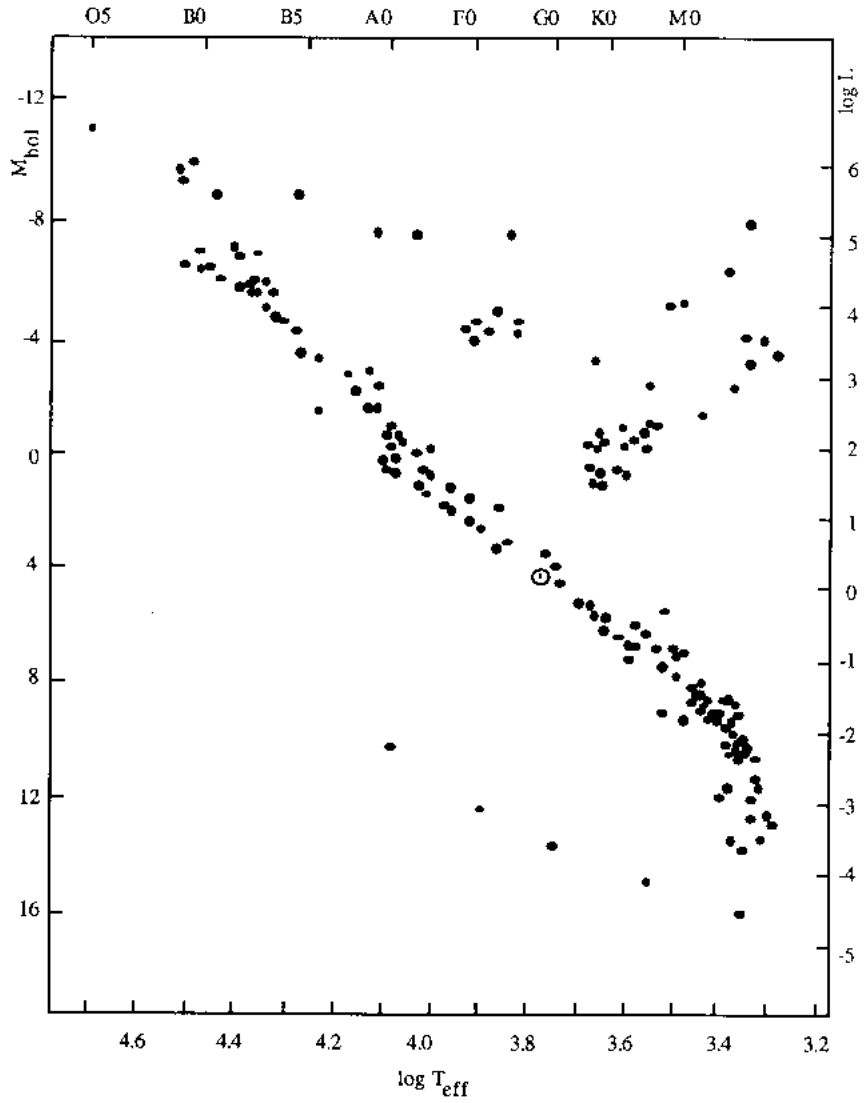

The Hertzsprung-Russel-Diagram of nearby stars (from dLD)

The *aim* of stellar structure theory is to understand the structure of such diagrams (and other observational results) and to derive more information about the stars from the basic photometric (spectroscopic) data.

1.2 The structure equations

1.2.1 Basic assumptions

Stars are considered as *self-gravitating* objects of hot plasma, emitting energy in the form of photons from the surface. In the absence of forces such as rotation and magnetic fields, *spherical symmetry* holds (only gravity and isotropic pressure are at work) and we have a one-dimensional problem to solve with *radius* r being the natural coordinate (Euler description).

1.2.2 Mass and radius

In Eulerian description, the mass $\mathrm{d}m$ contained in a shell at radius r and of thickness $\mathrm{d}r$ is

$$\mathrm{d}m = 4\pi r^2 \rho \mathrm{d}r - 4\pi r^2 \rho v \mathrm{d}t$$

because

$$\frac{\partial m}{\partial r} = 4\pi r^2 \rho$$

and

$$\frac{\partial m}{\partial t} = -4\pi r^2 v \rho$$

If we take the derivative of both equations with respect to the resp. other argument, we obtain

$$\frac{\partial \rho}{\partial t} = -r^{-2} \frac{\partial (\rho r^2 v)}{\partial r}$$

or

$$\frac{\partial \rho}{\partial t} = -\nabla(\rho v)$$

which is the continuity equation in 1-dimensional form and Eulerian description.
In *Lagrangian* description, we consider mass elements m (this is the mass contained in a concentric shell; also called M_r).

$$\Rightarrow r = r(m, t)$$

Perform a variable change $(r, t) \to (m, t)$:

$$\frac{\partial}{\partial m} = \frac{\partial}{\partial r} \frac{\partial r}{\partial m}$$

and

$$\left(\frac{\partial}{\partial t}\right)_m = \frac{\partial}{\partial r} \left(\frac{\partial r}{\partial t}\right)_m + \left(\frac{\partial}{\partial t}\right)_r$$

The first equation, when applied to m (l.h.s. $= 1$), gives on the r.h.s. from the first factor $4\pi r^2 \rho$ and this allows to solve for $\frac{\partial r}{\partial m}$ in Lagrangian coordinates:

$$\frac{\partial r}{\partial m} = \frac{1}{4\pi r^2 \rho} \tag{1.10}$$

This equation is our first structure equation, sometimes called the *mass equation* or *mass conservation*. It contains in general the recipe for the transformation between the two descriptions:

$$\frac{\partial}{\partial m} = \frac{1}{4\pi r^2 \rho}\frac{\partial}{\partial r} \tag{1.11}$$

Note that in this description, the l.h.s. of the second transformation formula contains the so-called "substantial time derivative" of hydrodynamics! It contains the complete change of some physical quantity of element m. The Lagrangian description gives much simples equations than the Eulerian.

1.2.2.1 Gravity

Gravitational field

$$\nabla^2 \Phi = 4\pi G\rho$$

($G = 6.673 \cdot 10^{-8}$ dyn cm^2 g^{-2}). In spherical symmetry:

$$\frac{1}{r^2}\frac{\partial}{\partial r}\left(r^2 \frac{\partial \Phi}{\partial r}\right) = 4\pi G\rho \tag{1.12}$$

With $g = \frac{\partial \Phi}{\partial r}$ we find that $g = \frac{Gm}{r^2}$ is the solution of Poisson's equation. Conventions are that g is one-dimensional and pointing towards $r = 0$ and that the potential Φ vanishes for $r \to \infty$. $-\int_0^\infty \Phi \mathrm{d}r$ is the energy required to disperse the complete star to infinity.

1.2.3 Hydrostatic equilibrium

Consider again a spherical shell of thickness dr. On it two forces (per unit volume) are acting: gravity $-g\rho \mathrm{d}r$ pointing towards the center and a pressure imbalance $\triangle P = -\frac{\partial P}{\partial r}\triangle r$. If the shell is supposed to be at rest (*hydrostatic equilibrium*), the sum is 0 and we obtain:

$$\frac{\partial P}{\partial r} = -\frac{Gm}{r^2}\rho$$

or, in Lagrangian coordinates:

$$\boxed{\frac{\partial P}{\partial m} = -\frac{Gm}{4\pi r^4}} \tag{1.13}$$

This is the second structure equation, that of *hydrostatic equilibrium*. Together with the mass equation, these two *mechanical* equations allow already some simple estimates of stellar conditions.
Replace the derivatives in the hydrostatic equation by differences between center (P_c) and surface ($P_0 \approx 0$) and you get

$$P_c \approx \frac{2GM^2}{\pi R^4}$$

where M and R are total mass and radius of the star ($M/2$ and $R/2$ were used on the r.h.s.).
For our Sun we obtain $P_c = 7 \cdot 10^{15}$ (cgs units).
Assume now an ideal gas equation of the form $\rho = \frac{\mu P}{\mathcal{R}T}$, where $\mathcal{R} = 8.315 \cdot 10^7$ erg K^{-1} g^{-1} is the Gas constant [1] and μ the *mean molecular weight* (defined later). We also define $\bar{\rho} = (3M)/(4\pi R^3)$ and get for the central temperature

$$T_c = \frac{8}{3}\frac{\mu}{\mathcal{R}}\frac{GM}{R}\frac{\bar{\rho}}{\rho_c} < 3 \cdot 10^7 \text{ K}$$

[1] $\mathcal{R}$ relates to the Boltzmann constant k_B through $\mathcal{R} = k_B N_A$, N_A being Avogadro's number $6.022 \cdot 10^{23}$.

The last term is in general < 1, because stars tend to have more concentrated cores. We already see that at the center of the Sun, T is of the order of 10^7 K and therefore nuclear reactions will take place there.

1.2.3.1 Motion

In case the mass layer is not at rest, the pressure equation becomes

$$\frac{\partial P}{\partial m} + \frac{Gm}{4\pi r^4} = -\frac{1}{4\pi r^2}\frac{\partial^2 r}{\partial t^2}$$

the last term being the *interia term*: the element is accelerated due to the net force resulting from gravity and pressure not balancing each other.
If $P = 0$ everywhere, m will move in free-fall $Gm/r^2 = \ddot{r}$. The timescale is $\tau_{ff} = \sqrt{R/|\ddot{r}|} \approx \sqrt{R/g}$. If $G = 0$, $|\ddot{r}| = R/\tau_{expl}^2$; $4\pi r^2 \frac{\partial P}{\partial m}$ can be transformed into $P/R\rho$ such that $\tau_{expl} \approx R\sqrt{\rho/P}$. $\sqrt{P/\rho}$ is the isothermal sound speed and τ_{expl} therefore the time needed for a sound wave to traverse the star.
If the star is near hydrostatic equilibrium, these two timescales must be about the same and are also called *hydrostatic timescale* τ_{hydro}, which is

$$\tau_{hydro} \approx \frac{1}{2}(G\bar{\rho})^{-1/2}$$

Examples: $\tau_{hydro} =$

- 27 minutes for the Sun
- 18 days for a Red Giant ($R = 100R_\odot$)
- 4.5 seconds for a White Dwarf ($R = R_\odot/50$)

Conclusion: even if somehow perturbed, stars can return to hydrostatic equilibrium within an extremely short time in most of their evolutionary phases.

1.2.3.2 The Virial Theorem

... describes the relation between global energy reservoirs of a star. It allows to understand evolutionary phases and global behaviour of stars.
By integrating the hydrostatic equilibrium equation over dm, one derives easily (only assuming $P(M) = 0$):

$$\int_0^M \frac{Gm}{r}\mathrm{d}m = 3\int_0^M \frac{P}{\rho},\mathrm{d}m \tag{1.14}$$

where the l.h.s. $= -E_g$ (gravitational energy).
In case of a monatomic ideal gas, $P/\rho = (2/3)u = (2/3)c_vT$ (u: specific internal energy), and therefore the r.h.s. corresponds to $2E_i = \int u\mathrm{d}m$.
The virial theorem for such a gas therefore is

$$E_g = -2E_i \tag{1.15}$$

For a general gas, $3(P/\rho) = \zeta u$, with $\zeta = 3(\gamma - 1)$, which, for a monoatomic gas is 2 ($\gamma = 5/3$) and for a photon gas 1. If $\zeta =$ const. throughout the star, the virial theorem reads

$$\zeta E_i + E_g = 0.$$

In the case of non-vanishing surface pressure P_0, the virial theorem becomes

$$\zeta E_i + E_g = 4\pi R^3 P_0. \tag{1.16}$$

The total energy is $W = E_i + E_g = (1-\zeta)E_i = \frac{\zeta-1}{\zeta}E_g$ and the luminosity L corresponds to the change of the total energy $\frac{\mathrm{d}W}{\mathrm{d}t}$ or $L = (\zeta-1)\frac{\mathrm{d}E_i}{\mathrm{d}t}$. For the standard case ($\zeta = 2$) we obtain

$$L = -\frac{\dot{E}_g}{2} = \dot{E}_i, \tag{1.17}$$

which means that if the star contracts ($\dot{E}_g < 0$), half of the energy gained is radiated away, while the other half is used to raise E_i (star is heated). Another interpretation is that since the star must radiate (because it is hotter than the universe at large), at the same time it heats up and shrinks (although parts – the envelope – might well and does expand, nevertheless). [2]

1.2.3.3 The Kelvin-Helmholtz timescale

$L \approx \left|\frac{\mathrm{d}E_g}{\mathrm{d}t}\right|$; define typical timescale

$$\tau_{\mathrm{KH}} = \frac{|E_g|}{L} \approx \frac{E_i}{L}.$$

$$|E_g| \approx \frac{GM^2}{2R} \Rightarrow \tau_{\mathrm{KH}} \approx \frac{GM^2}{2RL}.$$

For the Sun, $\tau_{\mathrm{KH}} = 1.6 \cdot 10^7$ yrs ($L_\odot = 3.827 \cdot 10^{33}$ erg s^{-1}). This implies that the Sun could shine only for about 10 million years, if the reactions at the center would be switched off. Stars evolve – in most cases – on much longer timescales, because they have energy sources much larger than $|E_g|$.

The constant density model:

ideal monatomic gas:

$$u = \frac{3}{2}\frac{nk_BT}{\rho} = \frac{3}{2}\frac{N_Ak_B}{\mu}T = \frac{3}{2}\frac{P}{\rho}, \tag{1.18}$$

(with Avogadro's number $N_A = 6.022 \cdot 10^{23}$ mole^{-1} and $k_B = 1.38 \cdot 10^{16}$ erg/K, the Boltzmann constant).

$$E_i = uV = u\frac{M}{\bar{\rho}} = \frac{3}{2}M\frac{\mathcal{R}}{\mu}T = -\frac{1}{2}E_g = -\frac{1}{2}\left(-\frac{3}{5}\frac{GM^2}{R}\right)$$

for a constant density model $\rho = \bar{\rho}$.
$\Rightarrow T = 4.09 \cdot 10^6 \mu \left(\frac{M}{M_\odot}\right)^{2/3} \rho^{1/3}$

If $\rho = \mathrm{const.}$, $r = (m/M)^{1/3}R$; insert this into hydrostatic equilibrium equation to obtain

$$\frac{\partial P}{\partial m} = -\frac{GM}{4\pi R^4}\left(\frac{M}{m}\right)^{1/3}.$$

Integration over M ($P(M) = 0$) yields $P(m) = P_c\left[1-(m/M)^{2/3}\right] = P_c\left[1-(r/R)^2\right]$ and

$$P_c = \frac{3}{8}\frac{GM^2}{R^4} = 1.34 \cdot 10^{15}\left(\frac{M}{M_\odot}\right)^2\left(\frac{R_\odot}{R}\right)^4$$

and

$$T(m) = T_c\left[1-(m/M)^{2/3}\right]$$

$$T_c = 1.15 \cdot 10^7 \mu \left(\frac{M}{M_\odot}\right)\left(\frac{R_\odot}{R}\right)$$

which is similar, but more exact than the previous estimate of the solar central temperature.

[2] **Note:** one can start with the total energy consideration, and search for equilibrium states; this returns the hydrostatic equation (see Hansen & Kawaler)

1.2.4 Energy conservation

Define L_r as the energy in (erg/s) passing outwards through a sphere of radius r; boundary conditions are $L(0) = 0$ and $L(M) = L(R) =: L$. L_r includes energy transported by radiation, convection and conduction, but not by neutrinos!
The energy gained (or lost) by a shell of thickness dm is

$$\mathrm{d}L_r = 4\pi r^2 \rho \epsilon \mathrm{d}m,$$

with ϵ in (erg/gs) being the specific *energy generation rate*.
Sources for ϵ are:

- in a stationary mass shell: $\epsilon = \epsilon_n(\rho, T, \vec{X})$: nuclear energy generation, depending also on composition $\vec{X}$;
- in a non-stationary mass shell: interaction with surrounding via $P\mathrm{d}V$ ($v := 1/\rho$ will be the specific volume in the following).

$$\left(\epsilon_n - \frac{\partial L_r}{\partial m}\right)\mathrm{d}t = \mathrm{d}q \tag{1.19}$$

$$\begin{aligned}\frac{\partial L_r}{\partial m} &= \epsilon_n - \frac{\partial u}{\partial t} - P\frac{\partial v}{\partial t} \\ &= \epsilon_n - \frac{\partial u}{\partial t} + \frac{P}{\rho^2}\frac{\partial \rho}{\partial t} \\ &= \epsilon_n - c_P\frac{\partial T}{\partial t} + \frac{\delta}{\rho}\frac{\partial P}{\partial t}\end{aligned} \tag{1.20}$$

From $\mathrm{d}q = T\mathrm{d}s$, one defines the *gravothermal energy*

$$\epsilon_g := -T\frac{\partial s}{\partial t},$$

which, as shown in the appendix on thermodynamical relations is

$$\epsilon_g = -c_P\frac{\partial T}{\partial t} + \frac{\delta}{\rho}\frac{\partial P}{\partial t} = -c_P T\left(\frac{1}{T}\frac{\partial T}{\partial t} - \frac{\nabla_{\mathrm{ad}}}{P}\frac{\partial P}{\partial t}\right) \tag{1.21}$$

Finally, both in nuclear reactions and in plasma processes neutrinos are produced. Since their free pathlength is so high that they do not interact with the stellar plasma, they are counted separately. In nuclear reactions, the energy loss due to neutrinos is already taken into account in the effective energy generation rate. The neutrinos from plasma processes, discussed later, are denoted by ϵ_ν. With this the *energy conservation equation* reads

$$\frac{\partial L_r}{\partial m} = \epsilon_n + \epsilon_g - \epsilon_\nu. \tag{1.22}$$

Note the conventions: ϵ_ν is positive for the energy of the neutrinos, therefore it is subtracted. ϵ_g is positive for contraction, which liberates energy, raising $L_r(m)$.

Note: Remember that we have assumed that the EOS and the internal energy do not depend on composition. If this is generalized, additional terms from the entropy change and from the chemical potential changes appear in ϵ_g. However, in general, these corrections are unimportant for ϵ_g, which itself is usually contributing only a minor fraction to L (Sun: 10^{-4}). The correction is largest in nuclear burning regions, but there ϵ_n dominates by many orders of magnitude. The correct (and complete) expression for ϵ_g is, however, necessary for precise solar models. [3]

[3] see Reiter, Walsh, Weiss: MNRAS 274, 899 (1995) and Reiter, Bulirsch, Pfleiderer: Astron. Nach. 315, 205 (1994)

1.2.4.1 Energy conservation – again

The energy budget of a star is (in complete form)

$$\dot{W} = \frac{\mathrm{d}}{\mathrm{d}t}(E_{\mathrm{kin}} + E_g + E_i + E_n) = -(L + L_\nu),$$

which must result from the energy conservation equation by integration over $\mathrm{d}m$, too.
The following terms are easy: $L = \int \frac{\partial L_r}{\partial m}\mathrm{d}m$, $L_\nu = \int \epsilon_\nu \mathrm{d}m$, $\int \epsilon_n \mathrm{d}m = -\frac{\mathrm{d}E_n}{\mathrm{d}t}$.
The integration over ϵ_g is more difficult. Use

$$\epsilon_g = -\frac{\partial u}{\partial t} + \frac{P}{\rho^2}\frac{\partial \rho}{\partial t}.$$

Integration of the first term gives $-\mathrm{d}E_i/\mathrm{d}t$. We also know that

$$E_g = -3\int_0^M \frac{P}{\rho}\mathrm{d}m,$$

which we differentiate w.r.t. t. The same is done for the hydrostatic equation, which, after multiplication by $4\pi r^3$ and integration gives:

$$\int_0^M 4\pi r^3 \frac{\partial \dot{P}}{\partial m}\mathrm{d}m = 4\int_0^M \frac{Gm}{r}\frac{\dot{r}}{r}\mathrm{d}m = 4\dot{E}_g$$

The l.h.s. is integrated by parts and becomes

$$\left[4\pi r^3 \dot{P}\right]_0^M - 3\int_0^M 4\pi r^2 \frac{\partial r}{\partial m}\dot{P}\mathrm{d}m$$

Again, $P(M) = 0$ is assumed, and the first term vanishes. In the second one $\frac{\partial m}{\partial r} = 4\pi r^2 \rho$ is used and then we get

$$-3\int_0^M \frac{\dot{P}}{\rho}\mathrm{d}m = 4\dot{E}_g.$$

This we use for the differentiated form of (E_g) and obtain finally:

$$\dot{E}_g = -\int_0^M \frac{P}{\rho^2}\dot{\rho}\mathrm{d}m$$

which is the last term in (ϵ_g), and therefore the equation for $\dot{W}$ is recovered, without the E_{kin}-term, however. If instead of the hyrostatic equation the one including the acceleration term had been used, this last missing term would have been recovered as well. We have shown, therefore, that our local energy conservation equation indeed yields the global one, if properly integrated.

1.2.4.2 The nuclear timescale

The nuclear timescale is defined as $\tau_{\mathrm{n}} := E_n/L$. The energy reservoir available to a star is approx. its mass of fuel times the erg/g of fuel.
For the Sun in hydrogen burning, where $q = 6.3 \cdot 10^{18}\ \mathrm{erg\,g^{-1}}$, this is (H-fraction by mass ≈ 0.7) in total $8.75 \cdot 10^{51}$ erg. With $L_\odot = 4 \cdot 10^{33}\ \mathrm{erg\,s^{-1}}$, we get

$$\tau_{\mathrm{n}} = 7 \cdot 10^7\ \mathrm{yrs}$$

.
Therefore: $\tau_{\mathrm{n}} \gg \tau_{\mathrm{KH}} \gg \tau_{\mathrm{hydr}}$
This is the timescale most important for most stars in most evolutionary phases. $\frac{\partial L_r}{\partial m} \approx \epsilon_n$ to high precision is an equivalent statement. It implies that $\epsilon_g \approx 0$ or that the star is said to be in *thermal equilibrium*. Together with the mechanical equilibrium this is also called *complete* equilibrium, because all terms involving $\mathrm{d}t$ are missing. Of course, complete equilibrium cannot be achieved accurately, as will be discussed later.

1.2.5 Energy transport

Star lose energy – generated deep inside – from the surface. This must be transported along the negative T-gradient, which can be estimated to be (for the Sun) $\triangle T/\triangle r \approx 10^7/10^{11} = 10^{-4}$ (K/cm). Means for this are radiation, convection and conduction, the latter being the least important. In a general form, the equation for the transport is written as

$$\frac{\partial T}{\partial m} = -\frac{T}{P}\frac{Gm}{4\pi r^4}\nabla \tag{1.23}$$

which is nothing else than the definition of ∇, which has to be replaced by the appropriate expression for the respective transport mechanism.

1.2.5.1 Radiative transport

The mean free path for a photon in the stellar interior is $l_{\rm ph} = 1/(\kappa\rho)$. κ is the mean absorption coefficient per mass unit, averaged over frequency. It depends on $\vec{X}, \rho, T$ and is ≈ 1 cm^2/g inside stars, but varies from 10^{-6} to 10^6. The typical value corresponds to $l_{\rm ph} = 2$ cm.
Together with the T-gradient this implies that the anisotropy in radiation is of order 10^{-10} only, and black body conditions prevail. The net transport is due to the small surplus of energy radiated from the more inner – hotter – parts over that from the – cooler – outer parts (within $l_{\rm ph}$).
In analogy to a particle diffusion equation, one derives that for radiation. The diffusive flux $\vec{j}$ of particles (per unit area and time) is

$$\vec{j} = -D\vec{\nabla}n = -\frac{1/}{3}vl_p\vec{\nabla}n$$

(D is called the diffusion constant; v the diffusion velocity; l_p is the particle free path length and n the particle density).
We now use $U := aT^4$ for the radiation density ($a = 7.57 \cdot 10^{-15}$ erg/(cm^{3}K^4) being the radiation constant) in place of particle density and c instead of v. I na 1-dimsnsional problem, we get for $\vec{\nabla}U$

$$\frac{\partial U}{\partial r} = 4aT^3\frac{\partial T}{\partial r}$$

and for the radiation flux F (replacing $\vec{j}$)

$$F = -\frac{4ac}{3}\frac{T^3}{\kappa\rho}\frac{\partial T}{\partial r}, \tag{1.24}$$

which can be written as $F = -K_{\rm rad}\nabla T$. $K_{\rm rad} = \frac{4ac}{3}\frac{T^3}{\kappa\rho}$ is interpreted as the radiative conductivity.
With $L_r = 4\pi r^2 F$, we obtain

$$\boxed{\frac{\partial T}{\partial m} = -\frac{3}{64ac\pi^2}\frac{\kappa L_r}{r^4T^3}} \tag{1.25}$$

This is the transport equation in the case of radiation. (A strict approach can be found in Hansen & Kawaler, chap. 4.)

1.2.5.2 The Rosseland mean opacity

κ as used in the transport equation, is actually an appropriate mean of κ_ν over frequency ν:

$$\frac{1}{\kappa} := \frac{\int_0^\infty \frac{1}{\kappa_\nu}\frac{\partial B_\nu}{\partial T}{\rm d}\nu}{\int_0^\infty \frac{\partial B_\nu}{\partial T}{\rm d}\nu} \tag{1.26}$$

where

$$B_\nu(T) = \frac{2h\nu^3}{c^2}\left(\exp\left(\frac{h\nu}{kT}\right) - 1\right)^{-1} \tag{1.27}$$

is the Planck-function for the energy density flux of a black body. ($U = aT^4 = (4\pi/c)\int B_\nu \mathrm{d}\nu$).
Note that the Rosseland mean is dominated by those frequency intervals, where matter is almost transparent to radiation!

1.2.5.3 Conduction

In regions of degeneracy, the mean free path of electrons is very large, because the probability for momentum exchange is very small due to the fact that all energy levels are occupied! We write

$$F_{\mathrm{cond}} = -K_{\mathrm{cond}}\nabla T$$

where the conductivity K_{cond} has to be calculated by quantum-mechanical means. With this we can write

$$F = F_{\mathrm{rad}} + F_{\mathrm{cond}} = -(K_{\mathrm{rad}} + K_{\mathrm{cond}})\nabla T \tag{1.28}$$

and introduce formally κ_{cond} by

$$K_{\mathrm{cond}} = \frac{4ac}{3}\frac{T^3}{\kappa_{\mathrm{cond}}\rho}. \tag{1.29}$$

This allows to replace κ_{rad} in (radtrans) by

$$\frac{1}{\kappa} = \frac{1}{\kappa_{\mathrm{rad}}} + \frac{1}{\kappa_{\mathrm{cond}}} \tag{1.30}$$

Physically, this means, that the mechanism with the smaller *opacity* κ or the higher conductivity K manages the transport.
For the general transport equation, in the case of radiation + conduction:

$$\nabla = \nabla_{\mathrm{rad}} = \frac{3}{16\pi acG}\frac{\kappa L_r P}{mT^4} \tag{1.31}$$

1.2.5.4 Perturbations and stability: convection

The stellar layers are subject to perturbations and motions. The question is, are the layers stable or unstable? Will the perturbations grow? If they grow they can transport energy and thus have to be considered in the energy transport equation.
Consider moving mass elements; assume no heat exchange with surrounding (adiabatic movement).

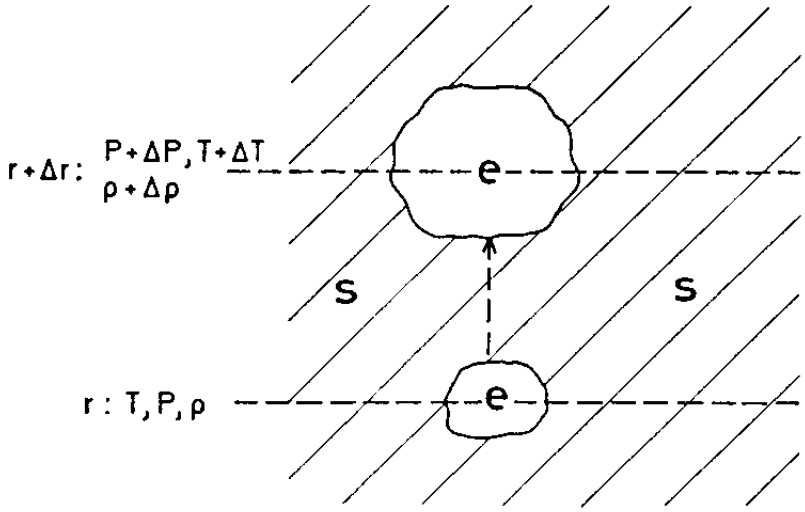

Illustration of blobs moving in unperturbed surrounding (from KW)

The figure illustrates the picture we have in mind: the temperature excess DT is positive, if the element is hotter than its surrounding. $DP = 0$ due to hydrostatic equilibrium. If $D\rho < 0$, the element is lighter and will move upwards. Take an element and lift it by $\triangle r$:

$$D\rho = \left[\left(\frac{\partial\rho}{\partial r}\right)_e - \left(\frac{\partial\rho}{\partial r}\right)_s\right] \triangle r$$

The stability condition therefore is $\left(\frac{\partial\rho}{\partial r}\right)_e - \left(\frac{\partial\rho}{\partial r}\right)_s > 0$, because then the buoyancy force $-gD\rho$ will be directed downward and the element will return.
With the EOS $\mathrm{d}\ln\rho = \alpha\mathrm{d}\ln P - \delta\mathrm{d}\ln T - \varphi\mathrm{d}\mu$; for an ideal gas, $\alpha = \delta = \varphi = 1$; $(\mathrm{d}\mu)_e = 0$.
Then the stability conditions changes into

$$\left(\frac{\delta}{T}\frac{\mathrm{d}T}{\mathrm{d}r}\right)_s - \left(\frac{\delta}{T}\frac{\mathrm{d}T}{\mathrm{d}r}\right)_e - \left(\frac{\varphi}{\mu}\frac{\mathrm{d}\mu}{\mathrm{d}r}\right)_s > 0 \tag{1.32}$$

Now define (for practical use) the *pressure scale height*

$$H_P := -\frac{\mathrm{d}r}{\mathrm{d}\ln P} = -P\frac{\mathrm{d}r}{\mathrm{d}P} = \frac{P}{\rho g} > 0 \tag{1.33}$$

(examples (cm): solar photosphere: $1.4 \cdot 10^7$; at $R_\odot/2$: $5.2 \cdot 10^3$; center $\to \infty$)
multiply the stability condition by H_P to obtain

$$\left(\frac{\mathrm{d}\ln T}{\mathrm{d}\ln P}\right)_s < \left(\frac{\mathrm{d}\ln T}{\mathrm{d}\ln P}\right)_e + \frac{\varphi}{\delta}\left(\frac{\mathrm{d}\ln\mu}{\mathrm{d}\ln P}\right)_s \tag{1.34}$$

$$\nabla_s < \nabla_{\mathrm{ad}} + \frac{\varphi}{\delta}\nabla_\mu \tag{1.35}$$

$$\nabla_{\mathrm{rad}} < \nabla_{\mathrm{ad}} + \frac{\varphi}{\delta}\nabla_\mu \tag{1.36}$$

The last equation holds in general cases and is called the *Ledoux-criterion* for dynamical stability. A special case of it is the *Schwarzschild-criterion*, which is obtained by simply setting $\nabla_\mu = 0$ (homogeneous medium). Note that since $\varphi/\delta > 0$, ∇_μ will stabilize, because usually μ increases inwards (as P).
If the stability criterion is fulfilled, the energy is transported by radiation, if not, by *convection*, i.e. by turbulent motion of element clumps (blobs).

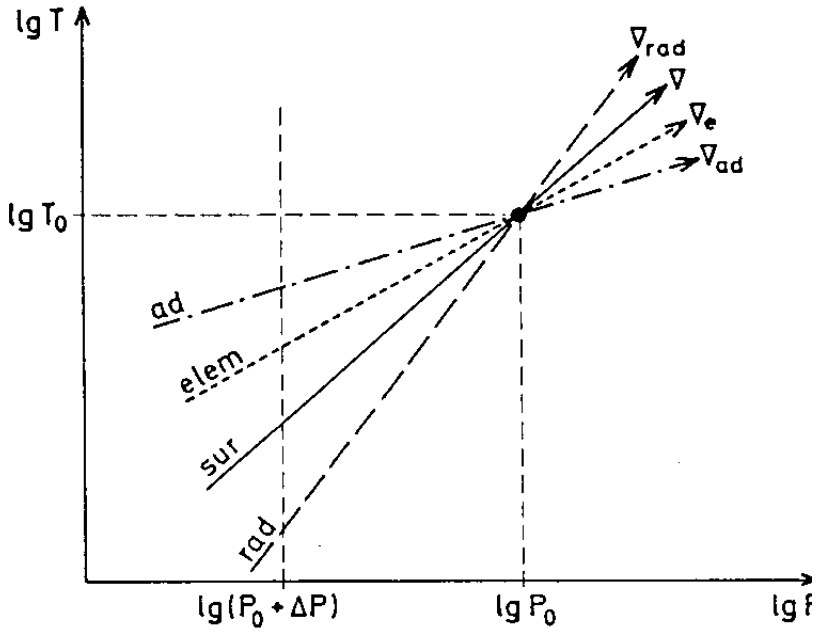

Illustration of the various temperature gradients in a convectively unstable region (from KW)

In an unstable layer, the following relations hold:

$$\nabla_{\rm rad} > \nabla > \nabla_e > \nabla_{\rm ad} \tag{1.37}$$

∇ is the actual gradient that will result in the convective layer. The first inequality arises from the fact that only part of the flux can be tranported by radiation, since convection is carrying some in any case. The last is due to the fact that the element will cool more than just adiabatic, because some energy will be lost by other means (radiation, conduction). The middle one is just the stability criterion for the blob not to be pushed back. The task of a convection theory is it to derive ∇!

1.2.5.5 Energy transport by convection

Convection in stars is a

- highly turbulent (Reynolds number Re $:= \frac{v\rho l_m}{\eta} \approx 10^{10}$; η viscosity; v speed of blobs $\approx 10^3$ cm/s $= 10^{-5} v_{\rm sound}$; $l_m = 10^9$ cm; in laboratory: turbulence sets in when Re > 100);
- 3-dimensional
- non-local

motion in compressible medium on dynamical timescales. This is impossible to be incorporated in stellar evolution calculations. One needs simple descriptions for the interesting quantities as ∇.
There exist different approaches of different level of sophistication:

1. full 3-d hydro-calculations: give a snapshot of turbulent convection, mostly in simplified situations or for the Sun (e.g. Nordlund, A&A 107, 1 (1982); Nordlund & Dravins A&A 228, 155 (1990))
2. 2-d hydro-models: can scan a wider stellar parameter range; applicable to shallow convection zones (as in White Dwarfs) or to surface convection in the Sun and other stars (e.g. Freytag, Steffen & Ludwig, A&A 313, 497 (1996))

3. Analytical solutions of the non-local convection equations with a momentum approach; describes mean values; several assumptions concerning fluctuations and viscosity, etc. (Grossman, MNRAS 279, 305 (1996))

4. Solution of full set of dynamical equations by using correlation functions (Xiong, Cheng & Deng, ApJS 108, 529 (1997)); similar to 3.

5. Local descriptions working with blob-picture of perturbations but keeping turbulent energy spectrum (e.g. Canuto, ApJ 467, 385 (1996) – also a review)

6. Local description in the most simplified way – the Mixing Length Theory (MLT) – with a free parameter (see Kippenhahn & Weigert for a detailed derivation)

While the purely numerical approaches are limited by the timescales, the full-equations approach suffers from inherent assumptions and the unsolved problem how to be incorporated in full stellar models. The local approaches are efficient, but lack physical justification, cannot describe non-local and time-dependent effects, and need a calibration (if possible at all!). Nevertheless, the MLT has been very successful in stellar structure theory and is used for all problems (sometimes with extensions to describe non-local effects like overshooting). Recently, it has received some justification from 2-d models.

A simplified derivation of the MLT equation:

$$F = \frac{L_r}{4\pi r^2} = F_{\rm conv} + F_{\rm rad}$$

be the total energy flux transported by convection and radiation (in as yet unknown parts). If it were transported by radiation only,

$$F =: \frac{4acG}{3}\frac{T^4 m}{\kappa P r^2}\nabla_{\rm rad};$$

instead, the radiative flux is

$$F_{\rm rad} = \frac{4acG}{3}\frac{T^4 m}{\kappa P r^2}\nabla$$

and

$$F_{\rm conv} = \rho v c_P (DT)$$

is the flux carried by a blob with $DT > 0$. v (now the velocity of the moving element) and DT must be average values to be derived.
Assume, a blob starts somewhere with $DT > 0$ and loses identity after a typical *mixing length* distance l_m. On average

$$\frac{DT}{T} = \frac{1}{T}\frac{\partial(DT)}{\partial r}\frac{l_m}{2} = (\nabla - \nabla_e)\frac{l_m}{2}\frac{1}{H_P}$$

DT leads to $D\rho$; the resulting buoyancy force is therefore $f_b = -gD\rho/\rho = g\delta DT/T$. The work done by it is (assume 50%)

$$\frac{1}{2} f_b \frac{l_m}{2} = g\delta(\nabla - \nabla_e)\frac{l_m^2}{8H_P}$$

Again, assume half of this goes into kinetic energy of the element, the rest be used up for "pushing away" the surrounding. Then,

$$v^2 = g\delta(\nabla - \nabla_e)\frac{l_m^2}{8H_P}$$

and

$$F_{\rm conv} = \rho c_P T \sqrt{g\delta} \frac{l^2 m}{4\sqrt{2}} H_p^{-3/2} (\nabla - \nabla_e)^{3/2}$$

T_e changes due to adiabatic cooling and radiation losses,

$$\left(\frac{{\rm d}T}{{\rm d}r}\right)_e = \left(\frac{{\rm d}T}{{\rm d}r}\right)_{\rm ad} - \frac{\lambda}{\rho V c_P v},$$

which can be transformed into $\nabla_e - \nabla_{\rm ad} = \frac{\lambda H_P}{8 V v T c_P}$; λ describes the radiation loss relative to the blob's energy. At this point, geometric factors and other assumptions come in (for the details see Kippenhahn & Weigert); finally, one obtains 5 equations for v, $F_{\rm conv}$, $F_{\rm rad}$, ∇ and ∇_e in terms of $P, T, \rho, l_m, \nabla_{\rm ad}, \nabla_{\rm rad}$. An analytical solution is possible and leads to a *cubic equation*:

$$(\xi - U)^3 + \frac{8U}{9}(\xi^2 - U^2 - W) = 0 \tag{1.38}$$

where

$$\begin{aligned} \xi^2 &= \nabla - \nabla_{\rm ad} + U^2 \\ U &= \frac{3acT^3}{c_P \rho^2 \kappa l_m^2} \sqrt{\frac{8H_P}{g\delta}} \\ W &= \nabla_{\rm rad} - \nabla_{\rm ad} \end{aligned}$$

W and U can be calculated at any point (local!) and (1.38) can be solved by numerical methods (more stable than analytical solution).
Physical interpretation: $U = \frac{\sigma_{\rm rad}}{\sigma_{\rm conv}}$ is the "ratio of conductivities", which are defined through $F_{\rm rad} = \sigma_{\rm rad} \nabla$ and $F_{\rm conv} = \sigma_{\rm conv} (\nabla - \nabla_{\rm ad})^{3/2}$. U is related to

$$\Gamma := \frac{(\nabla - \nabla_e)^{1/2}}{2U} = \frac{(\nabla - \nabla_e)}{(\nabla_e - \nabla_{\rm ad})}$$

which is the ratio of energy transported by the blob over that lost from it, or the "efficiency" of the convection.
If U small, Γ is large and almost all flux is transported by convection and the resulting gradient is $\approx \nabla_{\rm ad}$.
If U is large, Γ is small, and – although transport is by convection – the resulting gradient is almost $\nabla_{\rm rad}$.
In general, convection is *superadiabatic*:

$$\nabla = \nabla_{\rm ad} + \delta\nabla$$

The equations still contain the mixing length $l_m = \alpha_{\rm MLT} H_P$, where $\alpha_{\rm MLT}$ is the (in)famous *mixing-length parameter*. It is of order 1, and is determined usually by solar models (see later), $\alpha_{\rm MLT} \approx 1.2 \cdots 2.2$. It is assumed (without real justification) to be constant throughout a star and the same for all stellar masses, compositions and evolutionary phases.
Example for ∇: Sun, $r = R_\odot/2$, $m = M_\odot/2$, $T = 10^7$, $\rho = 1$, $\delta = \mu = 1$

$$\rightarrow U = 10^{-8} \rightarrow \nabla = \nabla_{\rm ad} + 10^{-5} = 0.4$$

(as long as $\nabla_{\rm rad} < 100 \cdot \nabla_{\rm ad}$); at center, $\nabla = \nabla_{\rm ad} + 10^{-7}$.
The Sun is in most parts almost adiabatic (in this case, l_m is unimportant). Red Giants can have very superadiabatic envelopes!

1.2.6 The chemical composition

So far, we have only treated m, L_r, P, T as the independent variables. However, many quantities depend also on the composition $\vec{X}$, and so does the structure. This composition *must* change with time, because L is mainly obtained from nuclear reactions and these change $\vec{X}$ on long timescales. It can furthermore change due to diffusion, convection and other mixing processes.
Notation: relative element mass fraction: $X_i := \frac{m_i n_i}{\rho}$, with $\sum_i X_i = 1$; special cases: hydrogen X, helium Y, "metals" $Z = 1 - X - Y$. m_i and n_i are particle masses and densities.
Examples (approximative numbers):

- Big Bang nucleosynthesis: $X \approx 0.75 \quad Y \approx 0.25 \quad Z \approx 0.0$;
- Population II stars: $X = 0.75 \quad Y = 0.25 \quad Z \approx 10^{-4}$
- Sun: $X = 0.70 \quad Y = 0.28 \quad Z = 0.02$

1.2.6.1 Changes due to nuclear reactions:

$$\frac{\partial X_i}{\partial t} = \frac{m_i}{\rho}[\sum_j r_{ji} - \sum_k r_{ik}] \tag{1.39}$$

The first term describes the creation of element i by a reaction of element j, and the second the destruction by the production of element k. The energy released is $\epsilon_{ij} = \frac{1}{\rho} r_{ij} e_{ij}$. r_{ij} is the number of reactions per second, and e_{ij} the energy released per reaction, per particle mass it is $q_{ij} = e_{ij}/m_i$
For the conversion of hydrogen into helium, for example, we get

$$\frac{\partial X}{\partial t} = -\frac{\epsilon_H}{q_H} = -\frac{\partial Y}{\partial t}$$

.

1.2.6.2 Changes due to diffusion:

Several effects work at same time:

1. Gradients in composition tend to be smoothed out; "concentration diffusion";
2. Heavier particles sink in potential; "pressure diffusion" or "sedimentation";
3. Heavier particles are slower, restricted to higher temperature regions; "temperature diffusion".

Formally:

$$\vec{v}_D = -\frac{1}{c} D \left(\vec{\nabla} c + k_T \vec{\nabla} \ln T + k_P \vec{\nabla} \ln P \right) \tag{1.40}$$

This is obtained by using Fick's law $\vec{j}_D = c\vec{v}_D = -D\vec{\nabla}c$, where $\vec{j}_D$ is the diffusive particle flux, D the diffusion constant, and c the concentration (relative number density).
From the continuity equation one gets (constand D assumed):

$$\begin{aligned} \frac{\partial c}{\partial t} &= -\vec{\nabla}\vec{j}_D \\ &= \vec{\nabla}(D\vec{\nabla}c) \\ &= D\nabla^2 c \end{aligned}$$

Corresponding equations can be derived for the other two terms of (1.40), with k_T and k_P describing relative diffusion speeds w.r.t. concentration diffusion. They are positive and of order 1.
In the sun, the timescale for diffusion is 10^{13} yrs, or, in 10^9 yrs composition changes of 10^{-4} can be expected. In fact, they are measurable, and diffusion has to be included in the solar models! The net effects are: due to P- and T-diffusion He is sinking towards the center of the Sun.
The general assumption has been that diffusion is unimportant, except for long-lived hot stars (e.g. White Dwarfs), where convection does not counteract diffusion.

1.2.6.3 Mixing by convection:

In completely convective regions, the mixing speed is so fast ($\approx 10^4$ cm/s; $\tau \approx 1$ yr) that *instantaneous* complete mixing can savely be assumed. Only in *semiconvective* regions – here the Ledoux-criterion for stability is fulfilled, but the Schwarzschild-criterion is violated – it is slow and resembles a diffusion process. In any case, formally, convective mixing can be treated as an additional diffusion process with appropriate constants.

1.2.7 The equations - summary

m is the Lagrangian coordinate;
r, P, T, L_r are the independent variables;
X_i are the composition variables, entering only through time derivatives;
$\rho, \kappa, \epsilon, \ldots$ are dependent variables;
The four structure equations to be solved are:

$$\frac{\partial r}{\partial m} = \frac{1}{4\pi r^2 \rho} \tag{1.41}$$

$$\frac{\partial P}{\partial m} = -\frac{Gm}{4\pi r^4} - \frac{1}{4\pi r^2}\frac{\partial^2 r}{\partial t^2} \tag{1.42}$$

$$\frac{\partial L_r}{\partial m} = \epsilon_n - \epsilon_\nu - c_P \frac{\partial T}{\partial t} + \frac{\delta}{\rho}\frac{\partial P}{\partial t} \tag{1.43}$$

$$\frac{\partial T}{\partial t} = -\frac{GmT}{4\pi r^4 P}\nabla \tag{1.44}$$

In the last equation, the appropriate ∇ has to be inserted; for radiation this is

$$\nabla_{\rm rad} = \frac{3}{16\pi acG}\frac{\kappa L_r P}{mT^4} \tag{1.45}$$

Finally, for the composition, we have

$$\frac{\partial X_i}{\partial t} = \frac{m_i}{\rho}\left(\sum_j r_{ji} - \sum_k r_{ik}\right) \tag{1.46}$$

1.2.8 Simple stellar models: Homology

Homology is the assumption that stars are related to each other by a very simple, linear similarity relation, which is that at

$$\frac{m_1}{M_1} = \frac{m_0}{M_0} \tag{1.47}$$

also

$$\frac{r_1}{R_1} = \frac{r_0}{R_0} \tag{1.48}$$

Insert this into mass equation:

$$\rho_1 = \rho_0 \left(\frac{M_1}{M_0}\right)\left(\frac{R_1}{R_0}\right)^{-3} \tag{1.49}$$

to obtain the homology scaling law for the density at the same relative mass fraction.
From the hydrostatic equation, one obtains similarly

$$P_1 = P_0 \left(\frac{M_1}{M_0}\right)^2 \left(\frac{R_1}{R_0}\right)^{-4} \tag{1.50}$$

or $P \propto (M^2/R^4)$.

To obtain even further insight, one assumes power laws for the dependent variables:

$$P = P_0 \rho^{\chi_\rho} T^{\chi_T} \quad (1.51)$$
$$\epsilon_n = \epsilon_{n,0} \rho^{\lambda} T^{\nu} \quad (1.52)$$
$$\kappa = \kappa_0 \rho^{n} T^{-s} \quad (1.53)$$

All exponents are assumed to be the same in homologous stars and at all m.
For example, since $\mathrm{d}\ln P = 2\mathrm{d}\ln M - 4\mathrm{d}\ln R$, we get also

$$4\mathrm{d}\ln R + \chi_\rho \mathrm{d}\ln\rho + \chi_T \mathrm{d}\ln T = 2\mathrm{d}\ln M$$

We want to obtain relations of the form $R \propto M^{\alpha_R}$, where the individual αs have to be determined from the structure equations and the homology assumptions.
From above equation it follows, for example, that

$$4\alpha_R + \chi_\rho \alpha_\rho + \chi_T \alpha_T = 2$$

This leads to a *matrix equation* for the α vector (α_R, α_T, α_ρ, α_L). The determinant of the matrix is, in the case of radiative transport:

$$D_{\rm rad} = (3\chi_\rho - 4)(\nu - s - 4) - \chi_T(3\lambda + 3n + 4) \quad (1.54)$$

For convection, it is:

$$D_{\rm conv} = 3(\chi_\rho - 4) + 3\chi_T(\Gamma_3 - 1) \quad (1.55)$$

where $(\Gamma_3 - 1) = \left(\frac{\mathrm{d}\ln T}{\mathrm{d}\ln\rho}\right)_{ad}$.
In the first case, one obtains, e.g. $\alpha_T = -2(\chi_\rho + \lambda + n)/D_{\rm rad}$

Application: homologous stars similar to Sun

$n = s = 0$ (electron scattering); $\lambda = 1$, $\nu = 15$ (CNO-cycle); $\chi_\rho = \chi_T = 1$ (ideal gas).
$\Rightarrow$ $\alpha_R = 0.78$: observed 0.75; $\alpha_L = 3.0$: obs. 3.5; $\alpha_T = 0.22$ $\alpha_\rho = -1.33$: correct dependencies (from numerical models); note that density decreases with mass!

From homology, it also follows for the hydrogen-burning lifetime of stars:

$$\tau_{\rm nuc} = 10^{10}\left(\frac{M}{M_\odot}\right)\left(\frac{L_\odot}{L}\right) = 10^{10}\left(\frac{M}{M_\odot}\right)^{1-3.5}$$

$\rightarrow$ more massive stars live shorter! (here we assumed for the numerical factor that about 10% of the mass is converted into helium).

1.3 The Microphysics: EOS, opacity, energy generation

1.3.1 Equation of State

1.3.1.1 Ideal gas with radiation pressure

$$P = nk_BT = \frac{\mathcal{R}}{\mu}\rho T \tag{1.56}$$

with $\rho = n\mu m_u$ ($m_u = 1.66 \cdot 10^{-24}$ g; $\mathcal{R} = k_B/m_u = 8.31 \cdot 10^7 \frac{\text{erg}}{\text{gK}}$ (gas constant); μ: molecular weight, mass of particle per m_u).
In stars, there are many components of the gas, with relative mass fractions $X_i = \frac{\rho_i}{\rho} \rightarrow n_i = \frac{\rho X_i}{m_u \mu_i}$ (electrons are neglected in partial densities)

$$P = P_e + \sum_i P_i = (n_e + \sum_i n_i)kT \tag{1.57}$$

a completely ionzied atom contributes $(1 + Z_i)n_i$ to n, such that

$$P = nkT = \mathcal{R}\sum_i \frac{X_i(1+Z_i)}{\mu_i}\rho T = \frac{\mathcal{R}}{\mu}\rho T \tag{1.58}$$

with $\mu := \left(\sum_i \frac{X_i(1+Z_i)}{\mu_i}\right)^{-1}$ being the *mean molecular weight.*
For a neutral gas, $\mu = \left(\sum_i \frac{X_i}{\mu_i}\right)^{-1}$.

The mean molecular weight *per free electron* is $\mu_e := \left(\sum_i \frac{X_i Z_i}{\mu_i}\right)^{-1} = \frac{2}{(1+X)}$, taking into account that $Z = 1 - X - Y$ and for helium and metals $\mu_i/Z_i \approx 2$.

Radiation pressure can be added to the ideal gas equation.

$$P_{\text{rad}} = \frac{1}{3}U = \frac{a}{3}T^4 \quad \left(a = 7.56 \cdot 10^{-15} \frac{\text{erg}}{\text{cm}^3\text{K}^4}\right)$$

Define $\frac{P_{\text{gas}}}{P} := \beta$. Then $\left(\frac{\partial\beta}{\partial T}\right)_P = -\frac{4(1-\beta)}{T}$ and $\left(\frac{\partial\beta}{\partial P}\right)_T = \frac{(1-\beta)}{T}$.

Furthermore

$$\begin{aligned}
\alpha &:= \left(\frac{\partial \ln\rho}{\partial \ln P}\right)_T = \frac{1}{\beta} \\
\delta &:= -\left(\frac{\partial \ln\rho}{\partial \ln T}\right)_P = \frac{4-3\beta}{\beta} \\
\varphi &:= \left(\frac{\partial \ln\rho}{\partial \ln\mu}\right)_{T,P} = 1 \\
c_P &:= \frac{\mathcal{R}}{\mu}\left[\frac{3}{2} + \frac{3(4+\beta)(1-\beta)}{\beta^2} + \frac{4-3\beta}{\beta^2}\right]
\end{aligned} \tag{1.59}$$

$$\begin{aligned}
\nabla_{\text{ad}} &:= \frac{\mathcal{R}\delta}{\beta\mu c_P} \\
\gamma_{\text{ad}} &:= \left(\frac{\text{d}\ln P}{\text{d}\ln\rho}\right)_{\text{ad}} = \frac{1}{\alpha - \delta\nabla_{\text{ad}}}
\end{aligned} \tag{1.60}$$

For $\beta \rightarrow 0$, $c_P \rightarrow \infty$, $\nabla_{\text{ad}} \rightarrow 1/4$ and $\gamma_{\text{ad}} \rightarrow 4/3$.
For $\beta \rightarrow 1$, $c_P \rightarrow \frac{5\mathcal{R}}{2\mu}$, $\nabla_{\text{ad}} \rightarrow 2/5$, and $\gamma_{\text{ad}} \rightarrow 5/3$.

Note: there are further thermodynamic derivatives in use in the literature, the so-called gammas. Here is a list of relations:

$$\begin{aligned} \gamma_{\rm ad} &=: \Gamma_1 \\ \nabla_{\rm ad} &=: \frac{\Gamma_2 - 1}{\Gamma_2} \\ \Gamma_3 &:= \left(\frac{{\rm d}\ln T}{{\rm d}\ln \rho}\right)_{\rm ad} + 1 \\ \frac{\Gamma_1}{\Gamma_3 - 1} &= \frac{\Gamma_2}{\Gamma_2 - 1} \end{aligned}$$

1.3.1.2 Ionization

The Boltzmann-equation describes the relative occupation numbers of different energy states in thermal equilibrium. If applied to atoms being ionized, taking into account the distribution of electrons in phase space, one obtains the *Saha-equation*[4]

$$\frac{n_{r+1}}{n_r} P_e = \frac{u_{r+1}}{u_r} 2 \frac{(2\pi m_e)^{3/2}}{h^3} (kT)^{5/2} \exp(-\chi_r/kT), \tag{1.61}$$

where n_r is the number density of atoms (of one species) in ionization state r, χ_r is the corresponding ionization energy, u_r is the partition function (usually the ground state statistical weight) and $h = 6.626 \cdot 10^{-27}$ erg s the Planck constant. $P_e = n_e kT$ is the electron pressure, finally.

Application: hydrogen ionziation in Sun
$n = n_0 + n_1$ (total of atoms in ground state 0 and ionized 1); $n_e = n_1$; $x := \frac{n_1}{n_0 + n_1}$
$P_e = P_{\rm gas} \frac{n_e}{n_e + n} = P_{\rm gas} \frac{x}{x+1}$

$$\Rightarrow \frac{x^2}{1 - x^2} = \frac{u_1}{u_0} \frac{2}{P_{\rm gas}} \frac{(2\pi m_e)^{3/2}}{h^3} (kT)^{5/2} {\rm e}^{-\chi_1/kT}$$

$u_0 = 2$, $u_1 = 1$ are ground-state stat. weights; $\chi_1 = 13.6$ eV.
At the solar surface, $T = 5700$ K, $P_{\rm gas} = 6.8 \cdot 10^4$, $\rightarrow x \approx 10^{-4}$; at $P_{\rm gas} = 10^{12}$, $T = 7 \cdot 10^5$, $\rightarrow x \approx 0.99$.

The mean molecular weight for a partially ionized gas is easily calculated by $\mu = \mu_0/(E+1)$, where μ_0 is the molecular weight of the unionized gas, and E the number of free electrons per all atoms. With μ again the ideal gas equation can be used.

For a mixture of atoms, a set of Saha-equations coupling all ionization states (P_e is coupling different atoms) is to be solved (numerically).
Here is an example for the run of ionization states:

[4] see Kippenhahn & Weigert, pp. 107, for a detailed derivation.

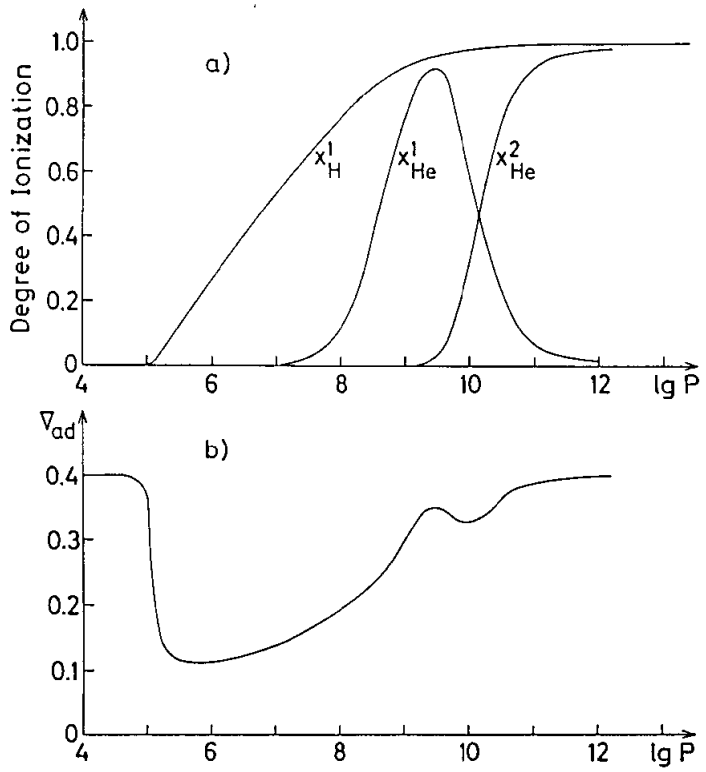

Illustration of ionization of hydrogen and helium within a stellar envelope. In panel (b) the corresponding run of $\nabla_{\rm ad}$ is shown. The depression is due to the increase in c_P due to ionziation. Since $\nabla_{\rm ad}$ is getting smaller, convection will set in. (from KW)

Note the following defect of the Saha-equation: the ionization increases with T and decreases with P. When $T \approx$ const., as in stellar cores, the ionization degree should decrease, which is unphysical. The explanation lies in the fact that the ionization potential is suppressed, if the atoms approach each other, and individual potentials overlap. This is called *pressure ionziation*, and is treated in practice by "complete ionziation"-conditions or a change in the χ_i.

1.3.1.3 Electron degeneracy

At high densities, the electrons are degenerate – from weak degeneracy as in the solar center to complete relativistic degeneracy as in massive giants' cores. The equation of state is then dominated by the electron pressure which arises from the fact that all quantum cells in phase space are occupied (Pauli-principle). The distribution of electrons in momentum space follows Boltzmann equation (p is momentum):

$$f(p)\mathrm{d}p\mathrm{d}V = n_e \frac{4\pi p^2}{(2\pi m_e kT)^{3/2}} \exp\left(-\frac{p^2}{2m_e kT}\right) \mathrm{d}p\mathrm{d}V \tag{1.62}$$

On the other hand, the Pauli-principle limits this:

$$f(p)\mathrm{d}p\mathrm{d}V \leq \frac{8\pi p^2}{h^3}\mathrm{d}p\mathrm{d}V \tag{1.63}$$

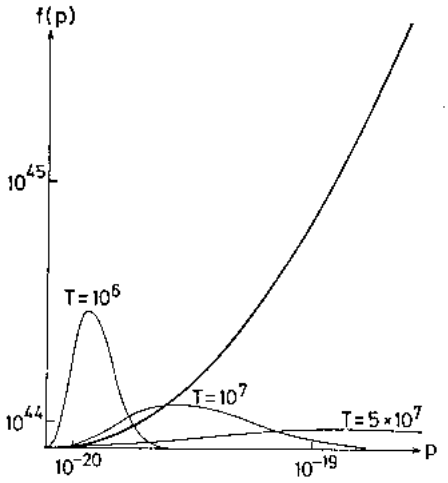

Run of $f(p)$ according to (f(p)) for three different temperatures and the limit imposed by Pauli's principle. Obviously, at lower T, the Boltzmann distribution can no longer be realized. (from KW)

Completely degenerate gas:

$$\begin{aligned} f(p) &= \frac{8\pi p^2}{h^3} \text{ for } p \leq p_F \propto n_e^{1/3} \\ &= 0 \text{ for } p > p_F \end{aligned} \tag{1.64}$$

$E_F = \frac{p_F^2}{2m_e} \propto n_e^{2/3}$ is the Fermi-energy (recall that $E_F > 0$ even if $T = 0$); for $E_F \approx m_e c^2$, $v_e \approx c$, this situation is called *relativistic complete degeneracy.*

1. $p_F \ll m_e c$ (non-relativistic)

$$P_e = 1.0036 \cdot 10^{13} \left(\frac{\rho}{\mu_e}\right)^{5/3} \qquad P_e = \frac{2}{3} U_e \tag{1.65}$$

2. $p_F \gg m_e c$ (relativistic)

$$P_e = 1.2435 \cdot 10^{15} \left(\frac{\rho}{\mu_e}\right)^{4/3} \qquad P_e = \frac{1}{3} U_e \tag{1.66}$$

(U_e is the internal energy per electron and unit volume). In all cases $P_i \ll P_e$ because of their much higher mass.

Partial degeneracy:
At any finite T, the electron gas deviates from complete degeneracy. Depending on T (and n_e), this can be neglected or has to be included. Increasing T enough must finally lead back to a Boltzmann-distribution. The appropriate statistics to describe the partially degenerate state is the *Fermi-Dirac* statistics:

$$f(p)\mathrm{d}p\mathrm{d}V = \frac{8\pi p^2}{h^3} \frac{1}{1 + \exp\left(\frac{E}{kT} - \Psi\right)} \mathrm{d}p\mathrm{d}V \tag{1.67}$$

with $\Psi = \frac{n_e}{T^{3/2}}$ called the *degeneracy parameter*. At constant Ψ, $T \propto \rho^{2/3}$ for the non-relativistic case, and $\propto \rho^{1/3}$ in the relativistic one.
From (1.67) one derives the following relations for Fermions:

$$
\begin{aligned}
n_e &= \frac{8\pi}{h^3}\int_0^\infty \frac{p^2 \mathrm{d}p}{1+\exp\left(\frac{E}{kT}-\Psi\right)} \\
P_e &= \frac{8\pi}{3h^3}\int_0^\infty \frac{p^3 v(p) \mathrm{d}p}{1+\exp\left(\frac{E}{kT}-\Psi\right)} \\
U_e &= \frac{8\pi}{h^3}\int_0^\infty \frac{E p^2 \mathrm{d}p}{1+\exp\left(\frac{E}{kT}-\Psi\right)}
\end{aligned}
$$

In the limiting cases, the known distributions are recovered. In practice, the EOS for this case has to be solved by either analytical approximative formulae or by numerical solution of the involved Fermi-Dirac integrals integrals. Numerical values can be found in Kippenhahn & Weigert, for example.

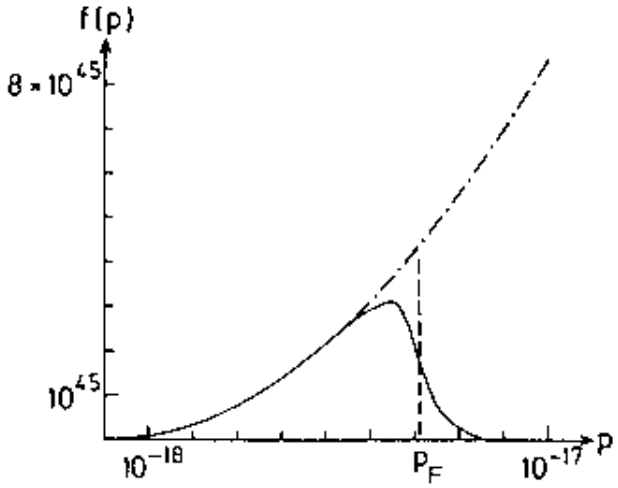

$f(p)$ for partially degenerate gas with $n_e = 10^{28}$ cm^{-3} and $T = 1.9 \cdot 10^7$ K corresponding to $\Psi = 10$. (from KW)

The equation of state for normal stellar matter:

$$P = P_{\mathrm{ion}} + P_e + P_{\mathrm{rad}} = \frac{\mathcal{R}}{\mu_0}\rho T + \frac{8\pi}{3h^3}\int_0^\infty \frac{p^3 v(p) \mathrm{d}p}{1+\exp\left(\frac{E}{kT}-\Psi\right)} + \frac{a}{3}T^4 \tag{1.68}$$

$$\rho = \frac{4\pi}{h^3}(2m_e)^{3/2} m_u \mu_e \int_0^\infty \frac{E^{1/2}\mathrm{d}E}{1+\exp\left(\frac{E}{kT}-\Psi\right)} \tag{1.69}$$

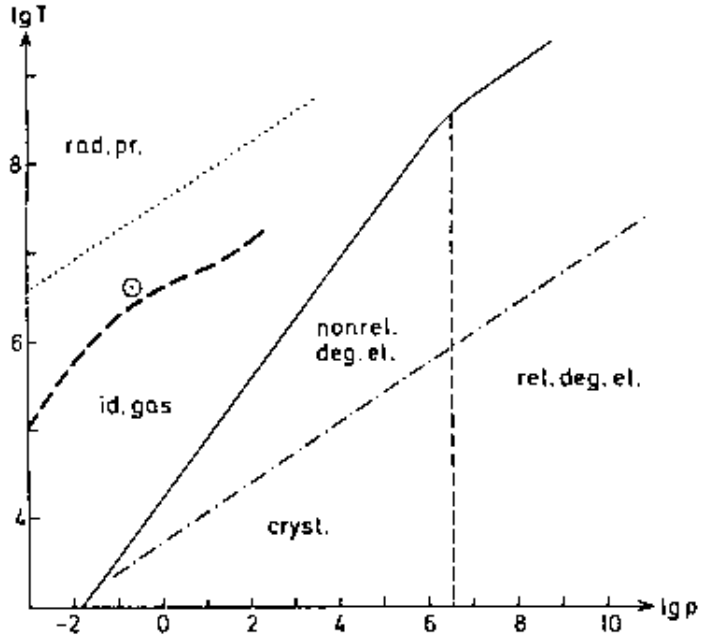

Sketch of the regions in the $\lg \rho$-$\lg T$ diagram, where the EOS is dominated by the different effects. (from KW)

At even higher densities ($\approx 8 \cdot 10^4$ higher) ions can become degenerate as well. Note further that for electron degeneracy, $P \approx P_e$, but $\rho \approx \rho_{\rm ion}$.

1.3.1.4 Further effects:

Up to now, we always have considered an ideal gas. Non-ideal effects like Coulomb screening or van-der-Waals forces have to be taken into count separately. The Debye-Hückel theory for screening is most easiest to implement. If the interaction between ions (Coulomb interaction) gets comparable to the thermal energy, collective effects like *crystallization* happen. This applies to White Dwarfs, for example. For details, see, the textbook by Shapiro & Teukolsky: Black Holes, White Dwarfs and Neutron Stars, Wiley (1983).
At nuclear matter densities, neutronisation sets in. Week interactions cause protons and electrons to become neutrons, which are degenerate. These objects are neutron stars.

1.3.1.5 EOS tables

In practice, for the EOS one has to use tabulated values for density and internal energy (and the various derivatives), if high accuracy is required. Presently, for normal densities, tables by Rogers, Swenson & Iglesias (ApJ 456, 902, 1996) are the best reference (OPAL-EOS); for higher densities (very low-mass stars, white dwarfs, etc.) the best choice is Saumon, Chabrier & van Horn (ApJ Suppl. 99, 713, 1995)

1.3.2 Opacity

Photons are absorbed and reemitted (scattered) while passing through the stellar interior. Therefore they transport energy from hotter to cooler layers. The "transparency" of the material determines the free pathlength and thus the resulting termperature gradient. The basic effects are

Electron scattering:
photons are electromagnetic waves giving rise to e^--oscillations which lead to re-emission of photons (Thomson-scattering). The opacity is described by

$$\kappa_{\rm sc} = \frac{8\pi}{3}\frac{r_e^2}{m_e m_u} = 0.20(1+X)\ {\rm cm^2 g^{-1}} \tag{1.70}$$

at $T > 10^8$ also momentum exchange can happen and $\kappa < \kappa_{\rm sc}$(Compton-scattering).
free-free transitions:
e^- in thermal motion coming close to ion, both particles form a system able to absorb and emit radiation. This effect is v-dependent. It is described by the classical *Kramers* formula

$$\kappa_{\rm ff} \propto \rho T^{-7/2} \tag{1.71}$$

The constant of proportionality includes quantum corrections.

bound-free transitions:
An atom from ground or excited state is converted into an ion by absorption of photons with the necessary energy. A Kramers-type approximation is

$$\kappa_{\rm bf} \propto Z(1+X)\rho T^{-7/2} \tag{1.72}$$

A special case is the H^--ion, which forms below 10^4 K, but is so loosely bound, that photon with $\lambda < 1655$ nm (infrared) can destroy it.

bound-bound transitions:
This is the dominant process below 10^6 K. It comes from the change of electrons into higher excited states and back, and depends strongly on the atomic level structure of the atoms. No simple formula is available.

e^-conduction:
This is no radiation process, but, as shown in Sect. 1.2.5, can be treated by the appropriated definition of a conduction opacity. It dominates at high densities (degenerate cores of stars).

$$\kappa_{\rm c} \propto \rho^{-2} T^2 \tag{1.73}$$

In practice, κ is calculated by specialized groups and provided in the form of *opacity tables* that depend on composition, T and ρ. About 18 metal species have to be taken into account to reach an accuracy of $\approx 10\%$.
The most recent tables are those of the Livermore group (OPAL), published in Rogers & Iglesias, ApJS 79, 507 (1992) and those of the Opacity Project, e.g. Seaton et al., MNRAS 260, 805 (1994). Older tables came from the Los Alamos group (e.g. Weiss, Keady & Magee, At. Data & Nuclear Data Tables 45, 209 (1990)). They include also molecules (important below ≈ 8000 K). Most recent low-T tables including molecules and dust are those by Alexander & Fergusson (ApJ 437, 879 (1994)).

1.3.3 Nuclear Energy Production

Principle: Nuclei have higher mass when existing separately than when combined into nucleus of higher mass A (in m_u). Difference in mass (mass defect) via $E = mc^2$ liberated as energy.
Example: 4 ^{1}H (protons) : $4 \cdot 1.0081 m_u$, but ^{4}He: $4.0089 m_u$. Difference (0.7%) : 26.5 MeV (931.1 MeV $= 1\ m_u$; 1 MeV $= 1.6 \cdot 10^{-6}$ erg). The solar luminosity in terms of mass is $4.25 \cdot 10^{12}$ gs^{-1}. If 0.7% of $M_\odot$ is available, the sun can shine for 10^{11} yrs.
The *binding energy* is defined as:

$$E_B := [(A - Z)m_n + Zm_p - M_{\rm nuc}]c^2 \tag{1.74}$$

and $f := E_B/A$ is the b.e. per nucleon, which is of order 8 MeV except for the lightest elements. Its maximum (8.4 MeV) is reached for ^{56}Fe, which is the most tightly packed nucleus. For H, it is 0 MeV by def., ^{4}He = 6.5, ^{12}C = 7.5.
All reactions transforming nuclei into ^{56}Fe will release energy. For $A < 56$ this works by fusion (and happens in stars), for $A > 56$ by fission (nuclear reactors; and stars with excessive energies - supernovae).

Nuclear fusion:
To merge two nuclei, the Coulomb barrier between them, being $\approx Z_1 Z_2$ MeV high, must be overcome such that nuclear forces (attractive) work. The nuclei must come as close as

$$r_0 \approx A^{1/3} 1.44 \cdot 10^{-13} \text{ cm}.$$

In thermonuclear reactions, the thermal motion ($E_{\rm kin}$) is used. In a Maxwell-Boltzmann-distribution of temperature T, there are always some particles fast enough, but their number is much too small; e.g. at $T = 10^7$ K, $kT/E_{cb} \approx 10^{-3}$, such that only a fraction of 10^{-434} particles will have the necessary energy. The solution has been found by Gamov: quantum-mechanical tunnelling.

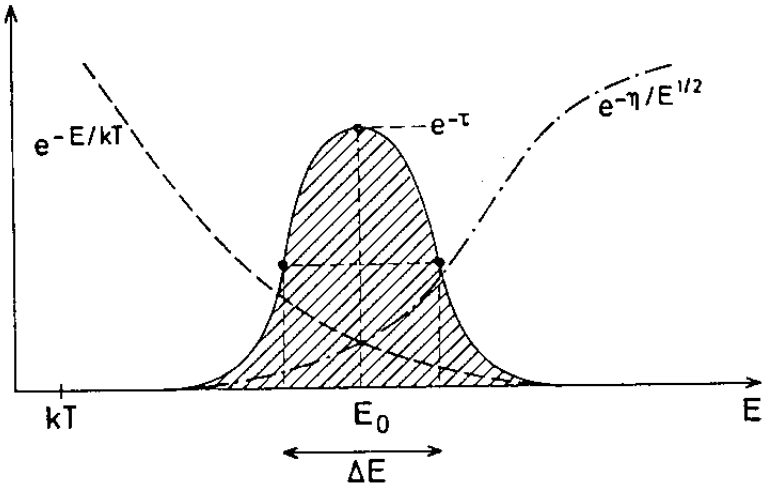

The Gamow peak (strongly magnified); the dashed line is the Maxwell-distribution, the dot-dashed one the tunnelling probability (from KW)

We skip the derivation of nuclear cross sections, which can be found in great detail in Clayton's book (Principles of stellar structure and nucleosynthesis). We mention only, that for non-resonant reactions, it usually is brought into a form

$$\sigma(E) = S(E) E^{-1} \exp -\pi\eta \quad \eta = \sqrt{(m/2)} \frac{2\pi Z_1 Z_2 e^2}{h E^{1/2}} \tag{1.75}$$

m being the reduced mass of the reacting nuclei. $S(E)$ is measured in laboratories, but usually at energies much higher than that of stellar plasmas. The extrapolation is critical. Resonant reactions have to be measured in the laboratory or predicted by nuclear theories. They can be most critical for reactions to occur.

The *thermonuclear reaction rate*

$$r_{jk} = \frac{n_j n_k}{1+\delta_{jk}} \langle \sigma v \rangle \tag{1.76}$$

is the number of reactins per unit volume and time; $\langle \sigma v \rangle$ is the reaction probability per pair of reacting nuclei and second, it is averaged over the Maxwellian velocity distribution

$$f(E)\mathrm{d}E = \frac{2}{\sqrt{\pi}} \frac{\sqrt{E}}{(kT)^{3/2}} e^{-E/kT} \mathrm{d}E \tag{1.77}$$

$$\langle \sigma v \rangle = \int_0^\infty \sigma(E) v f(E) \mathrm{d}E \tag{1.78}$$

The energy released by the reaction is then

$$\epsilon_{jk} = \frac{1}{1+\delta_{jk}} \frac{q_{jk}}{m_j m_k} \rho X_i X_k \langle \sigma v \rangle \tag{1.79}$$

with q_{jk} being the energy released per reaction.
One can approximate ϵ_{jk} by $\epsilon_{jk,0} \left(\frac{T}{T_0}\right)^\nu$. One finds that for H-burning $\nu = 5 \ldots 15$ and for He-burning $\nu = 40$. That implies that nuclear reactions are a very efficient thermostat.

Electron shielding:
The cloud of e^- reduces the repulsive Coulomb force. This leads to an *increase* in the reaction probability by about 10%. Usually, the *weak* limit is appropriate, which holds, if $E_D = \frac{Z_1 Z_2 e^2}{r_D} \ll kT$ ($r_D = \sqrt{\frac{kT}{4\pi\chi n e^2}}$ is the Debye-Hückel length and χ an average particle density)

In practice, we use published fit formulae for the individual rates. Most famous are those by Fowler and collaborators, for example Caughlan & Fowler 1988 (At. Data & Nuc. Data Tables, 40, 283).

1.3.3.1 Major burning stages in stars

In stars, fusion takes place in well-separated phases of burning lighter elements to heavier ones. The sequence is hydrogen → helium → carbon/oxygen → neon → silicon → iron. For us, only the first two are of interest, since the temperatures needed for the subsequent phases are not reached in stars of low and intermediate mass discussed in later lectures.

Hydrogen-burning takes place via two major mechanisms. The p-p-chain, so-called after the initial reaction $p(p, \nu e^+)d$ (the positron will annihilate with one of the electrons and the energy is added to the radiation field).

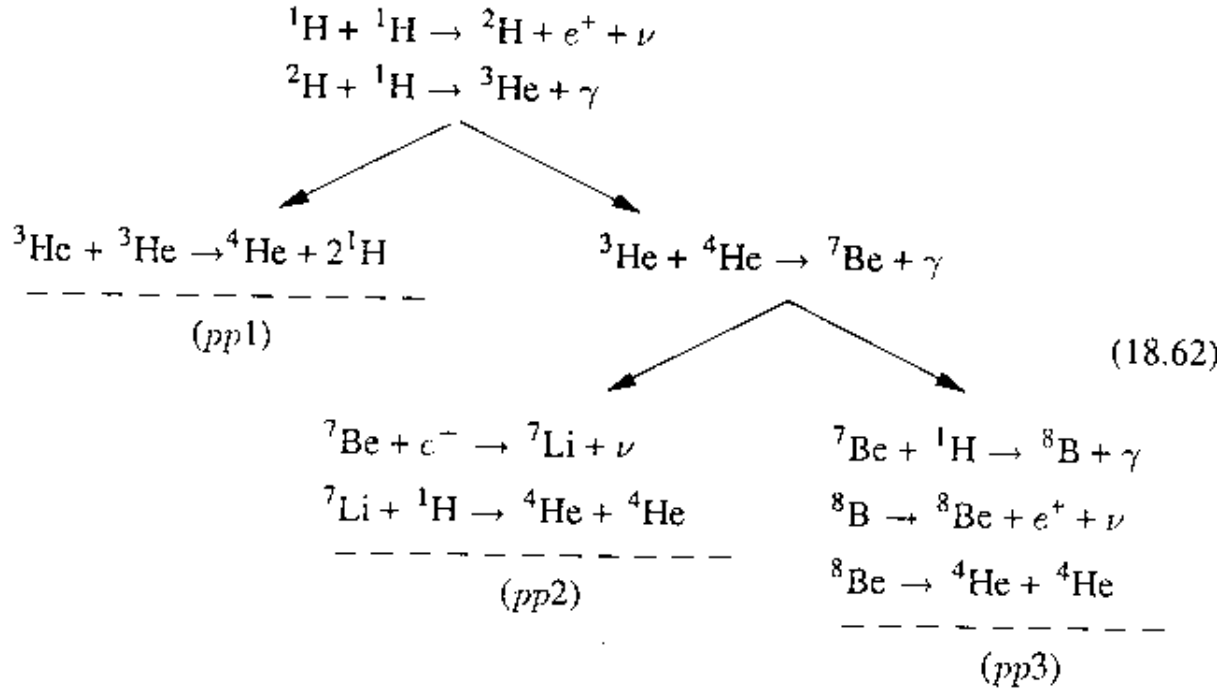

The pp-chain for the fusion of hydrogen to helium. (from KW)

It consists actually of three different paths, with ppI being the most important one. ppII and ppIII become more important the higher T. Note the neutrinos emitted. They carry away energy and the three chains deliver 26.20, 25.67 and 19.20 MeV per completion.

The second way to create helium in stars is the *CNO-cycle*, where these three elements serve as catalysts.

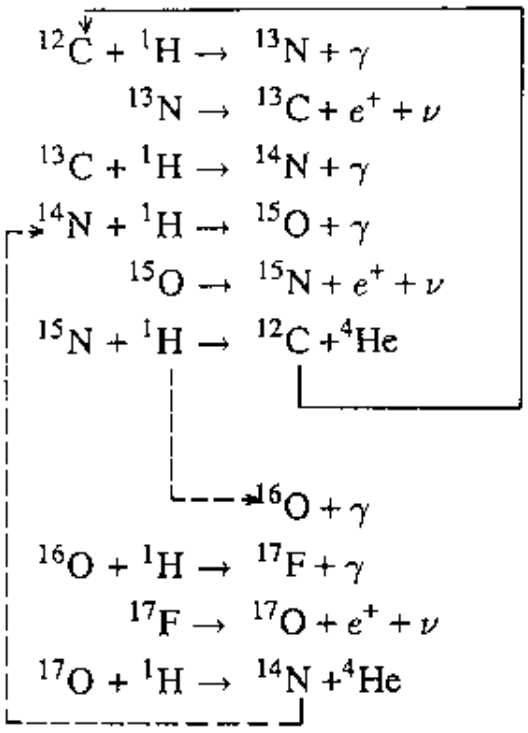

The CNO-cycle. (from KW)

Here, a few particularities have to be noted:

- The e^+ reactions are so fast that they can be assumed to happen instantaneously.
- The proton-capture reactions have different speed. Therefore, the complete cycle is dominated by the slowest reaction, which is $^{14}N(p,\gamma)^{15}O$.
- $q_{\mathrm{CNO}} \approx 25MeV$
- In equilibrium, almost all nuclei are converted into ^{14}N.
- The isotope ratio $^{12}C/^{13}C$ is much smaller than in cosmic matter (3-6 instead of 40)
- At low T (solar center), the cycle is too slow to be important, but the $C \rightarrow N$ transformation is working.
- Equivalent cycles involving Na and Mg exist and operate partially at higher temperature ($\approx 5 \cdot 10^7$ K).

With increasing temperature, the CNO-cycle becomes more dominant.

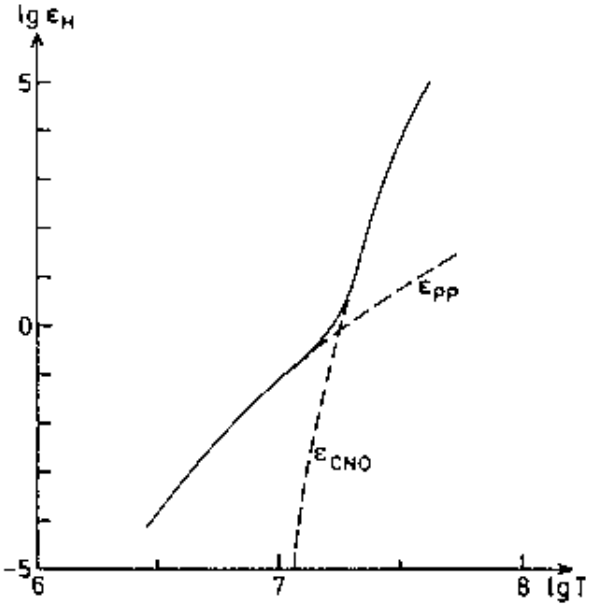

The contribution of pp-chain and CNO-cycle to the total energy production ϵ. (from KW)

Helium-burning starts at about 10^8 K, reached in most stars easily. Three major reactions are important (recall that no protons are left):

1. $3-\alpha$-process: $2\alpha(\alpha,\gamma)^{12}C$; actually two steps: $\alpha(\alpha,\gamma)^{8}Be$ and $^{8}Be(\alpha,\gamma)^{12}C$; the first one results in a state of ^{8}Be which, although unstable, has a much longer lifetime than a simple $\alpha-\alpha$-scatter; together with the third α is in resonance with a level of ^{12}C at 7.664 MeV. Without this resonant state, no carbon would exist in large abundance (and no life as we know it?). $q = 7.27$ MeV.

2. $^{12}C(\alpha,\gamma)^{16}O$: this process becomes important, as soon as enough carbon has been built up and the helium abundance gets lower (the $3-\alpha$-process is prop. to the cubic power of the helium abundance). Its reaction is uncertain by a factor of 2! $q = 7.6MeV$

3. $^{16}O(\alpha,\gamma)^{20}Ne$: important only during the end of helium burning; $q = 4.77$ MeV

The balance of the three reactions determine the abundances in the C/O-core that results from helium-burning. Calculations give 50/50 to 20/80 results.

Burning times:

Since the luminosity of a star is roughly determined by its mass and composition, the burning time in each phase is then determined by the q-values. L is increasing, and q decreasing. Both effects lead to ever shorter burning times (in yrs):

H	:	10^{10}
He	:	10^{8}
C	:	10^{4}

⋮ : ⋮

Si : hrs

1.3.4 Plasma neutrino emission

We have mentioned that the stellar plasma emits neutrinos, which leave the star almost unhindered (their mean free path under stellar conditions being of order 100 pc!) and lead to an energy loss L_ν.
Processes are:

1. Pair annihilation: $e^- + e^+ \to \nu + \bar{\nu}$ at $T > 10^9$ K.
2. Photoneutrinos: $\gamma + e^- \to e^- + \nu + \bar{\nu}$ (as Compton scattering, but with ν-pair instead of γ).
3. Plasmaneutrino: $\gamma_{\rm pl} \to \nu + \bar{\nu}$; decay of a plasma state $\gamma_{\rm pl}$.
4. Bremsstrahlung: inelastic nucleus–e^- scattering, but emitted photon replaced by a ν-pair.
5. Synchroton neutrinos: as synchroton radiation, but again a photon replaced by a ν-pair.

The most important process for stellar interiors are plasma-neutrinos. Tables or formulae for the emission rates have been calculated by Itoh and group (e.g. ApJS 102, 411, 1996) and (for plasma-neutrinos) by Haft, Raffelt & Weiss (ApJ 425, 222, 1994).

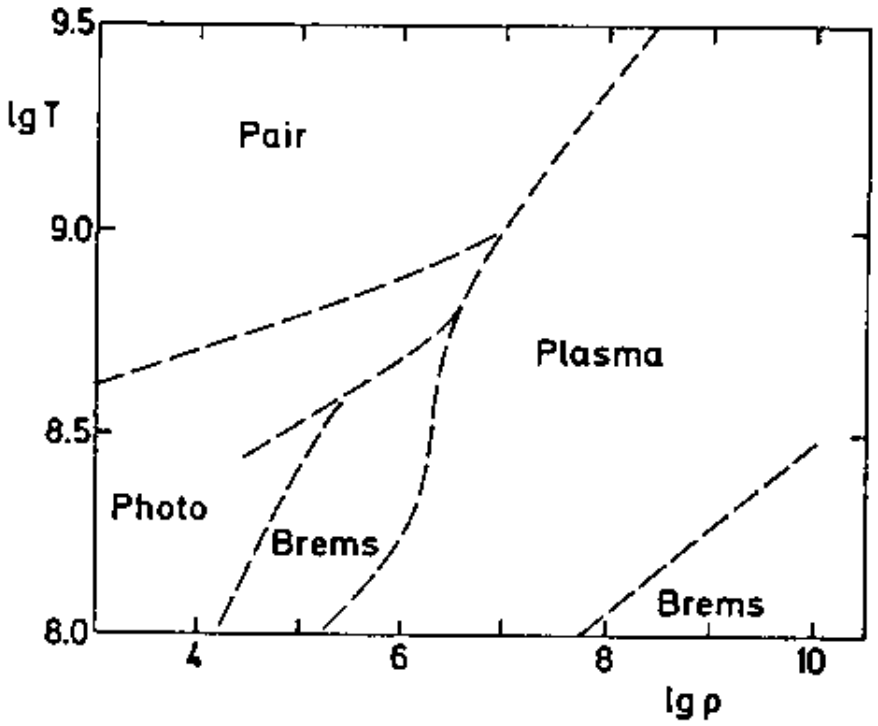

The regions in the ρ–T plane, where the different plasma-neutrino processes are dominant (from KW)

1.4 The complete problem - and its solution

We repeat here again the structure equations:

m is the Lagrangian coordinate;
r, P, T, L_r are the independent variables;
X_i are the composition variables, entering only through time derivatives;
The four structure equations to be solved are:

$$\frac{\partial r}{\partial m} = \frac{1}{4\pi r^2 \rho} \tag{1.80}$$

$$\frac{\partial P}{\partial m} = -\frac{Gm}{4\pi r^4} - \frac{1}{4\pi r^2}\frac{\partial^2 r}{\partial t^2} \tag{1.81}$$

$$\frac{\partial L_r}{\partial m} = \epsilon_n - \epsilon_\nu - c_P \frac{\partial T}{\partial t} + \frac{\delta}{\rho}\frac{\partial P}{\partial t} \tag{1.82}$$

$$\frac{\partial T}{\partial t} = -\frac{GmT}{4\pi r^4 P}\nabla \tag{1.83}$$

In the last equation, the appropriate ∇ has to be inserted; for radiation this is

$$\nabla_{\rm rad} = \frac{3}{16\pi acG}\frac{\kappa L_r P}{mT^4}$$

Finally, for the composition, we have

$$\frac{\partial X_i}{\partial t} = \frac{m_i}{\rho}\left(\sum_j r_{ji} - \sum_k r_{ik}\right) \tag{1.84}$$

$$\sum_i X_i = 1;$$

In addition, we have to provide $\rho(P,T,X_i)$, $\kappa(P,T,X_i)$, $r_{jk}(P,T,X_i)$, $\epsilon_n(P,T,X_i)$, $\epsilon_\nu(P,T,X_i)$, ...

In space (mass) we have a boundary value problem between $0 \le m \le M$ with boundary conditions:

- at center: $r(0) = 0$, $L_r(0) = 0$
- at $r = R$: P and T either from simple assumption $P = 0$, $T = 0$ or from atmospheric lower boundary and Stefan-Boltzmann-law $L = 4\pi\sigma R^2 T_{\rm eff}^4$

In calculations, the innermost region is expanded around the center into a series in m:

$$r = \left(\frac{3}{4\pi\rho_c}\right)^{1/3} m^{1/3} \tag{1.85}$$

and

$$P = P_c - \frac{3G}{8\pi}\left(\frac{4\pi}{3}\rho_c\right)^{4/3} m^{2/3} \tag{1.86}$$

and

$$L_r = (\epsilon_g + \epsilon_n - \epsilon_\nu)_c m \tag{1.87}$$

where the central b.c. have already been used.
The outer boundary condition involves stellar atmosphere calculations, not treated here. Two concepts are worth being noted:

1. optical depth: $\tau := \int_R^\infty \kappa\rho \mathrm{d}r = \bar{\kappa}\int_R^\infty \rho \mathrm{d}r$; for $\tau > 1$ matter is said to be optically thick and the diffusion approximation for radiative transport is valid; below: detailed radiation transport; at $\tau = 2/3$ the Stefan-Boltzmann-law holds.
2. pressure at R: $P(R) := \int_R^\infty g\rho \mathrm{d}r \approx g_R \int_R^\infty \rho \mathrm{d}r \Rightarrow P = \frac{GM}{R^2}\frac{2}{3}\frac{1}{\bar{\kappa}}$

In *time*, we have an initial value problem (zero-age model).

1.4.1 Numerical methods

Treat spatial and temporal problem separately. At any t, X_i are given. Solve then the spatial problem:

1.4.1.1 Approaches

1. **Direct integration** : conceptually the easiest method; start at one boundary, integrate (e.g. Runge-Kutta-type integrator) all equations and check other boundary conditions; repeat if necessary; Problem: solutions diverge (outer regions) and iterative process not likely to succeed. Improvement: start 2 integrations from outer and inner boundary, try to merge midway. (Schwarzschild integration; used for simple models)
2. **Difference method** : divide star in many mass shells, setup difference equations to replace differential equations; example:

$$\frac{P_{i+1} - P_i}{m_{i+1} - m_i} = -\frac{G\bar{m}}{4\pi\bar{r}^4}$$

where $\bar{m}$ is a mean mass over that shell, e.g. $\frac{m_{i+1}+m_i}{2}$.
This approach couples neighbouring grid-points, the solution is found by requiring that the equations are fulfilled, and by varying the variables y_i; this leads to a Newton-type algorithm involving a large matrix of dimension Nx4 (N grid-points); it needs for each model a good guess for the solution, otherwise the Newton-method will not converge.
This method is the standard one used and will be elaborated below.
3. **Hybrid methods** : Here a direct integration between fixed mesh-point is performed. It is equivalent to a multiple-fitting method, but the variation of the guesses at the fixed points is done via a Newton-method. (see the book by de Loore and Doom for a description)

1.4.1.2 The Henyey-method:

This is the realization of the second method and it concerns the solution of the matrix inversion. A complete description is found in Kippenhahn, Weiger, Hofmeister (1967) and in the textbook by Kippenhahn & Weigert.
Write the equations in a general form:

$$A_i^j := \frac{y_i^{j+1} - y_i^j}{m_i^{j+1} - m_i^j} - f_i(y_1^{j+1/2}, \ldots, y_4^{j+1/2}) \tag{1.88}$$

where the upper index stands for grid-point ($j + 1/2$ is a mean value) and the lower for the i-th variable (out of 4). A solution is found, if $A_i^j = 0$.
Similarly, the outer and inner boundary conditions are cast into equations

$$B_i = 0 \quad i = 1, 2 \tag{1.89}$$

and

$$C_i = 0 \quad i = 1, \ldots, 4 \tag{1.90}$$

where the inner one are to be taken at grid-point $N - 1$ and the expansions around $m = 0$ have been used already.

A simple counting reveals that we have $2 + 4 + (N-2) \cdot 4 = 4N - 2$ equations and 4 unknowns at N grid-points -2 at the outer boundary, which again is $4N - 2$. A solution is therefore well-determined. The solution is found via the ordinary Newton-approach:

$$A_i^j + \sum_i \frac{\partial A_i^j}{\partial y_i} \delta y_i = 0 \tag{1.91}$$

which gives the corrections δy_i to the previous variable values. This can be expressed as a matrix equation:

$$H \begin{pmatrix} \delta y_1^1 \\ \delta y_2^1 \\ \vdots \\ \delta y_3^N \\ \delta y_4^N \end{pmatrix} = \begin{pmatrix} B_1 \\ \vdots \\ A_i^j \\ \vdots \\ C_4 \end{pmatrix} \tag{1.92}$$

The matrix H contains all the derivatives and is called Henyey-matrix. It contains non-vanishing elements only in blocks. This leads to a particular method of solving it (Henyey-method).

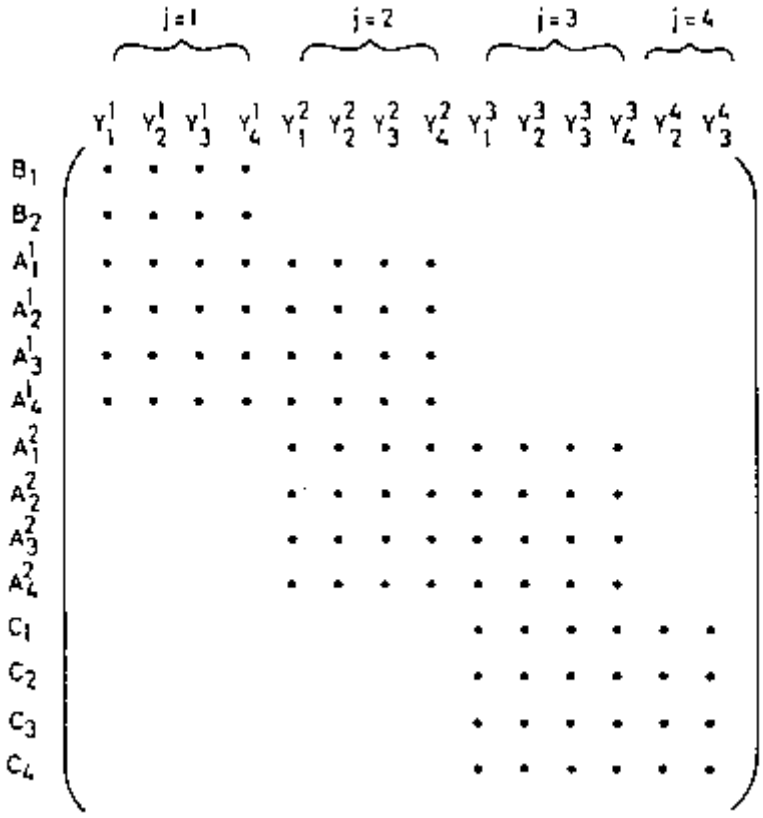

The Henyey-matrix for a $N = 4$ resolution indicating the non-vanishing elements. (from KW)

The henyey-method expresses some of the corrections to be calculated in terms of others, e.g.

$$\delta y_1^1 = U_1 \delta y_3^2 + V_1 \delta y_4^2 + W_1 \tag{1.93}$$

This leads to matrix equations for the U_i, V_i, W_i, which can be solved for and the coefficients be stored. Consider the first block-matrix:

$$\begin{bmatrix} \frac{\partial B_1}{\partial y_1^1} & \frac{\partial B_1}{\partial y_2^1} & \cdots & 0 \\ \frac{\partial B_2}{\partial y_1^1} & \frac{\partial B_2}{\partial y_2^1} & \cdots & 0 \\ \frac{\partial A_1^1}{\partial y_1^1} & \frac{\partial A_1^1}{\partial y_2^1} & \cdots & \frac{\partial A_1^1}{\partial y_2^2} \\ \vdots & \vdots & \vdots & \vdots \\ \frac{\partial A_1^4}{\partial y_1^1} & \frac{\partial A_1^4}{\partial y_2^1} & \cdots & \frac{\partial A_1^4}{\partial y_2^2} \end{bmatrix} \begin{bmatrix} U_1 & V_1 & W_1 \\ U_2 & V_2 & W_2 \\ U_3 & V_3 & W_3 \\ \vdots & \vdots & \vdots \\ U_6 & V_6 & W_6 \end{bmatrix} = \begin{bmatrix} 0 & 0 & -B_1 \\ 0 & 0 & -B_2 \\ -\frac{\partial A_1^1}{\partial y_3^2} & -\frac{\partial A_1^1}{\partial y_4^2} & -A_1^1 \\ \vdots & \vdots & \vdots \\ -\frac{\partial A_4^1}{\partial y_3^2} & -\frac{\partial A_4^1}{\partial y_4^2} & -A_4^1 \end{bmatrix} \tag{1.94}$$

In the next block, again y_1^2 and y_2^2 are replace as before, and the other variables are expressed in terms of y_3^3 and y_4^3. This reduces the block of four equations in 8 unknowns into one of 4 unknowns only. This is repeated until the last block, which consists of 4 equations for 6 unknowns, of which two can be expressed by the previous coefficients. This block can then be solved for the unknown corrections $\delta y_1^N, \ldots, \delta y_4^N$. Once they are known, the coefficient equations of the previous block allow to calculate the corrections of the previous block, and so on, until the first one is reached again. This done, the A_i^j can be computed again (with the derivatives) and the next iteration starts.
Note that this method is linear in grid-points, not quadratical as a simple matrix inversion would be!

Once the spatial problem is solved, the integration in time can be done:

$$X_i(t + \triangle t) = X_i(t) + \frac{\partial X_i}{\partial t}(T(t), P(t), \ldots)\triangle t \tag{1.95}$$

The most simple approximation is to keep T constant over $\triangle t$. An improvement is to estimate its run (from previous evolution).

The nuclear network equation is solved by backward differencing:

$$X_i(t + \triangle t) = X_i(t) + \triangle t \sum_i r_{ij}(t) X_i(t + \triangle t) Y_j(t + \triangle t) \tag{1.96}$$

The $X_i(t + \triangle t)$ are written as $X_i(t) + \triangle X_i$ and in the product the resulting term $\triangle X_i \triangle X_j$ is neglected (linearization). This leads to a linear system in the $\triangle X_i$. Since we have linearized the equations, we have to ensure that the X_i do not change too rapidly. Therefore, the $\triangle t$ between two consecutive stellar models (of order 10^6 yrs) is subdivided into smaller timesteps for the network integration. A similar method is possible for diffusion equations as well.

1.4.2 Polytropes

Polytropes have been used widely in the pioneer days of stellar evolution theory and are still of conceptual interest to understand the numerical results. We briefly review the concept, which, for one and all times, has been discussed in Chandrasekhar's book "An introduction to the study of stellar structure" (Dover 1958; Chicago 1939).
The idea is that the EOS sometimes takes the form $P \propto \rho^\gamma$ (e.g. degenerate gas). One imagines stars for which the EOS *and* the actual run of P is of this form; these are polytropes:

$$P(r) = K\rho^{1+1/n}(r) \tag{1.97}$$

n: polytropic index. This equation can also be written as

$$P(r) = P_c\theta^{(1+n)} \tag{1.98}$$

$$\rho(r) = \rho_c\theta^n \tag{1.99}$$

From the hydrostatic equation and Poisson's equation, one can derive

$$\frac{(n+1)P_c}{4\pi G\rho_c}\frac{1}{r^2}\frac{\mathrm{d}}{\mathrm{d}r}\left(r^2\frac{\mathrm{d}\theta}{\mathrm{d}r}\right) = -\theta^n \tag{1.100}$$

and with the substitution $r = r_n\zeta$, where r_n is the factor in front of the l.h.s., we get

$$\frac{1}{\zeta^2}\frac{\mathrm{d}}{\mathrm{d}\zeta}\left(\zeta^2\frac{\mathrm{d}\theta}{\mathrm{d}\zeta}\right) = -\theta^n \tag{1.101}$$

This is the *Lane-Emden-equation*, which uses only the hydrostatic and the polytropic equation. It is a second order ordinary differential equation easily to be solved numerically. The boundary conditions are: $\theta(\zeta = 0) = 1$ ($\rho = \rho_c$) and $\theta'(0) = 0$ ($\frac{\mathrm{d}P}{\mathrm{d}r} = 0$). The star's surface corresponds to the first root of θ, where $P = T = \rho = 0$, but M and R might be finite.
Analytic solutions exist for $n = 0, 1, 5$. For $n = 5$, the radius becomes infinite.
Interesting cases are $n = 1.5$ corresponding to $P \propto \rho^5/3$ (completely degenerate, non-relativistic gas) and $n = 3$, which is $P \propto \rho^4/3$ (fully relativistic, deg. gas). Adiabatic convection zones are polytropes with $n = 1.5$, isothermal cores have $n = \infty$.
In Schwarzschild's book and the textbooks you will find also discussions of composite polytropes, such with singular b.c.s, and more.

Chapter 2

The Sun – example of a low-mass main-sequence star

Our Sun is a typical low-mass star in the longest-lasting phase of evolution, the so-called main-sequence phase, when the energy production is due to hydrogen fusion in the stellar center. At the same time, due to its proximity, it provides the best information available about stars. Therefore it always has been the standard test case for theory. We use the Sun as an example for illustrating structure and evolution of stars of similar type. The known problems, in particular the classical "Solar Neutrino Problem" will be discussed as well.

Literature:

- Stix M.: The Sun, Springer, 1989 (a textbook containing everything about the Sun, from structure to coronal activity; also included a very concise introduction to stellar structure theory)
- Bahcall J.N., Pinsonneault M.H.: Reviews of Modern Physics, vol. 64, 885 (1992) and vol. 67, 781 (1995); the latest reviews by *the* authority (JNB) on solar models.
- Turch-Chièze S., The Solar Interior, Physics Reports, vol. 230, 57 (1993), a very extendend and detailed review, discussing technical details to a greater extend.

2.1 Facts about the Sun as a star

Solar quantities:

Quantity	value	accuracy	source
distance	$1.4959 \cdot 10^{13}$ cm	10^{-8}	triangulation; radar & laser ranging
mass	$1.959 \cdot 10^{33}$ g	10^{-3}	Kepler's 3$^{\text{rd}}$ law
radius	$6.963 \cdot 10^{11}$ cm	10^{-4}	geometry
expansion	2.4 cm/yr		
surf. gravity	$2.74 \cdot 10^{4}$ cm/s^2		
luminosity	$3.845 \cdot 10^{33}$ erg/s	10^{-4}	solar constant
T_{eff}	5777 K	$\pm$4.5 K	Stefan-Boltzmann law
composition	$Z/X = 0.0245$	$\pm$0.0010	solar photospere; meteorites
rel. metal	$O = 0.49$, $C = 0.30$		
number fractions	$N = 0.05$, $Fe = 0.07$		
H & He abundance	$X = 0.713$ $Y = 0.270$		solar models
age	$4.57 \cdot 10^{9}$ yrs	$\pm 0.03 \cdot 10^{9}$ yrs	meteorites

If put into HRD of nearby stars, the Sun falls right onto the line of the highest number of stars, which is called *main sequence*. From statistical considerations (most stars are where they live longest) and from the timescales discussed in Chapter 1, this should be the phase of hydrogen fusion.

2.2 Interlude on star formation

2.2.1 General considerations

The theory of star formation is a different field than that of stellar evolution, which usually starts with the onset of hydrogen burning. The general picture is that out of a cold molecular cloud, clumps begin to contract, heat up, lose their energy and contract further. The virial theorem already tells us that they get hotter nevertheless. During the contraction phase the energy lost is taken from contraction only (ϵ_g), but at some point T is high enough for nuclear reactions setting in, and finally hydrogen begins to fuse to helium. Since T is always highest in the core, this phase is that of *core hydrogen burning*, when $\epsilon_g \approx 0$, i.e. all energy is taken from nuclear reactions.
Below a critical mass – $M \approx 0.08\,M_\odot$ – the star is never able to get L from nuclear reactions, but continues to contract forever. (L is so low – $10^{-4}\,L_\odot$ – that the gravothermal energy is sufficient.) Such stars are called brown dwarfs. At the lower mass end of those the giant planets follow.
While the details of star formation are a subject of active research, after a certain point, stellar structure theory can begin to treat the approach to the main sequence. This is, when the star can be identified as a separate body, contracting on a thermal timescale. In this case, all structure equations are valid. This is called the *pre main sequence phase*.

2.2.2 Pre-main sequence evolution

The energy equation is

$$\frac{\partial L_r}{\partial m} = -T\frac{\partial S}{\partial t};$$

The whole configuration is very cool: $T_c \approx 10^5$ K and $T(R) \approx 3000$ K. The star is very luminous – $\lg L/L_\odot \approx 3$ – and the opacities very high.
$\Rightarrow$ the pre-main sequence star is completely convective, therefore homogeneous in composition and is contracting along the so-called *Hayashi-line* which is an almost vertical line in the HRD and describes, where solutions for completely convective stars are possible.

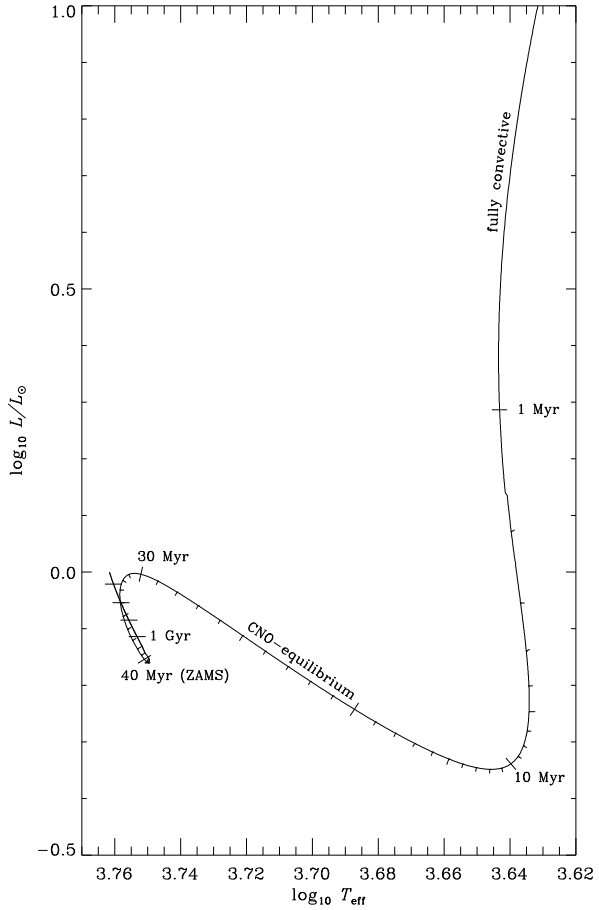

The evolution of the Sun (courtesy H. Schlattl, MPA)

During the contraction, the central temperature rises and subsequently nuclear reactions set in:

- after $< 10^6$ yrs, $T_c \approx 6 \cdot 10^5$ K, and *deuterium* from the Big Bang is converted into ^{3}He by proton capture. Since the star is fully convective, all D is converted.
- after $\approx 10^7$ yrs, $T_c \approx 8 \cdot 10^6$ K, and *CN-equilibrium* can be achieved; formally, the CNO-cycle is operating, but its cycle-time is so long that it does not produce relevant energies. The initial $C \rightarrow N$ conversion, however, is able to make the core convective again, which became radiative earlier due to decreasing opacities.
- after $\approx 3 \cdot 10^7$ yrs, the *pp-chain* begins to operate. The additional energy leads to a decrease in L during which the pp-nuclei assume their equilibrium abundances (esp. ^{3}He).
- after $\approx 4 \cdot 10^7$ yrs, $\epsilon_g \approx 0$ and L is due to ϵ_n only. The star has reached the *zero-age main sequence* (ZAMS). Note that at that time the star is no longer strictly homogeneous, because nuclear reactions have taken place and the star is radiative almost everywhere (except for the outermost layers). The central X is about 10^{-3} smaller than at the surface.

The structure of the ZAMS-Sun is shown in the next figure:

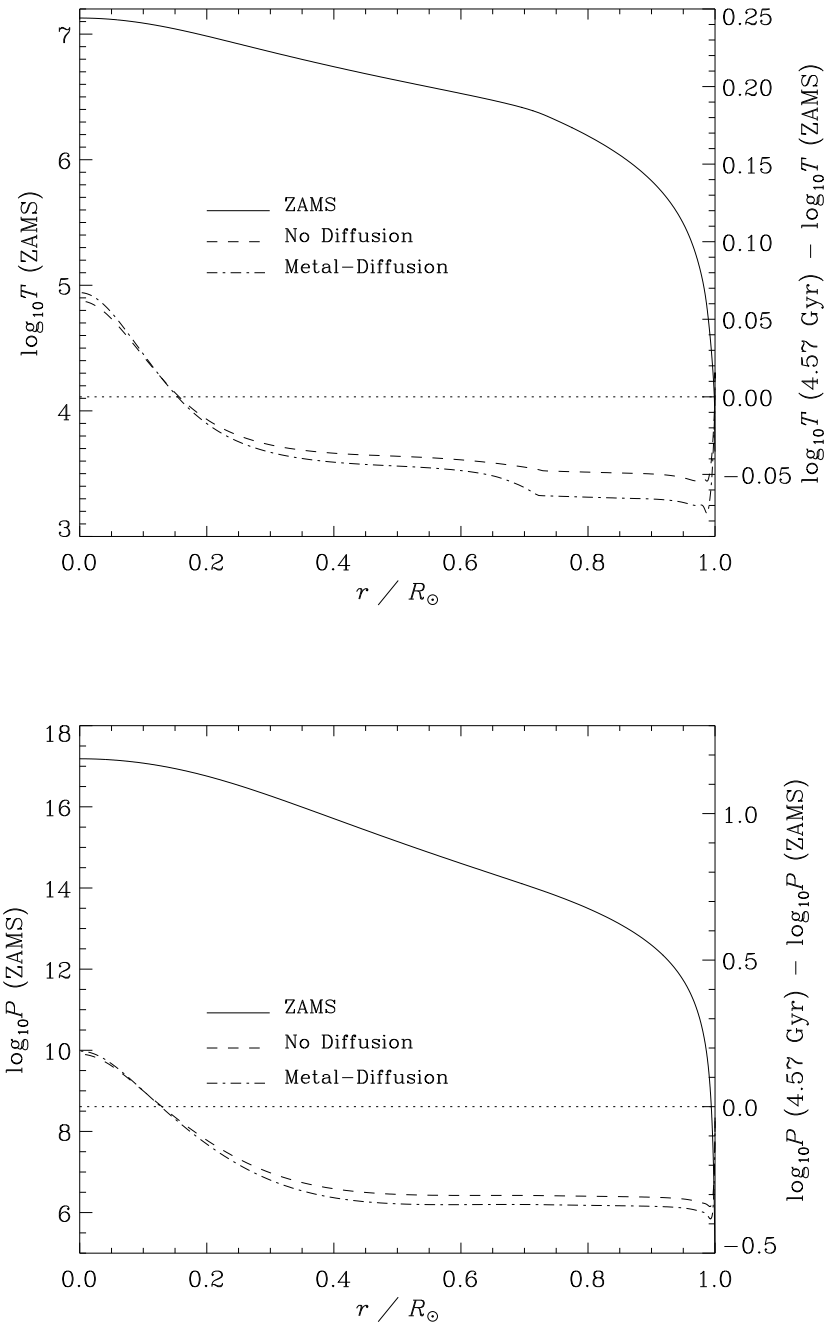

The structure of the Sun when on the ZAMS ($t = 0$) and the changes in the course of the evolution: T and P. (courtesy H. Schlattl, MPA)

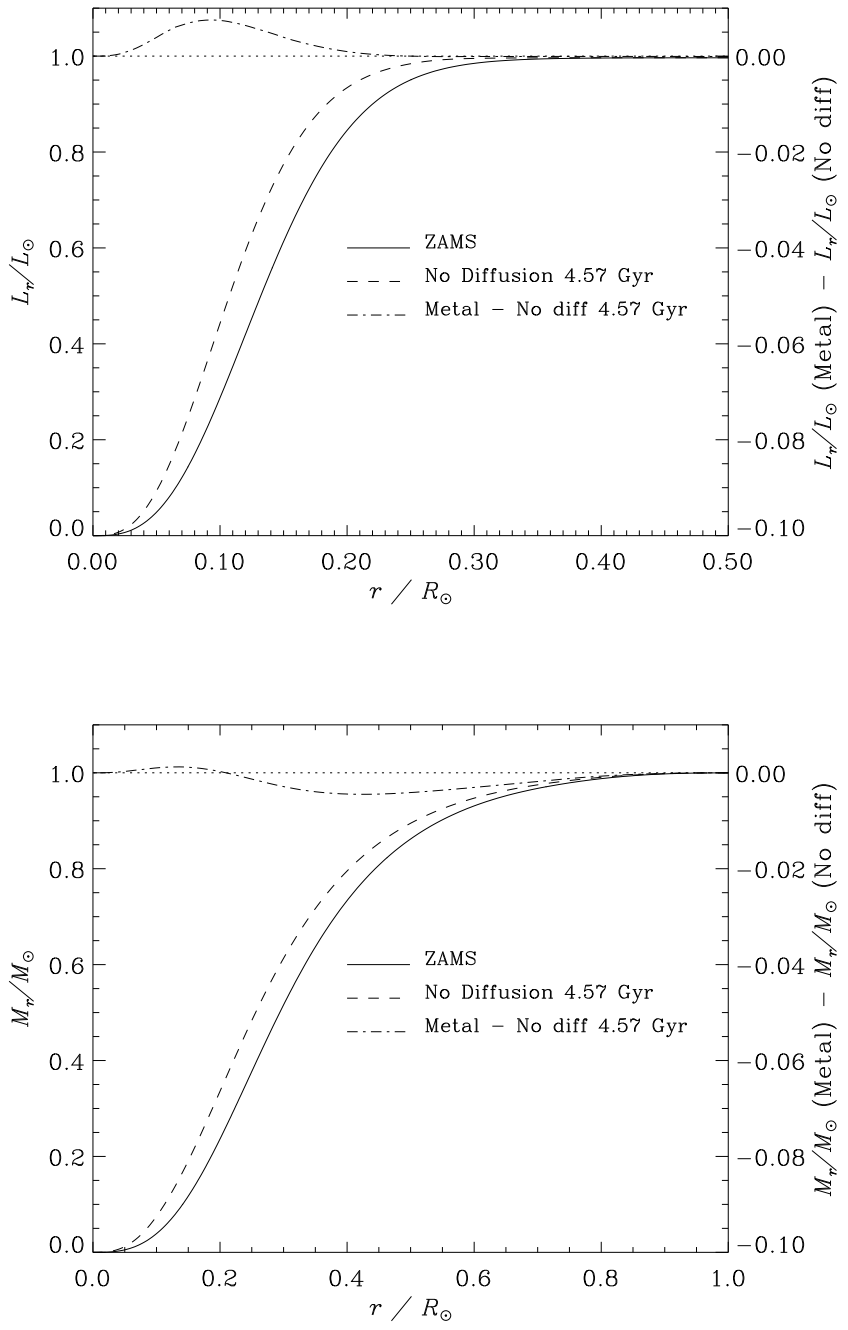

The structure of the Sun when on the ZAMS ($t = 0$) and the changes in the course of the evolution: L_r and m (courtesy H. Schlattl, MPA)

The calculation can also be started on the ZAMS, assuming $\epsilon_g = 0$ and homogeneous composition. This is a rather good approach, and technically much easier, because all ∂t-terms vanish. If the energy generation is calculated from equilibrium formulae, the composition will change only for hydrogen and helium. If a nuclear network is used, the participating isotopes will assume their equilibrium abundances. This leads to an unphysical, but short-lived adjustment phase (and a small loop in the HRD).

2.3 Evolution on the main-sequence

The Sun, up to its present age, has evolved about half-way through the main-sequence phase (see HRD-figure). In the course of this evolution, the luminosity has risen from $L = 0.68 L_\odot$ and $T_{\rm eff}$ from 5600 K. Central temperature and pressure have increased by 7% and 30%. Energy generation and relative mass got more concentrated towards the center. The hydrogen abundance has decreased, where energy is produced. In the center it has gone from $X_0 = 0.715$ to $X_c(t_\odot) = 0.36$. The energy produced in the center is to 98% from the pp-chain; the CNO-cycle contributes less than 2%.

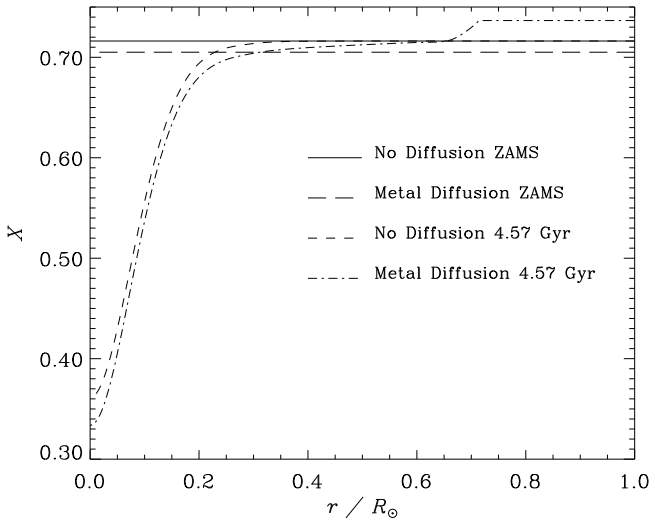

The hdyrogen abundance in the present Sun (courtesy H. Schlattl, MPA)

The temperature gradients in the outermost layers are shown in the next figure:

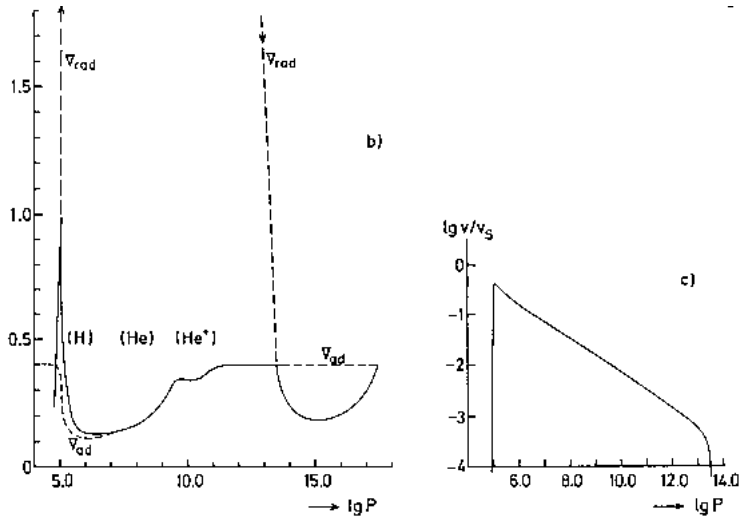

The temperature gradients in the solar envelope as a function of P. The depression of $\nabla_{\rm ad}$ in the ionization zones and the corresponding rise of $\nabla_{\rm rad}$ leads to convection (from KW)

2.3.1 The solar neutrino problem

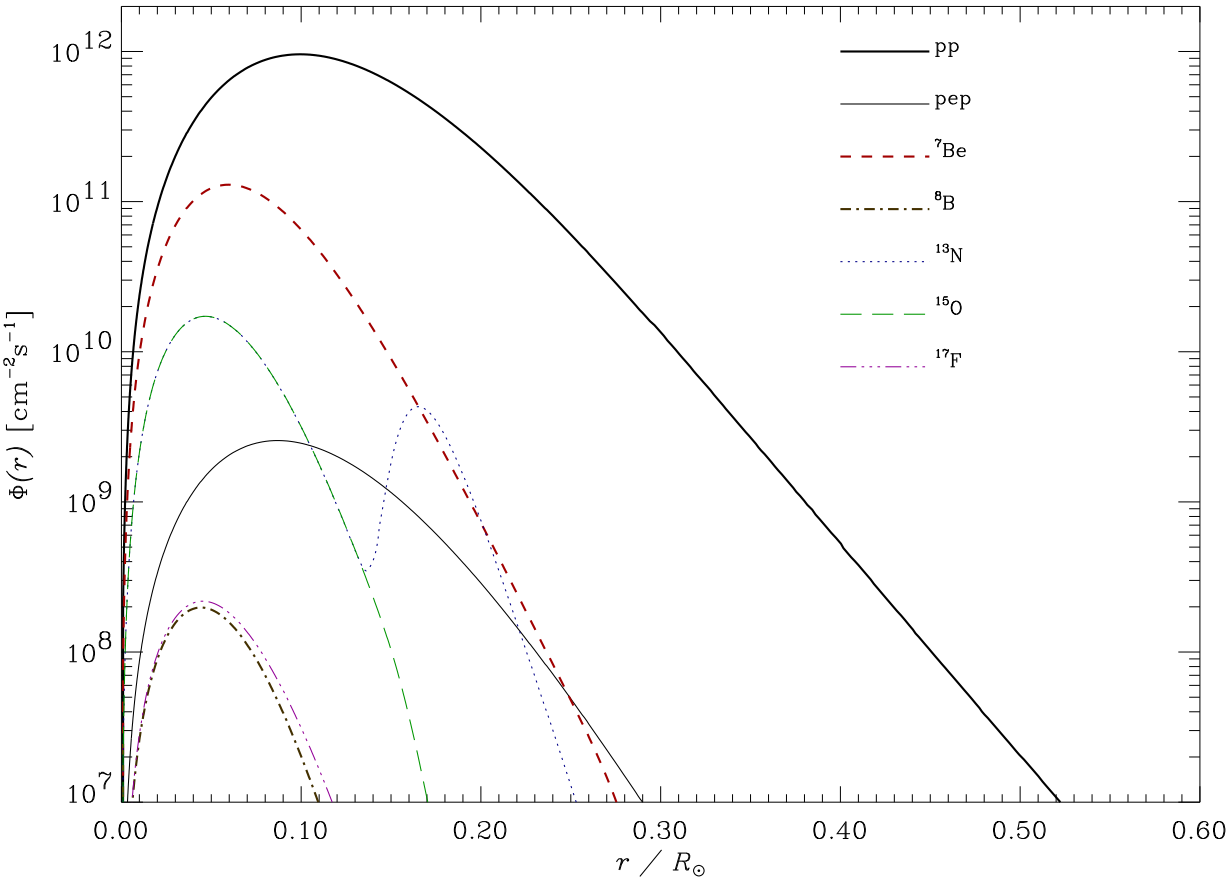

The neutrino flux as produced within the solar core as a function of relative radius (courtesy H. Schlattl, MPA)

The neutrinos produced in the nuclear reactions leave the Sun unimpeded and reach Earth (through which they pass as well – most of them). Inspite of their extremely low cross-sections they are numerous enough that some of them can be captured in experiments. The counts in these experiments are clearly lower than the predictions of the theory (by a factor of 2). This constitutes the *Solar Neutrino Problem*. However, the experiments have proven that the flux is of the order as predicted and Kamiokande, which is direction sensitive (scattering experiment), has shown that the measured neutrinos come from the Sun. This is the final proof that the sun burns hydrogen to helium!

Detector	type	reaction	threshold (MeV)	ν from:
Homestake	liquid target	$\nu_e + {}^{37}Cl \rightarrow {}^{37}Ar + e^-$	0.8	^{7}Be & ^{8}B
(Super-)Kamiokande	Cerenkov	$\nu_e + e^- \rightarrow \nu_e + e^-$	7.5 (5.0)	^{8}B
GALLEX & Sage	radiochemical	$\nu_e + {}^{71}Ga \rightarrow {}^{71}Ge + e^-$	0.23	pp, ^{7}Be & ^{8}B

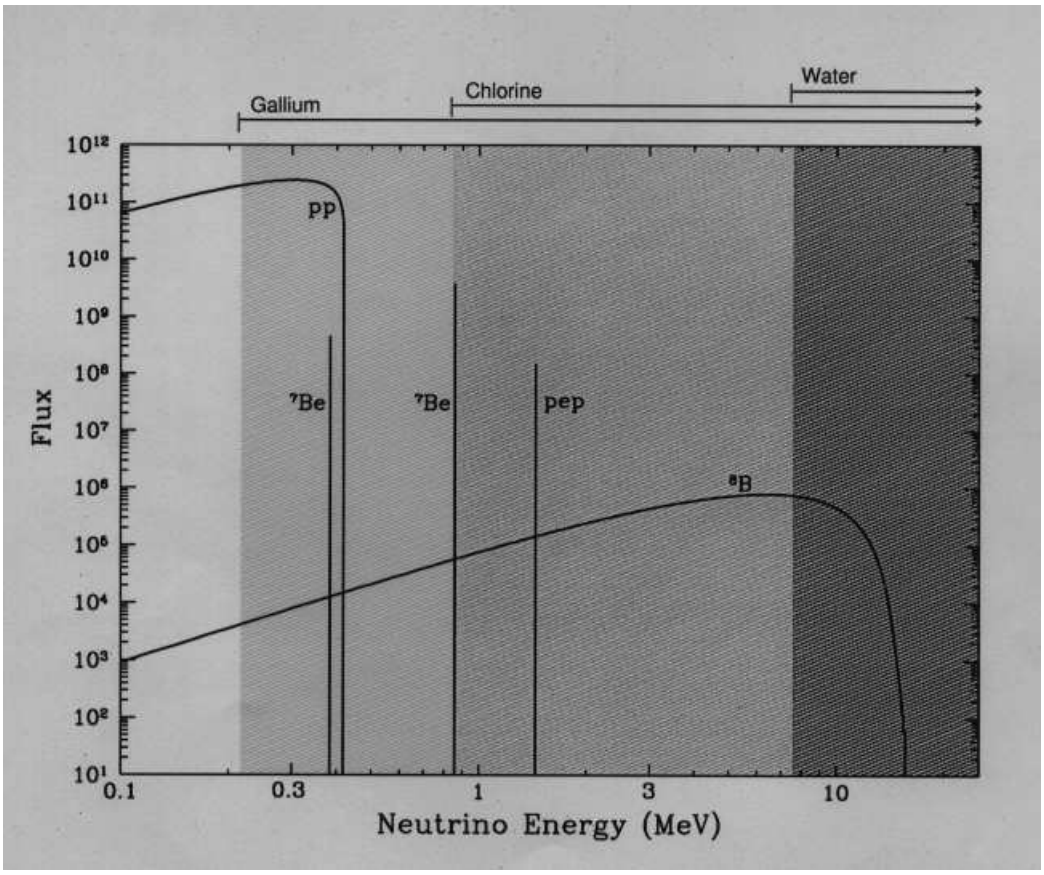

The solar ν-spectrum (pp-chain only) and the detector ranges (J. Bahcall)

This figure shows the predicted ν-spectrum. The next one shows the experimental results, compared to the predictions. (1 SNU = 10^{-36} events/target atom and second)

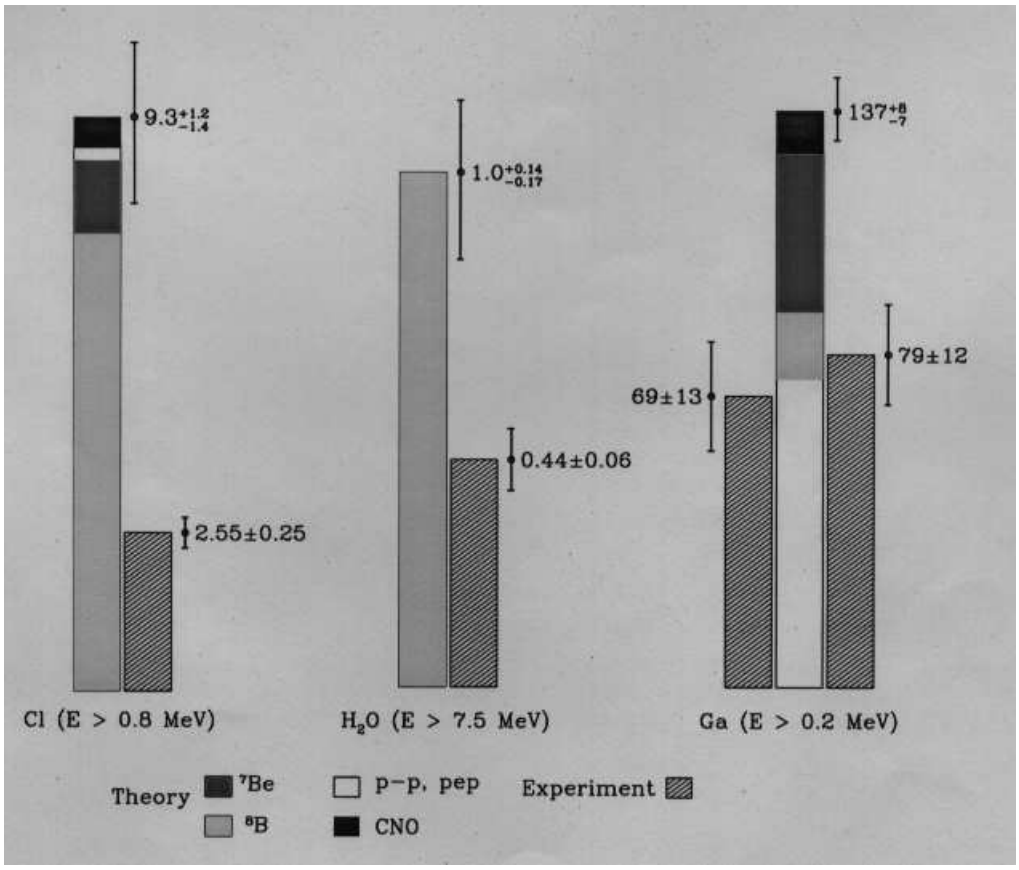

The solar ν-experiment results (J. Bahcall)

What is the solution for this problem? It can be excluded that the experiments are wrong (different types; calibration of GALLEX,...).

Astrophysical solutions: the easiest explanation would have been that T_c is lower (by $\approx 5\%$) than predicted. However, such a solution is not consistent with the experiments any longer. Their collective analysis shows that most likely the $^7Be - \nu$s are missing primarily.

Nuclear explanations: Given the experiments, it could be that the pp-branching is calculated wrongly, due to unknown features in the reaction rates (resonances). While this does not solve the problem completely, recent experiments have confirmed the rates as used in energy regions previously not measured.

Particle physics explanations: This is the most likely answer to the problem. Most extensions of the standard model of particle physics allow or predict the conversion of neutrinos either into other flavours or sterile right-handed νs. Such neutrinos are not measurable in the present experiments. The standard explanation now is the MSW (Mikeyev, Smirnov, Wolfenstein) effect, which describes the resonant conversion of ν_e into ν_μ in the present of matter. For a specific parameter range (mass difference and mixing angle) the experiments can be explained completely.

2.3.2 Solar Models

A *solar model* is in fact the final model of a whole sequence of stellar models starting at time $t = 0$ (pre-ms or ZAMS) and calculated until $t = t_\odot$. In the model sequence, certain parameters are free to choose, e.g. $\alpha_{\rm MLT}$, Y_i. The final model will, most likely deviate from the Sun in terms of observed quantities like $L_\odot$ and $R_\odot$. The initial parameters have to be changed accordingly, until finally the Sun is reproduced by the model.
In the simplest case, $\alpha_{\rm MLT}$ and Y_i are the free parameters and $L_\odot$ and $R_\odot$ the quantities to be matched (M, X/Z and age are fixed).
The dependencies are as follows (they depend on the particular solar model calculation):

$$\begin{aligned} \frac{\partial \lg L}{\partial \alpha_{\rm MLT}} &= 0.02 \\ \frac{\partial \lg L}{\partial Y_i} &= 6.24 \\ \frac{\partial \lg T_{\rm eff}}{\partial \alpha_{\rm MLT}} &= 0.017 \\ \frac{\partial \lg T_{\rm eff}}{\partial Y_i} &= 0.26 \end{aligned} \tag{2.1}$$

and demonstrate that to first approximation, L depends on Y_i, and $T_{\rm eff}$ on $\alpha_{\rm MLT}$.
Due to the high accuracy of all observations concerning the Sun, the stellar evolution codes and the physics included have to be of highest quality. In fact, solar models have always been the testing ground for stellar evolution theory and triggered many improvements, e.g. accurate opacities (OPAL & Opacity Project) and EOS.
In the last years, it has become evident that diffusion has to be included in the solar models as well. This implies that $Y_\odot \neq Y_i$ and $Z_\odot \neq Z_i$ (if metal diffusion is included as well). Therefore, the correct Z_i has to be iterated as well.
The effect of diffusion on the composition is such that $Y_i \approx 0.27$, but the present $Y_\odot$ (abundance at surface and convective envelope) has been reduced to ≈ 0.25. Also, the structure changes slightly (and the neutrino problem becomes even more serious). The figures showing the structure evolution of the Sun demonstrate the influence of diffusion.

2.3.3 Helioseismology

This will be treated in a separate lecture. Suffices to say here that the Sun is ringing like a bell in many non-radial modes with periods around 5 min. From these the structure can be infered. The results are in excellent agreement with the theoretical models.
In particular, we learned that the depth of the convective zone is $R_{cz} = 0.713 R_\odot$, the helium content in it is $Y_\odot = 0.245$, the run of sound speed, and the importance of diffusion.
The results also rule out many non-standard solar models invented to solve the neutrino problem (such as low-Z at center, WIMPS, etc.)

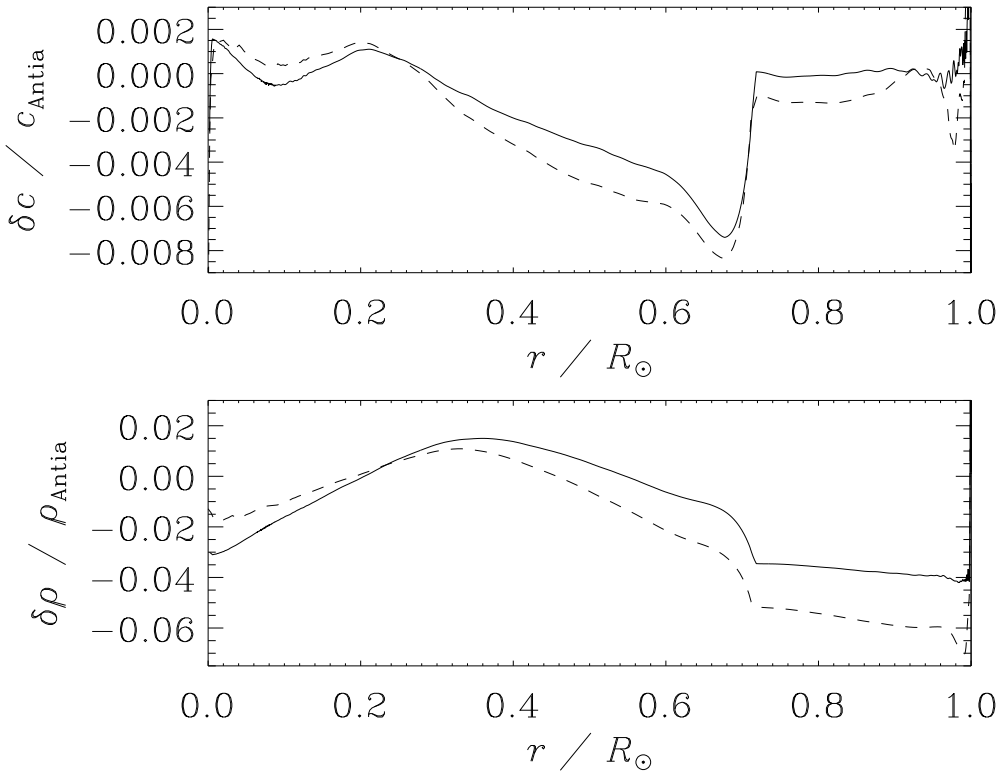

The agreement between solar models (Schlattl, Weiss & Ludwig, 1997) and observationally infered sound speed and density.

2.4 Other stars on the main sequence

2.4.1 ZAMS

$L \propto M^3\mu^4$ and $R \propto \mu^{\frac{\nu-4}{\nu+3}} M^{\frac{\nu-1}{\nu+3}}$ (from homology).
For the pp-chain (for $M \leq 1.5M_\odot$),

$$R \propto \mu^{0.15} M^{0.5},$$

while for the CNO-cycle

$$R \propto \mu^{0.6} M^{0.8};$$

a mean value (keeping composition constant) would be

$$R \propto M^{0.75}.$$

With $L \propto R^2 T_{\rm eff}^4$ it follows that

$$\lg L = 8 \lg T_{\rm eff} + \text{const.}$$

for the ZAMS, and the lines of constant R in the HRD are

$$\lg L = 4 \lg T_{\rm eff} + \text{const.}$$

The (zero-age) main sequence is the place of stars in core hydrogen burning with mass being the parameter along it. Radius increases with mass.
For the central values, one finds:

$$T_c \propto M^{\frac{4}{\nu+3}} \quad P_c \propto M^{\frac{-2(\nu-5)}{\nu+3}} \quad \rho_c \propto M^{\frac{-2(\nu-3)}{\nu+3}} \quad T_c \propto \rho_c^{\frac{-2}{\nu-3}}$$

Central temperature increases, but density decreases with mass!

2.4.2 Evolution on the main sequence

- low-mass stars evolve as Sun
- $M > 1.2M_\odot$: develop small convective core, but have no convective envelope; CNO-cycle becomes important
- the MS-lifetime decreases
- $M < 0.4M_\odot$: completely convective stars
- at the lowest M non-ideal effects in EOS very important (pressure ionzization, ...)

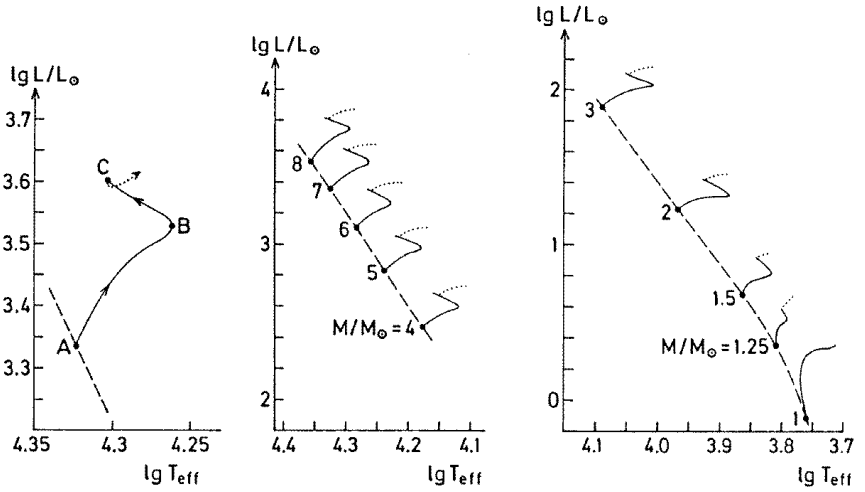

Theoretical HRDs with main-sequence evolutionary paths for stars of composition similar to the Sun. (from KW)

Chapter 3

Low-mass star evolution: Globular clusters

The lecture will demonstrate, how we learned to understand complex stellar systems. Globular Clusters are systems of many thousands of stars that have the same age and composition. They provide a snapshot of a population of stars, with mass being the quantity dictating the differences. In the turn of the discussion of the various evolutionary stages, the general run of stellar evolution can be illustrated easily. One of the most important applications of Globular Clusters is the determination of their age, which appears to be close to that of the universe. Methods and results will be reviewed. Globular Clusters in many respects connect stellar evolution with cosmology and particle physics. This will be included in the lecture.

Literature:

- Renzini A., Fusi Pecci F.: Annual Review of Astronomy and Astrophysics, vol. 26, 199 (1988); a classical review discussing the importance of globular cluster diagrams;
- Iben I., Renzini A.: Physics Reports, vol. 6, 329 (1984); a review discussing some of the classical stellar evolution problems; suited for those who want to look for unsolved questions
- Stetson P.B., VandenBerg D.A., Bolte M.: Publications of the Astronomical Society of the Pacific, 108, 560 (1996); a very recent review discussing methods of cluster age determinations; not including the latest development
- Degl'Innocenti S., Salaris, M., Weiss, A.: Astrophys. Journal 479, 665 (1997); our own paper deriving new and lower ages for the oldest cluster; supplemented by Salaris & Weiss, preprint astro-ph 9704238 inspecting 25 halo clusters

Note that all principal features of stellar evolution can of course be found in the two textbooks as well.

3.1 Facts about globular clusters

3.1.1 General facts

Globular clusters (GCs) are groups of $10^4 \cdots 10^5$ stars bound together by their mutual gravitation. The clusters live mostly in isolation from other stars. They are found in a spherical halo around the galaxies, but also close to the disk and the bulge of our own Mily-Way. They move on orbits passing through the disk. Thereby clusters can be perturbed and even destroyed by tidal forces. Only the tightest bound clusters have survived over the evolution of the Galaxy. Today, the number is about 150. Other galaxies have similar numbers, but examples with many more clusters are known as well.
Most of the clusters, in particular those in the halo, have low metallicities of $Z \approx 2 \cdot 10^{-4} \cdots 10^{-3}$. [1]
From CMDs and also spectroscopic observations it appears that all stars within one cluster have almost exactly the same $[Fe/H]$. In particular this can be infered from the narrowness of the so-called Red Giant Branch (RGB).
From the same argument the suspicion arises that they also have the same age, and the structure arises just from the different initial mass. The CMD-features are common to all clusters, but they are expressed to different extends.

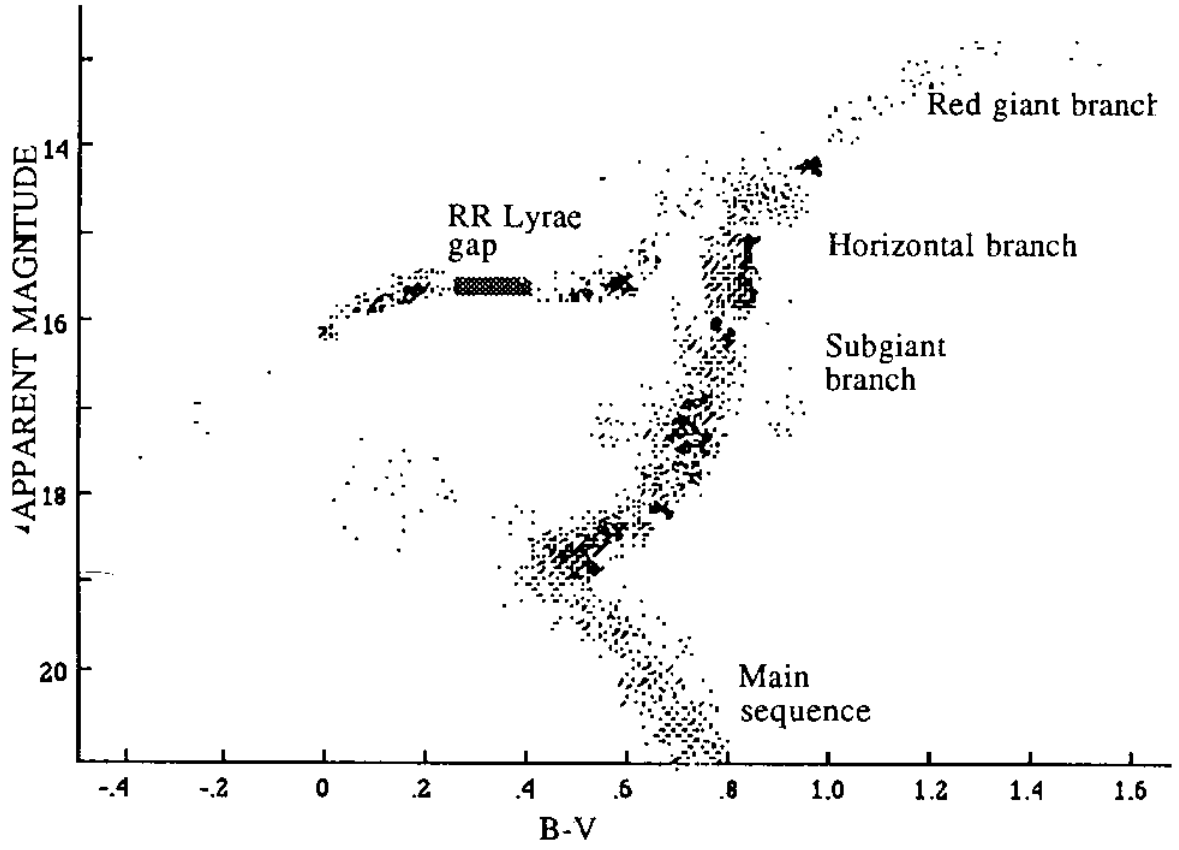

The CMD of M3 with the different branches indicated (from dLD)

[1] Obervers express this by $[Fe/H] := \log(Fe/H)_{\rm GC} - \log(Fe/H)_{\odot}$; this is $-2 \cdots -0.5$ for clusters

3.1.2 The physical meaning of the CMD-features

- MS (main sequence) — core hydrogen burning
- SGB (sub-giant branch) — transition to shell burning
- RGB (red giant branch) — shell burning; deep convective envelope; degenerate helium core
- He-flash — ignition of helium under degenerate conditions; termination of RGB
- HB (horizontal branch) — core helium burning (non-degenerate) plus hydrogen-shell; L depends on core mass, and $T_{\rm eff}$ on envelope mass; star distribution unexplained!
- AGB (Asymptotic Giant Branch) — double-shell burning

3.2 Evolution of globular cluster stars

After the core hydrogen burning phase ends, the maximum of the energy production establishes where X is still high and T is highest, which is somewhere within the formerly "slightly" burning core. The shell uses up its own fuel and therefore has to move out on a nuclear timescale. The helium core (isothermal, because $\epsilon_n = 0$) contracts and stays at the burning temperature of the shell. Its degeneracy increases and due to the high density, neutrino emission becomes more and more important, until the cooling by neutrinos is high enough to invert the temperature! The T-maximum is inside the core, but not at the center!
The envelope keeps expanding right after the MS. It also becomes cooler until it is convective. Why stars evolve to Red Giants is an open question and not understood. With the envelope being convective, the expansion cannot take place by lowering T (Hayashi-line!), but by increasing L. This is the ascent on the RGB. During this, the convective envelope gets ever deeper, until regions are reached that had experienced some nuclear burning on the MS. The ashes are mixed to the surface, where Y, and CNO-abundances change (this is observed!). This phase is called the *first dredge-up*. After that the approaching shell is pushing the convective envelope back. At the deepest penetration point a discontinuity in X is left behind. When the shell passes through this, ϵ_n increases suddenly, leading to a vertical loop in the HRD. Star counts confirm this *Thomas-peak*.

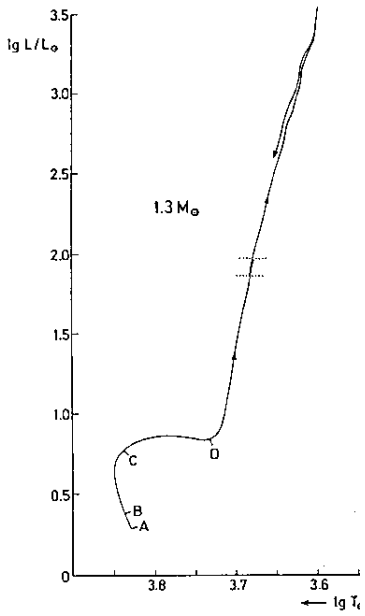

Evolution of a low-mass star in the HRD (from KW; originally Thomas, 1967)

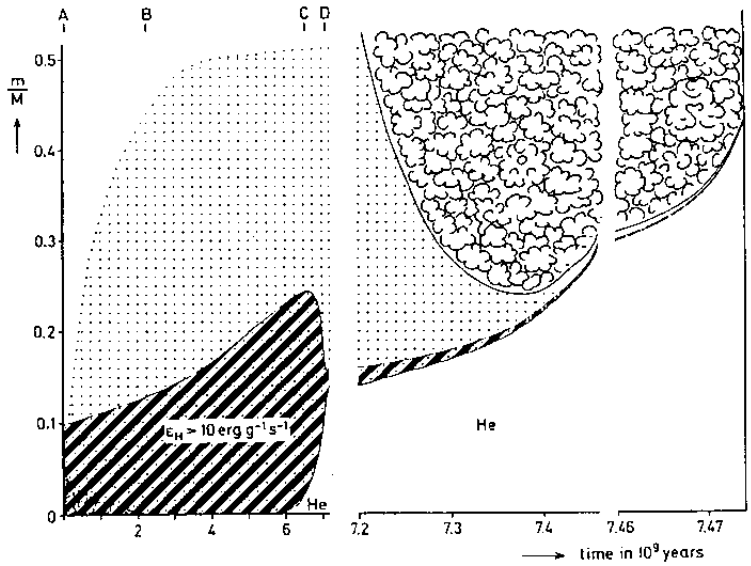

Interior evolution of the $1.3M_\odot$ star (from KW; originally Thomas, 1967)

For the RGB stars, analytical (homology) models are possible, which show that $L \propto M_c^7$, i.e. they predict a core-mass–luminosity relation, which is confirmed by the theoretical models computed. A typical RG has $L = 1000L_\odot$, $T_{\rm eff} = 3500$ K, $R = 100R_\odot$ and $g = 10^{-4}g_\odot$.
At some point, the maximum temperature is sufficient for the ignition of helium. Nuclear energy generation under degenerate conditions is unstable, as can be shown analytically (see Kippenhahn & Weigert). The reasoning is that for degenerate matter $P = P(\rho)$ and does not depend on T. Energy liberated by nuclear reactions is therefore put into T, heating the core and therefore ($\nu > 20$) raising ϵ_n even more: a runnaway situation occurs. No expansion occurs, only a smoothing of the Fermi-edge of the electrons, which finally will lead to a reduction of degeneracy. At that point the core expands, $T_{\rm max}$ is at the center and ordinary central He-burning will commence.
For the core-mass at which the ignition happens, the following relation results from calculations:

$$M_c = 0.475 - 0.22(Y_e - 0.25) - 0.010(3 + \lg Z) - 0.025(M - 0.80) + 0.03\mu_{12}$$

(The last term is a postulated neutrino magnetic moment affecting the cooling, which could be shown to be $< 3 \cdot 10^{-12}$.)
The timescale during the ignition gets extremely short (days to seconds!), almost dynamical. The helium luminosity rises to $L_{\rm He} = 10^6 L$ for a few days and $L_{\rm He} = 10^4 L$ for 1000 yrs. The whole event is called *core helium flash.*

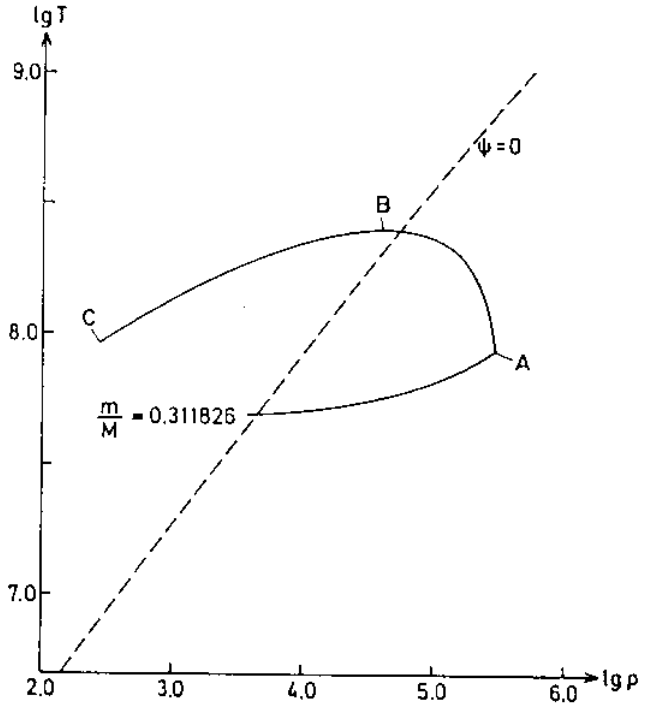

T-evolution during the core helium-flash (from KW)

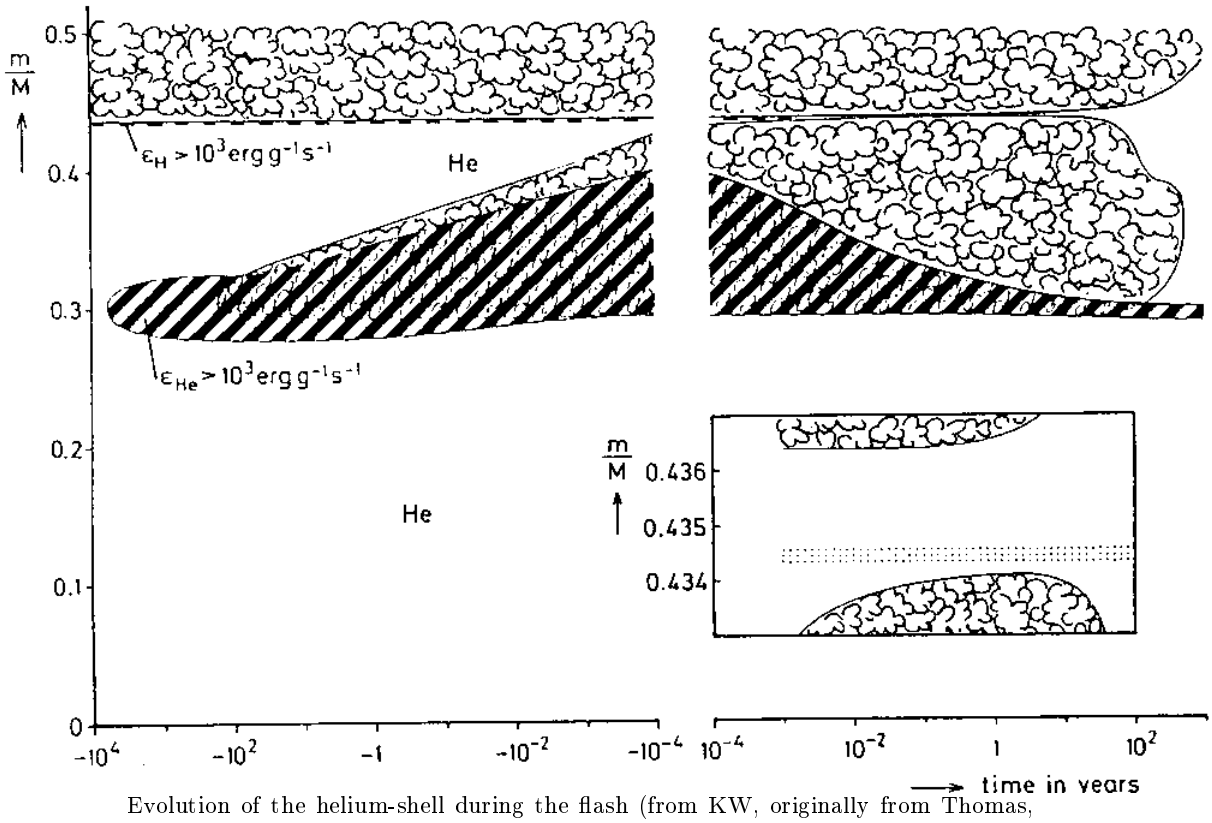

Evolution of the helium-shell during the flash (from KW, originally from Thomas, 1967)

RGB and helium flash can be used to ...

- restrict μ_{12}
- determine distances (if good statistics of stars)
- determine extragalactic distances
- compare clusters differentially

The timescales during the MS and RGB evolution determine the number of stars in each V-bin. This is the so-called luminosity function used to check theory and to determine the initial mass function (IMF).

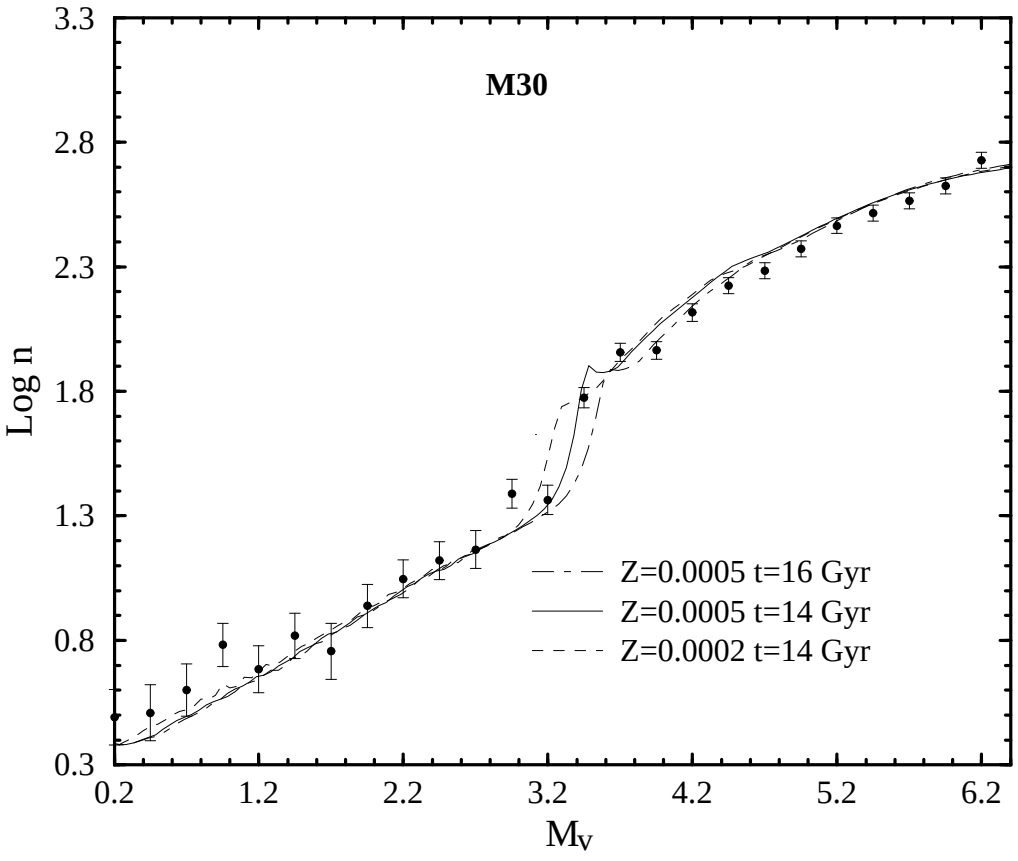

The luminosity function of the cluster M30 and theoretical comparisons (Degl'Innocenti, Weiss & Leone, A&A 319, 487 (1997))

After the flash, the stars settle on the *Horizontal Branch*. Again, L depends on core-mass, but $T_{\rm eff}$ on the total and therefore envelope mass. It is unclear, how the distribution of stars along the HB comes about. Apparantly, stars must lose different amount of mass on the RGB by stellar winds ($0.0 \cdots 0.3 M_\odot$). This constitutes the so-called *second parameter problem*.

3.3 Age determination of globular clusters

We already mentioned that GCs appear to have stars of common age. The CMD can be compared to theoretical *isochrones*: these are lines in a CMD of stars of different mass but same age. (Note that for each mass the evolution up to the RGB has to be calculated!). On the lower main-sequence, the stars appear to be almost ZAMS-models, and only mass varies; on the RGB, the mass is nearly constant, because the evolution is so fast.
The point, where the stars leave the MS, after core hydrogen burning has ceased, is called *turn-off* (TO). It is the bluest (hottest) point on the main-sequence of GC CMDs. The lower MS, the RGB and the HB are almost age-idependent, but the TO is not! Therefore, its position is a good age indicator! By comparison with theoretical isochrones of different age, the one fitting the TO-luminosity will give the cluster age.

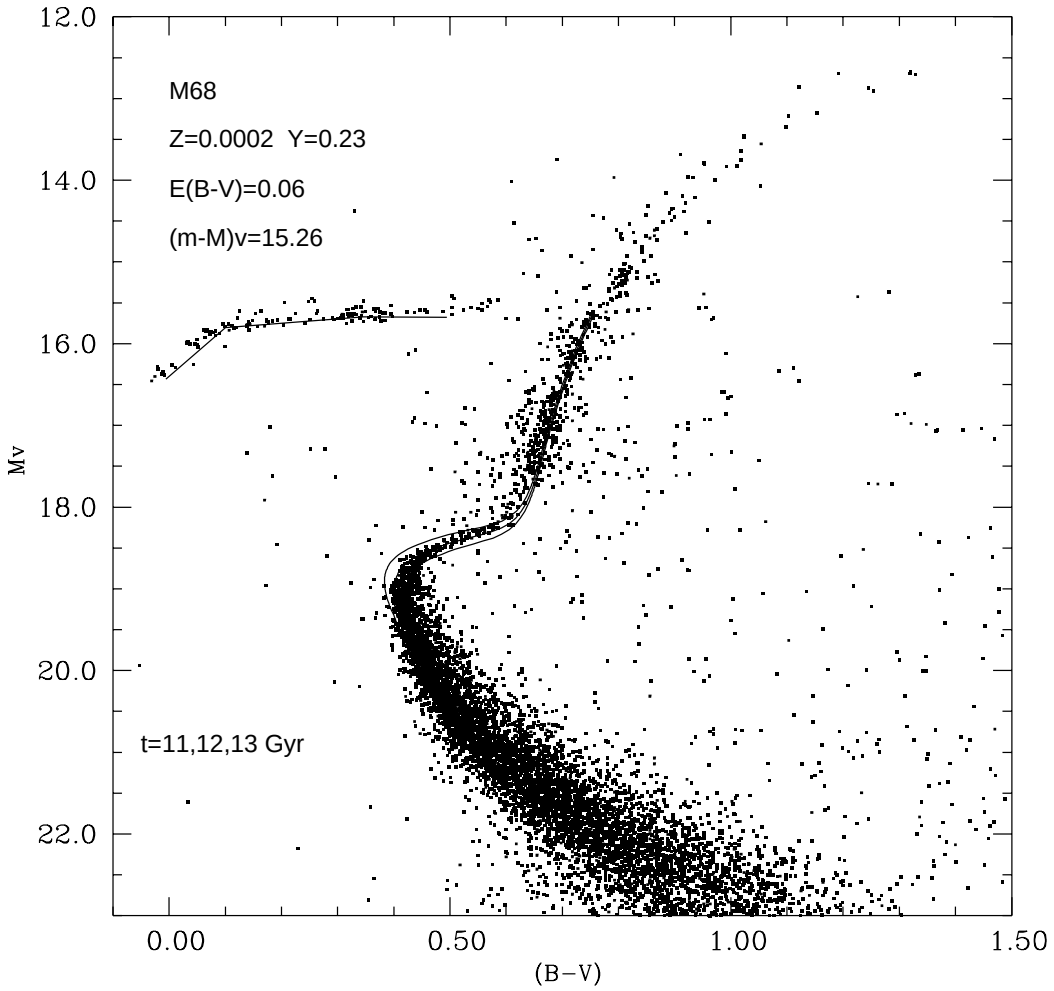

The CMD of M68 and isochrones (Degl'Innocenti, Salaris &Weiss, ApJ 479, 665 (1997))

The result is that clusters indeed can be described by isochrones of a single age and one composition, and that GCs are the oldest objects in the Galaxy. Their age is almost as high as that of the Universe!

Age determinations are not as simple as might appear. The crucial problem is that the distance to the clusters are unknown. Only when this is known, M_V of the TO is known and can be compared to that of the models of different age. How can distances be determined?

3.3.1 Distance indicators

1. Some stars on the HB are pulsating with periods of hours (RR Lyr stars). It is known that their mean brightness depends almost on metallicity alone. If $[Fe/H]$ is known, the absolute brightness of them is known, and therefore, by the distance modulus, the distance to the HB and GC. The problem is that determined $M_V - [Fe/H]$-relations differ so much that the age derived from them differs by several billion years (Gyr). Also, not all clusters have RR Lyr stars.

2. Some nearby stars are hardly evolved lower MS stars (subdwarfs). Their distances are known from parallaxes (recently HIPPARCOS has greatly improved this). Therefore, their luminosity can be determined. The colours (temperatures) are know as well. By determining the distance modulus between such stars and stars of same $T_{\rm eff}$ on the cluster MS, the distance is known again. The problems here lie in the parallax errors, the different metallicities and the photometric errors on the lower MS of clusters.

3.3.2 Distance independent methods

Since RGB and HB are almost age-independent, the brightness difference between HB and TO and/or the colour difference between RGB and TO are age-dependent and can be used for age determinations. This is what Salaris & Weiss (1997) have done for a large sample of clusters. The first method (called the *vertical* one) is independent of errors concerning the colour (temperature) of the TO. It needs a well-developed HB, however. It can be used to determine absolute ages. The second method (the *horizontal*), if used for absolute ages, depends on the mixing-length parameter and the conversion from $T_{\rm eff}$ to $(B-V)$. The uncertainties get small, when clusters of same metallicity are compared to determine their differential age. The combination of both methods gives best results.

In addition, the HB models needed for the vertical method give distances. These can be compared with observations to check the method.

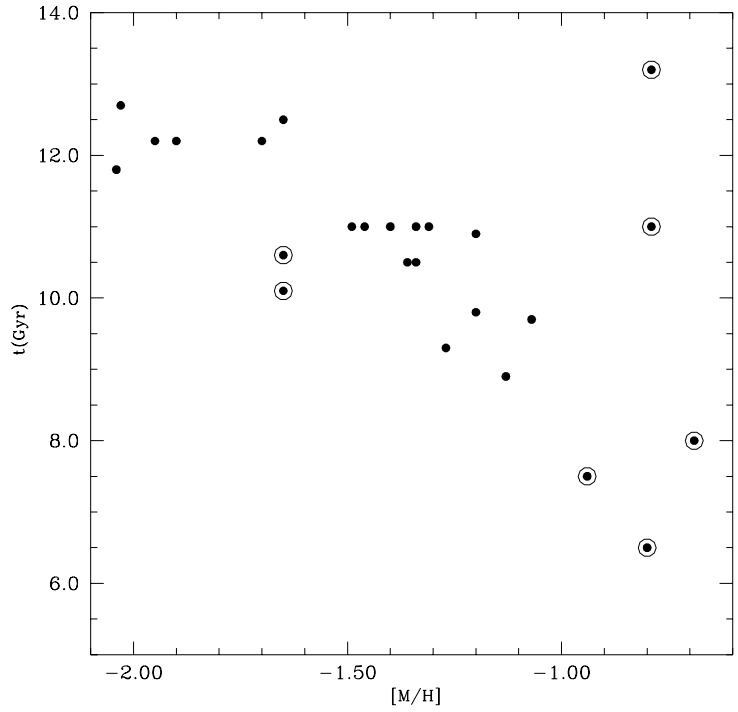

The ages of 25 clusters as a function of metallicity (from Salaris & Weiss, 1997)

Chapter 4

Late evolutionary phases of intermediate-mass stars

Stars of $\approx 3 - 8 M_{\odot}$ develop into phases not accessible to low-mass stars like the Sun. These phases are characterized by thermal instabilities and strong mass loss. Nucleosynthesis of rare elements happens here as well. Some theoretical and observational aspects will be discussed on a very introductory level.

Literature:

- Iben I., Renzini A.: Annual Review of Astronomy and Astrophysics, vol. 21, 271 (1983); the standard review explaining in detail the Asymptotic Giant Branch phase;
- Vassiliadis E., Wood P.R.: Astrophys. Journal 413, 641 (1993); presently one of a few standard articles on evolutionary calculations of AGB stars;
- Weinberger R., Acker A. (eds.): Planetary nebulae, IAU Symp. 155, Kluwer, 1993; proceedings of the largest meeting in the last few years about planetary nebulae and their connectin to late stages of stellar evolution

4.1 General features of the evolution of intermediate-mass stars

As intermediate-mass-stars we consider here stars with $2.5 \leq M/M_\odot < 8$. Their early evolution (main sequence and RGB) differs from that of low-mass stars ($M \leq 1.3M_\odot$). The mass range of $1.3 < M/M_\odot < 2.5$ shares properties from both groups and in the literature is sometimes added to the low-mass range, but sometimes to the intermediate-mass range, depending on point of view. [1]
Intermediate-mass stars have the following properties:

- convective core and radiative envelope on the MS (for $M > 1.3M_\odot$)
- hydrogen-burning via CNO-cycle
- rapid transition from MS to RGB; not observable (so-called Hertzsprung gap in HRD)
- helium core remains non-degenerate
- non-violent ignition of He at center
- double-shell burning phase with degenerate C/O-core

4.1.1 The post-MS evolution

As for low-mass stars, the exhausted core of stars at the end of the MS-phase consists of helium only and is isothermal, because $\epsilon = 0$. From the virial theorem applied to the core we get

$$E_g = -\int_0^{M_c} \frac{Gm}{r}\mathrm{d}m = [4\pi r^3 P]_0^{M_c} - \int_0^{M_c} 3\frac{P}{\rho}\mathrm{d}m \tag{4.1}$$

with

$$\int_0^{M_c} 3\frac{P}{\rho}\mathrm{d}m = 2E_i \approx 3\frac{\mathcal{R}}{\mu}T_c M_c \tag{4.2}$$

where we have used the ideal gas equation and the fact that $T = T_c$. Thus,

$$3\frac{\mathcal{R}}{\mu}T_c M_c - C_g\frac{GM_c}{R_c} - 4\pi R_c^3 P_c = 0 \tag{4.3}$$

Here we have replaced E_g by an approximation with a "structure" constant C_g. It follows that

$$\Rightarrow P_c = \frac{3\mathcal{R}}{4\pi\mu}\frac{T_c M_c}{R_c^3} - \frac{C_g G}{4\pi}\frac{M_c^2}{R_c^4} = C_1\frac{T_c M_c}{R_c^3} - C_2\frac{M_c^2}{R_c^4}, \qquad C_1, C_2 > 0 \tag{4.4}$$

For fixed M_c, T_c, search the maximum, i.e. $\left(\frac{\partial P_c}{\partial R_c}_{M_c,T_c} = 0\right)$. This yields

$$P_c = \frac{2187\mathcal{R}^4}{1024\pi^2 C_g^3 G^3 \mu^4}\frac{T_c^4}{M_c^2} \propto \frac{T_c^4}{\mu^4 M_c^2} \tag{4.5}$$

The pressure from the weight of the envelope is (homology) $P_e \propto T_c^4/M^2$ (T_c is the temperature of the H-shell as well!) and is independent of R_c. In hydrostatic equilibrium, both pressures should balance. If the maximum of $P_c > P_e$, two solutions are possible: one with a larger R_c (non-degenerate core), and one with a degenerate core. If, however, the maximum of $P_c < P_e$, no solution in equilibrium is possible and the core has to contract (which actually happens on a thermal timescale). The core-mass, for which exactly one solution is possible, and for which the isothermal non-degenerate core can just balance the weight of the overlying envelope, is called the *Schönberg-Chandrasekhar mass* and is in terms of relative core mass $q := M_c/M$:

$$q_{\mathrm{SC}} = 0.37\left(\frac{\mu_e}{\mu_c}\right)^2 \tag{4.6}$$

[1] All mass limits are to be taken as approximate; they vary by $0.1 \cdots 0.3M_\odot$, even if a clear definition is made, due to slightly different numerical results.

and depends on the ratios of the molecular weights of core and envelope. Its numerical value for solar-type stars is 0.08. If this value of the isothermal core is exeeeded, it has either to become degenerate (additional pressure source) or non-isothermal (by contraction energy).
This explains the fact that stars of intermediate mass, when having finished the MS-phase, suddenly start an evolution on a thermal timescale. The core contraction triggers an envelope expansion, with the node in the H-shell. *It is unclear, why this so-called mirror-principle holds.* All "explanations" in the literature about the question, why stars become red giants, are disputed!
After the large expansion of the envelope, it becomes more and more convective until – as for low-mass stars – the ordinary RGB evolution starts. During this ascent or even earlier (for higher mass) core temperatures reach the critical 10^8 K for the ignition of helium burning.

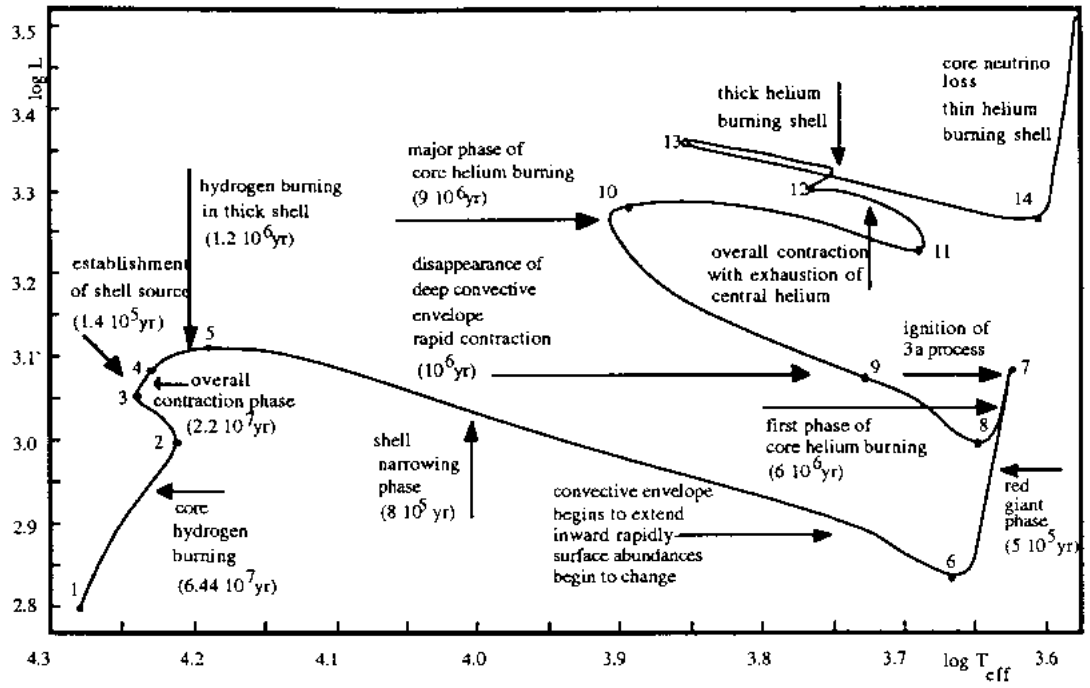

Evolution of a $5M_\odot$ star (from dLD)

Above figure shows the evolutionary track of a $5M_\odot$ star from the main sequence into helium-shell burning and the duration of each phase. This is a typical mass and evolutionary scheme for all stars in this mass range.

4.1.2 The helium-burning phase

Helium ignites in these stars under non-degenerate conditions with ν-losses being unimportant. For smaller masses, the ignition takes place during the RGB ascent. The stars for a short time retraces its own track backwards, spends a rather long time at a miimum luminosity and then begins to evolve back. Higher mass stars ($M > 4M_\odot$) extend this excursion also to much higher $T_{\rm eff}$ - they *loop*. These loops depend on many details of the structure of the stars, and their extend and duration is rather uncertain. In particular, since the helium burning takes place in a core smaller than the previous H-burning regions, the H-profile in the star still remembers the end of the MS-phase. When the H-shell eats through this profile of increasing H-content, the evolution is influenced by it.
After the end of core helium burning, as in the hydrogen phase, a helium-burning shell develops around an exhausted C/O core and a double-shell phase starts. The star will develop again a deep convective

envelope and evolve along the Hayashi line. This second ascent of the giant branch is called the *Asymptotic Giant Branch* (AGB). During the transition from core- to shell-burning, the H-shell might extinguish. After the MS-phase and during the first RGB phase, the stars can experience, as their lower-mass counterparts, the first dredge-up. After the core-helium burning, during the second approach to the RGB, a second dredge-up might occur, when the deep convective zone for a short time penetrates into regions, where the extinguished H-shell had already converted all hydrogen to helium.

4.2 The AGB-phase

The double-shell phase is one of the most interesting and complicated phases of stellar evolution. It is not only reached by intermediate mass stars, but in principle by all stars with $M > 0.8 M_\odot$. However, whether they really develop as far, depends on the mass lost during the RGB phase. (It is unclear, whether the Sun will ever become an AGB star, as well.) In any case, intermediate-mass stars are the prototype stars for the discussion of the AGB phase, which is characterized by *thermal pulses*, nucleosynthesis of rare elements (*s-process*) and strong mass-loss.

4.2.1 Thermal pulses

The thermal pulses are rather regular runaway events in the helium shell, which last for a hundred years and repeat every few thousand years. A pulse is a complicated sequence of changes in both shells, the layer between them, and the envelope above. An example is shown in the figure below, taken from the thesis of J. Wagenhuber (1996, MPA).
A pulse starts with the quiet phase A, in which practically all luminosity is produced in the H-shell. Then the He-shell becomes unstable and produces more and more energy (see panel (c)), although the stellar values remain constant. At the maximum, convection between the two shells sets in, then expansion, during which the H-shell extinguishes. Finally, the He-luminosity drops due to the expansion and the quiet phase resumes. This is a very simplified description of the events shown in the figure. Notice, for example, the extremely thin shells, the reaction of the envelope convection, the interplay between the various luminosities.
Why is the helium shell unstable? A simple sequence of arguments is the following:

1. assume the shell expands a little bit, e.g. due to a small T-fluctuation or an increase in Y;
2. if the shell is very thin, the increase in thickness $\frac{\mathrm{d}D}{D}$ is $\frac{\mathrm{d}\rho}{\rho}$;
3. the change of the mean radius of the shell, $\frac{\mathrm{d}r}{r}$, however is almost 0, because the shell is very thin;
4. the pressure in the shell depends (hydrostatic equilibrium) on the pressure exerted from the envelope;
5. due to $\frac{\mathrm{d}r}{r} \ll 1$ the envelope does not "feel" any change in the gravitational potential, and P_e stays constant;
6. with $\frac{\mathrm{d}\rho}{\rho} < 0$ but $\mathrm{d}(P) = 0$, for an ideal gas it follows that $\frac{\mathrm{d}T}{T} > 0$, that is, the shell gets even hotter;
7. and the runaway has started and continues until the pressure is changing as well, or the excessive energy can be carried away fast enough (e.g. by convection)

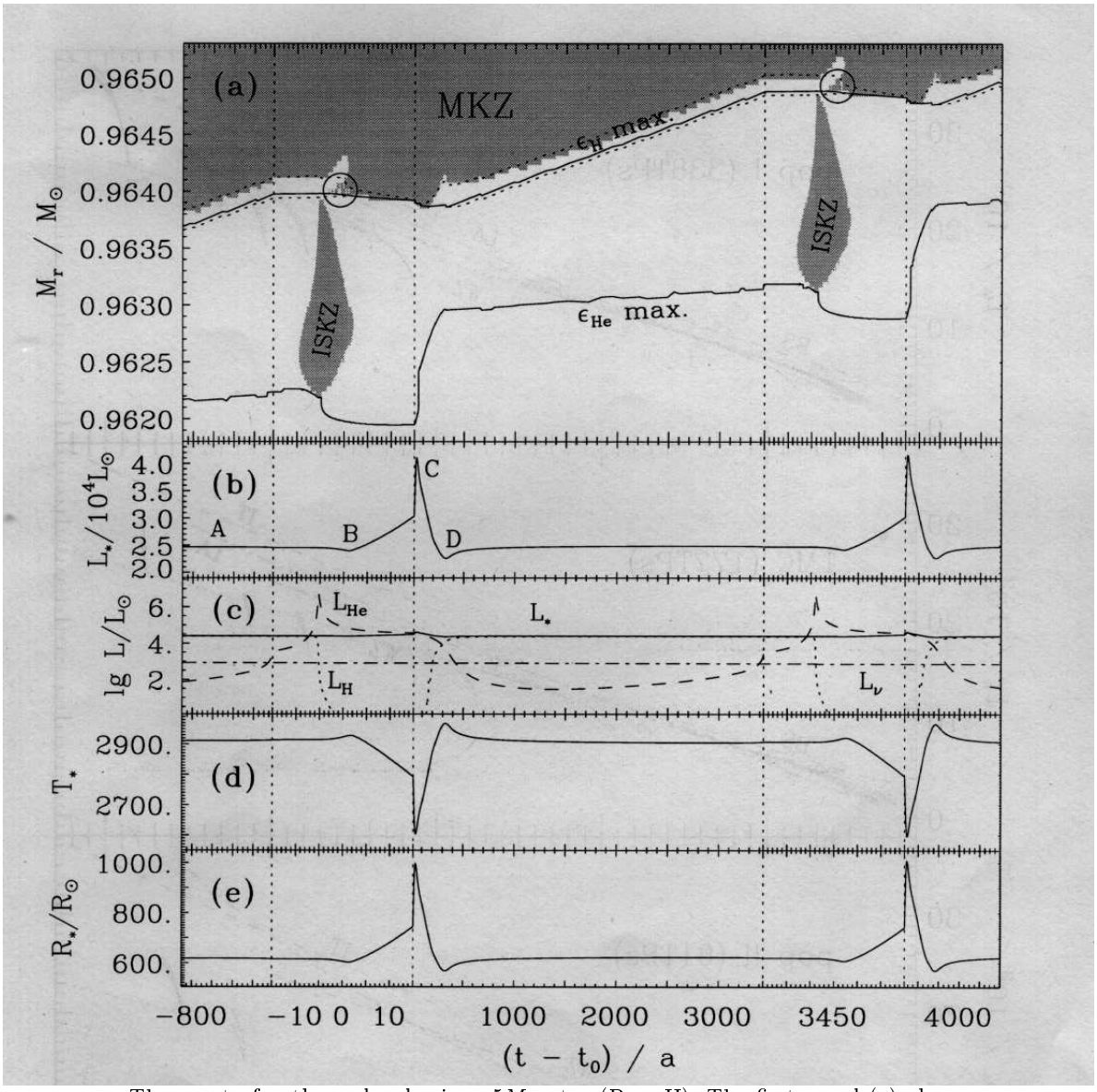

The event of a thermal pulse in a $5M_\odot$ star (Pop. II). The first panel (a) shows the location of the two shells and the convective regions; the second (b) the stellar luminosity, the third (c) the luminosity produced in H- and He-shell, (d) $T_{\rm eff}$ and (e) the stellar radius. The time axis has a varying scale. (from Wagenhuber, thesis 1996)

The thickness of the shell is of the order of 10^{-4} or less in relative radius and 10^{-2} in mass. Since helium-burning has a higher T-dependence ($\nu \approx 40$), it is always thinner than the H-shell and therefore gets unstable earlier.

The timescales, as seen in the figure, become extremely short. In some cases dynamical terms can no longer be neglected. At the same time, the structure gets very complex (large gradients in P and T). Both facts lead a high computational effort. Due to the instability nature, numerical instabilities trigger physical ones and the models tend to refuse to converge. The problem has been solved by Wagenhuber & Weiss (A&A 286,121 (1994)). Now a complete sequence of many pulses (needing 10^5 models with $3 \cdot 10^3$ grid points can be calculated in one computational run (about 1 week on a RISC workstation).

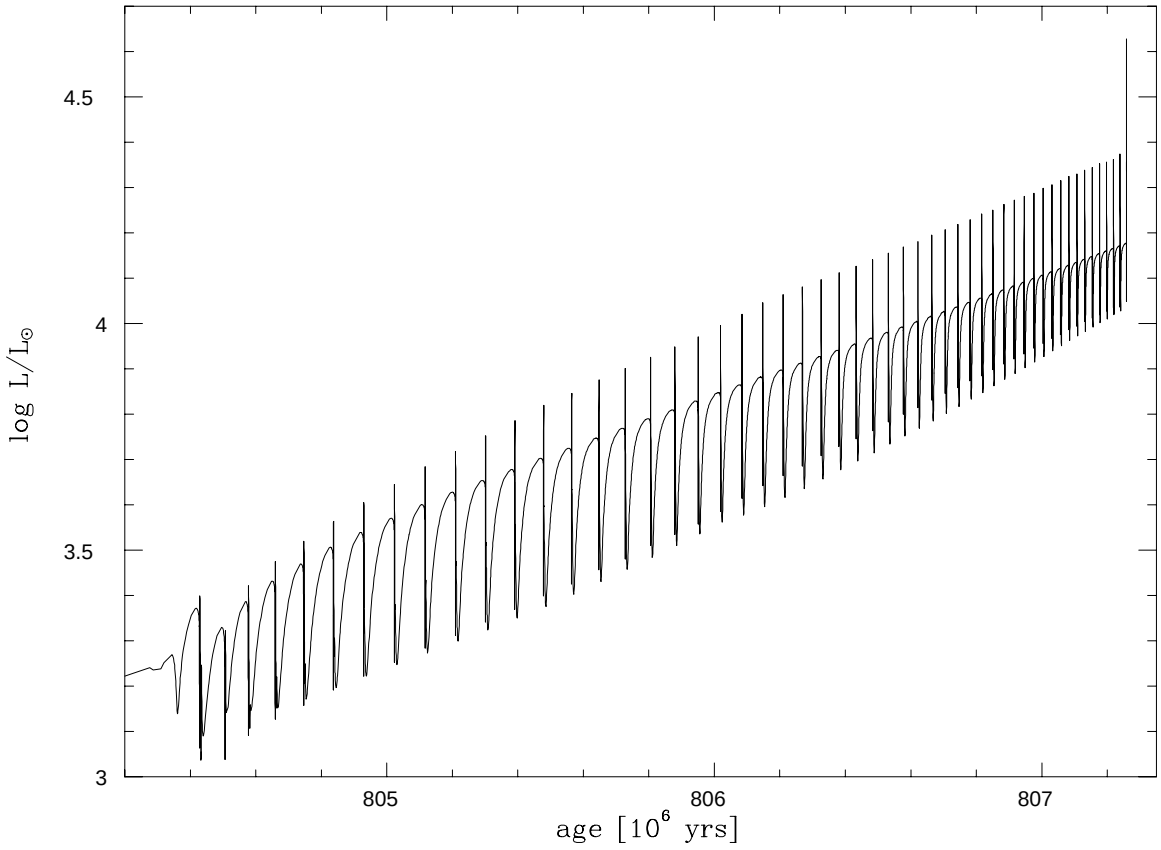

Thermal pulses in a $2.5M_{\odot}$ star over the whole AGB evolution (Wagenhuber & Weiss, 1994)

Since the calculations are so time-consuming and difficult, simple relations for the main quantities of interest are needed. This is possible. The most important example are *core mass - luminosity relations* for L in the quiescent phases. The simplest form is

$$L/L_{\odot} = 5.92 \cdot 10^4 (M_c - 0.495) \tag{4.7}$$

which is asymptotically valid for $0.6 < M_c/M_{\odot} < 0.9$. Asymptotically means that the first few pulses and nuclear energy generation at the hot bottom of convective envelopes in the more massive AGB stars are ignored.

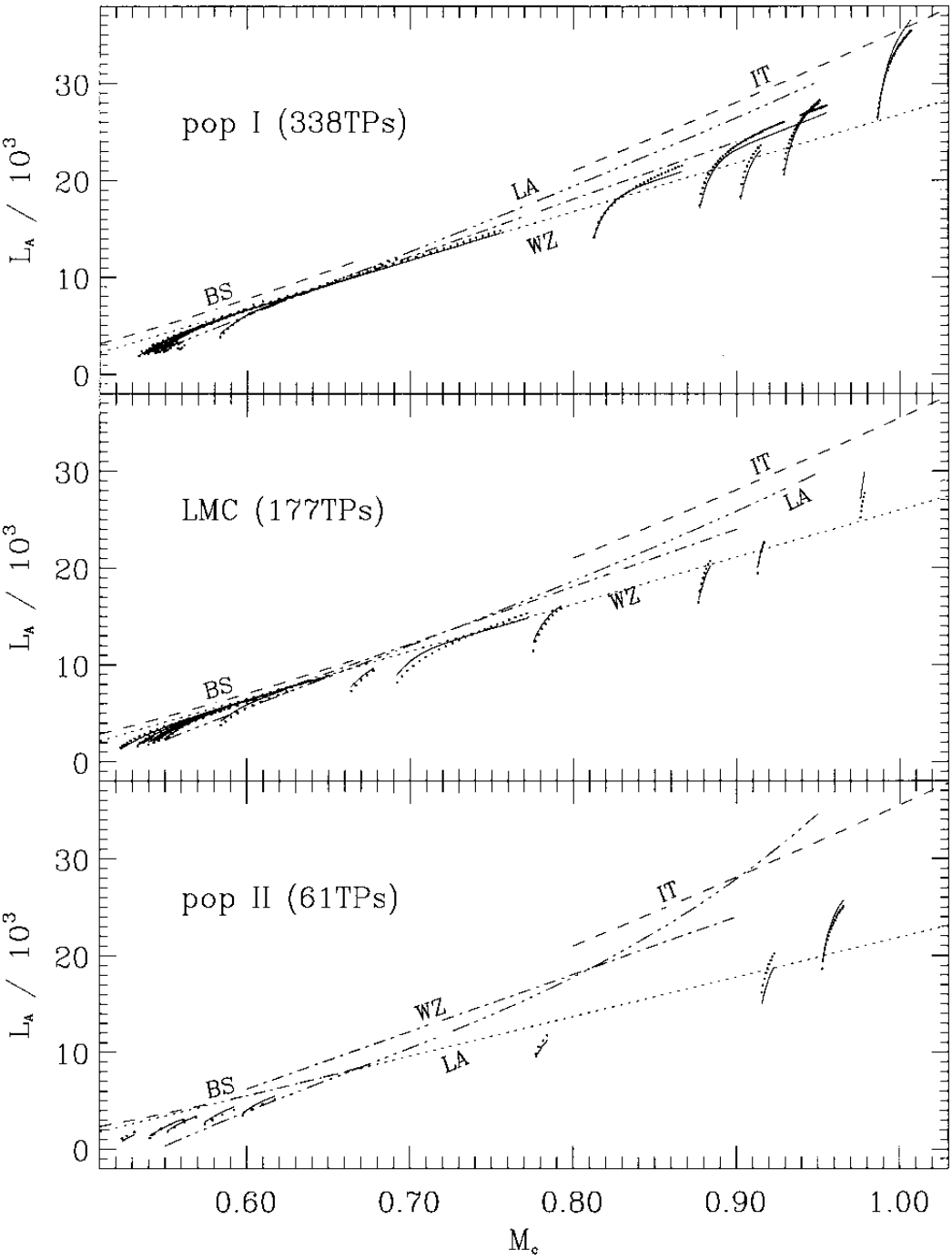

$M_c - L$ relations for three different compositions compared to many calculated thermal pulses (from Wagenhuber 1996)

4.2.2 Mass loss on the AGB

In principle, an AGB-star could evolve until its degenerate core reaches the Chandrasekhar mass of $\approx 1.4 M_\odot$, where not even electron degeneracy can stop further collapse. This would need hundreds of pulses. Observations show that the end-products of intermediate-mass star evolution, the *White Dwarfs*, which have been the cores of AGB-stars, have masses of $\approx 0.6 M_\odot$, depending on total initial mass ($0.8 M_\odot$

as a maximum). This means that AGB stars must lose their envelopes during that phase and only the cores remain. Further evidence comes from the existence of circumstellar shells and *Planetary Nebulae*, which are circumstellar shells illuminated by UB-light from the post-AGB star. The conclusion is that AGB stars lose most of their envelopes by stellar winds, which at the end of the AGB-phase increases dramatically; up to $10^{-4} M_\odot$/yr (*superwind*).
The physical mechanism for the wind is not yet completely clear, but the picture emerges that dust forms in the extended, cool atmospheres, which is then accelerated by radiation pressure and drags along the gas. Empirical and theoretical mass loss formulae, which are included in the stellar models, all have a functional form like

$$\dot{M} = \eta \frac{L^\alpha}{T_{\rm eff}^\beta M^\gamma} \tag{4.8}$$

(α, β, $\gamma > 0$), which says that increasing L and decreasing $T_{\rm eff}$ and mass lead to higher mass loss. Wagenhuber (thesis, 1996) has shown that with theoretical dust-driven winds the termination of the AGB-phase can be achieved in a self-constistent way leading to good agreement with observations. Previous work very often used parametrized mass-loss rates calibrated to observations (Vassiliadis & Wood, for example).

4.3 The post-AGB phase

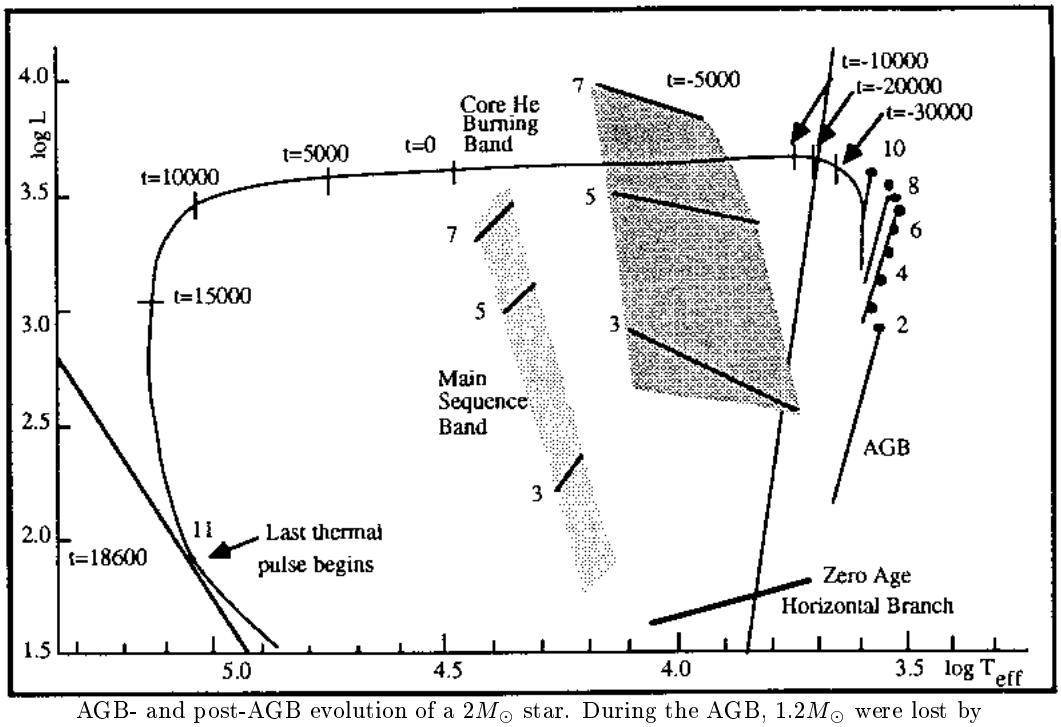

AGB- and post-AGB evolution of a $2M_\odot$ star. During the AGB, $1.2M_\odot$ were lost by an "ordinary" stellar wind; the superwind led to the rapid ejection of $0.2M_\odot$, such that a remnant of $0.6M_\odot$ was left (from Iben & Renzini 1983)

In the above figure an example evolution is shown that resulted from a parametrized calculation. After the envelope is lost almost completely, the shells are no longer able to sustain the remaining envelope, which contracts and heats up. The star begins a horziontal evolution through the HRD with a crossing-time of a few 10^5 yrs (depending on mass). At about 30000 K, the UV-flux is high enough to ionize an existing circumstellar shell, which re-emits in several forbidden lines (e.g. [OIII] λ5007 Å); such an object is called a *Planetary Nebula*.

Later, the shells extinguishes because either the fuel is used up or hot winds have led to the loss of it. The star then begins the cooling-phase of a White Dwarf, which takes its luminosity from thermal energy as did the star when it started its life on the pre-main sequence. Stars that lose their envelopes already on the RGB, evolve into WDs as well. This is the fate of the Sun. Since the cooling-time of WDs gets longer and longer as they get dimmer, the oldest WDs in the Galaxy are still visible. Determining their age gives a limit to the age of the Galaxy. In the solar neighbourhood, the oldest WDs are about 10 Gyr old. The disk of the Galaxy appears to be slightly younger than the globular clusters. In them, only intrisically bright WDs can be found up to now, which are much younger (3-5 Gyr).

4.4 Nucleosynthesis on the AGB

Possibly the most important aspects of the AGB-stars for the universe is that they are believed to be the place where many rare earth elements are processed in the *s-process* nucleosynthesis. The 's' stands for slow, because it operates via neutron captures, which are relatively slow compared to the β-decays occuring in these reaction chains. The advantage is that neutrons do not suffer from the Coloumb-wall. The disadvantage is that one needs a sufficient number of neutrons, which do not occur in the ordinary H- and He-burning chains.
There are two favourite n-sources,

$$^{13}C(\alpha,n)^{16}O \quad \text{and} \quad ^{22}Ne(\alpha,n)^{25}Mg$$

called the ^{13}C and ^{22}Ne source.

During the thermal pulses, the outer convective zone may reach layers usually lying below the H-shell. These layers, He-rich, get mixed with debris from the He-shell, when the intershell convection starts at the top of a pulse. Therfore, He-burning ashes can reach the surface, in particular carbon, which is easy to observe. Indeed, stars with too high C-abundances (*carbon stars*) have been observed all along the AGB, indicating that this so-called *third dredge-up* does indeed happen. In the theoretical models, unfortunately, it occurs rarely, if at all. The second effect of the 3$^{\text{rd}}$ dredge-up is that protons from the H-rich layers will get mixed into the very hot He-shell. They will not be burned to helium, but rather used for p-captures in C and O in the He-shell:

$$^{12}C(p,\gamma)^{13}N(\beta+\nu)^{13}C \quad \rightarrow \quad \begin{matrix}(p,\gamma)^{14}N \\ (\alpha,n)^{16}O\end{matrix} \tag{4.9}$$

$$^{16}O(p,\gamma)^{17}F(\beta+\nu)^{17}O \quad \rightarrow \quad \begin{matrix}(p,\alpha)^{14}N \\ (\alpha,n)^{20}Ne\end{matrix} \tag{4.10}$$

This process would therefore lead to the ^{13}C source.
Alternatively, the following could happen. The H-shell converts C and O mostly into ^{14}N, which gets mixed into the He-shell. Then

$$^{14}N(\alpha,\gamma)^{18}F(\beta^{+}\nu)^{18}O(\alpha,\gamma)^{22}Ne(\alpha,n)^{25}Mg \tag{4.11}$$

The efficiency of all processes and reactions involved depends on pulse-strengths, mixing efficiency and more details. Parametrized nuclear network calculations have shown that for appropriate neutron-exposures the solar system s-process abundances can be obtained.
In general, the calculations of the stellar models are more likely to obtain 3$^{\text{rd}}$ dredge-up, proton injection, and s-process, if

- pulse number is high
- Z is low
- non-standard convection (overshooting, semiconvection) is used

An example for a typical s-process chain is the cadmium, indium, tin chain:

$$^{110}Cd + n \rightarrow ^{111}Cd + n \ldots ^{115}Cd \xrightarrow{e^{-}} ^{115}In + n \rightarrow \ldots$$

Chapter 5

Pecularities: Pulsations, Helium Stars, Abundance Anomalies

The stellar zoo is full of stars not fitting into the general picture developed in the previous sections. Also, stars do not only evolve on very long timescales, but sometimes vary on dynamical timescales (regular pulsations). In the final lecture, a relaxed look at those peculiar features which are the salt in the soup of our daily work in stellar evolution will be taken.

Literature:

- Cox J.P., Theory of Stellar Pulsations, Princeton University Press, 1980; the standard textbook containing the theory of pulsation;
- Jeffery C.S., Heber U. (eds.): Hydrogen-deficient stars, A.S.P. Conference Series, vol. 96, 1996; proceedings of the latest workshop of helium and related stars; contains the up-to-date knowledge about these stars
- Kraft, R.P., Publications of the Astronomical Society of the Pacific, 106, 553 (1994); the standard review article on abundance anomalies found in globular cluster stars;

5.1 Pulsating stars

5.1.1 Observational evidence

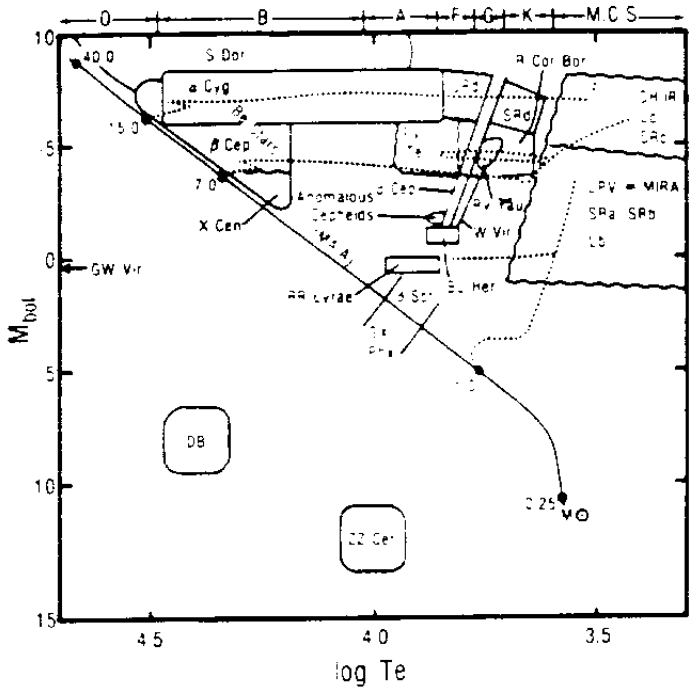

A brief visit to the zoo of pulsating stars (from Becker, 1987)

- periodic brightness variations observed all over the HRD
- pulsations are radial and non-radial (as in the Sun)
- periods from hours to years
- connected – but not completely in phase – with temperature (radius) variations
- existence of an *instability strip* crossing core He-burning loop of intermediate-mass stars, the horizontal branch and the main sequence
- existence of a period-density relation $\Pi\sqrt{\bar{\rho}/\bar{\rho_\odot}} = 0.03 \cdots 0.12$ days

5.1.2 The physical view

The pulsations are dynamical waves of motion through the stellar envelope. Their characteristic time is the free-fall time τ_{ff}.
From the virial theorem and the sound-crossing time estimate the observed period-density relation can be explained; one gets

$$\Pi\sqrt{\bar{\rho}} = \text{const.} = 2\left(\frac{4}{3}\Pi G\bar{\rho_\odot}\right)^{-1/2} \approx 0.04 \text{ days} \tag{5.1}$$

During pulsation, mass elements are compressed and expanded. During compression T rises and the element will lose energy to the surroundings. During expansion, the situations is the other way round. If

more energy is lost during compression than gained during expanion, the element damps the oscillation. It is stable. If this applies for most of the envelope or star, any excited pulsation will die again.[1]
An unstable situation occurs for example, when the element is producing nuclear energy. A rise in T leads to a large intrinsic heat gain. This is unstable and refered to as the ϵ-mechanism. Due to this, the most massive stars become unstable as a whole. However, for most stars, any excitation in the energy producing regions is easily damped by overlying regions.
The situation becomes also unstable, when during compression the element loses less energy than it would under adiabatic conditions. This happens, when the opacity gets much higher for higher T. This is called the κ-mechanism and is the one that drives almost all pulsating stars.
For the classical Kramers opacity, we have $\kappa = C\rho T^{-3.5}$. For a completely ionized gas, $T \propto \rho^{2/3}$ and $\kappa = C\rho^{-4/3}$. This means that during compression, κ gets smaller, and the situation is stable. This led Eddington to the conclusion that pulsations cannot be due to variations in opacity.
He did not have access to opacities that take ionization into account. In the case of partial ionization, compression leads to an increase in ionization, i.e. $\frac{\partial \ln T}{\partial \ln \rho} = \lambda \ll 1$. Thus, in this case, with $T \propto \rho^{\lambda}$ and $\lambda \approx 0$, $\kappa \propto \rho^{1-3.5\lambda}$, which, for $\lambda < 2/7$ will lead to an increase in κ upon compression. Whether the total effect of the κ-variation and that of $\left(\frac{\partial \ln T}{\partial \ln \rho}\right)_{\rm ad}$ lead to an unstable situation, depends on the opacity details.

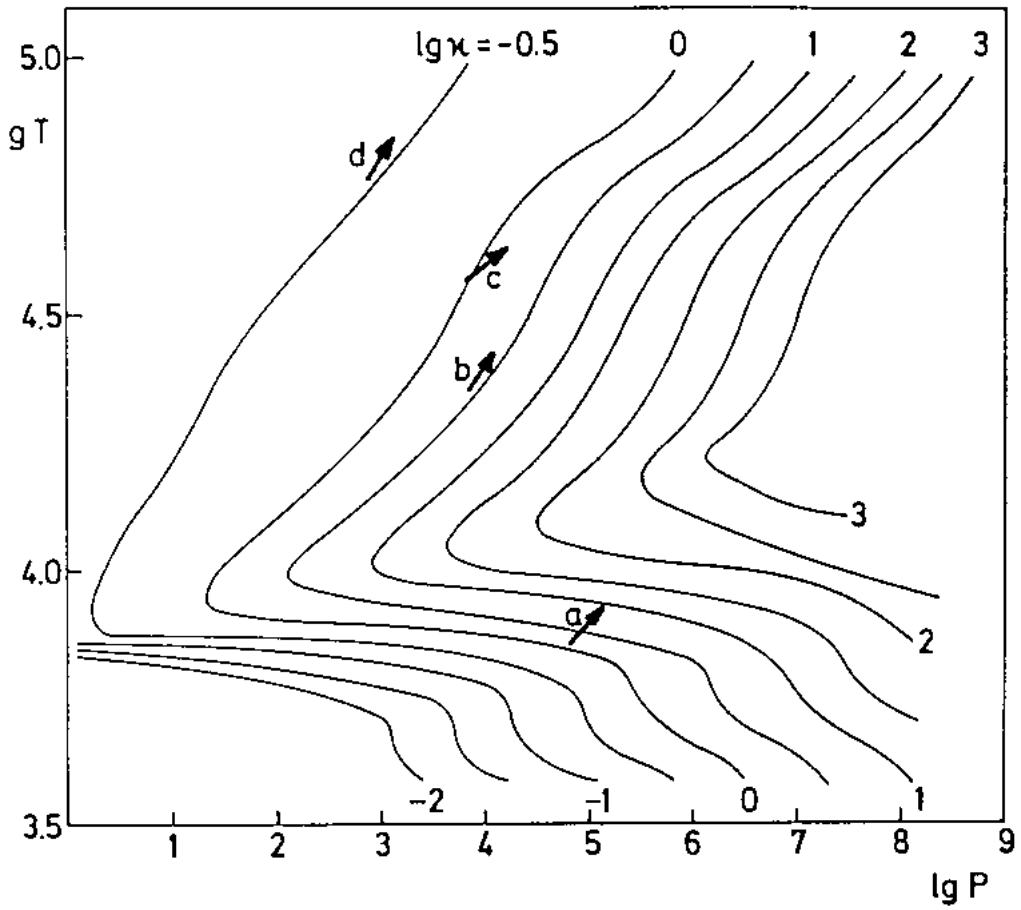

Lines of constant opacity and arrows indicating $\left(\frac{\partial \ln T}{\partial \ln \rho}\right)_{\rm ad}$. (from KW)

In this figure some typical situations are shown: (b) and (d): in both cases, compression leads to a lower

[1] This is actually the case for all solar oscillations; however, they are permanently excited due to the random motion in the convective turbulence.

κ, equivalent to damping. (a) is unstable, because κ rises sharply. However, the star would have only a very small mass in this region, so that the envelope would not really start to pulsate. (c) is the most interesting case, since $\left(\frac{\partial \ln T}{\partial \ln \rho}\right)_{\rm ad}$ is reduced due to the second ionization of helium and κ increases. If the stellar envelope has a large enough mass fraction in the ionization region, it will become unstable.

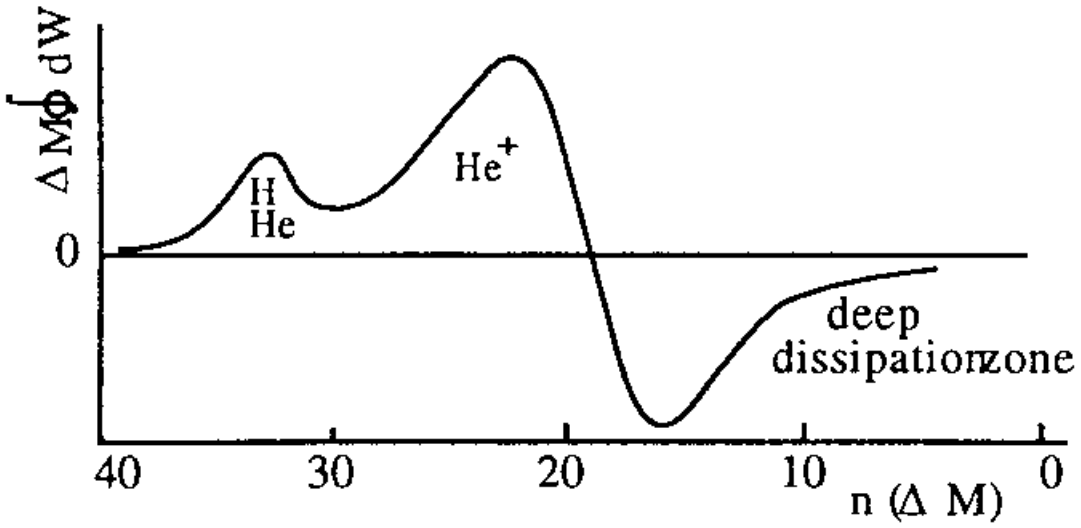

Sketch of exciting and unstable regions within a stellar envelope. The abscissa is the work-integral over mass layers. (from dLD)

Whether a star is stable or not is described by the *work integral*. It arises from the consideration that a mass element, while passing through a compression–expansion–cycle, either gains heat or loses it. The integral over mass describes than whether a whole envelope gains energy. It is then going to pulsate.

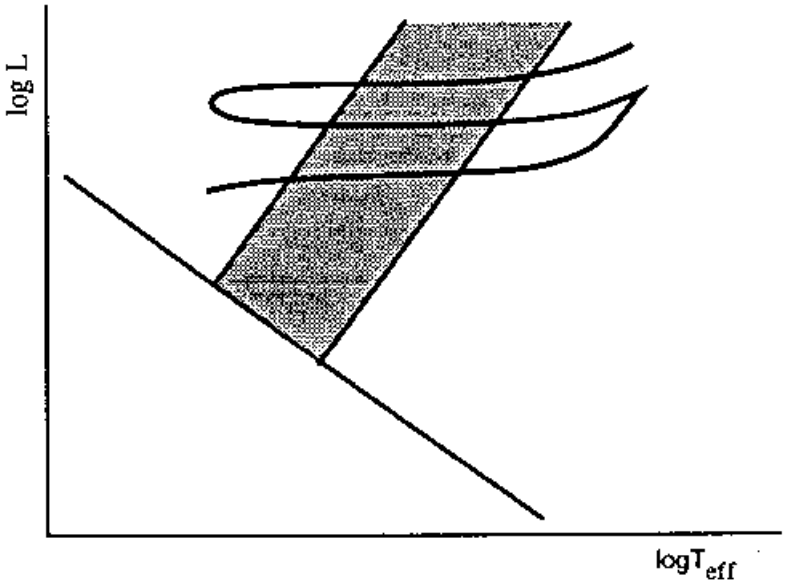

Sketch of the instability strip and an evolutionary path through it. (from dLD)

5.1.3 Numerical calculations

- full non-linear calculations are difficult and time-consuming
- standard approach: linear stability analysis; gives period and growing times
- convection usually "frozen in", i.e. considered not to take part in the pulsation
- results in very good agreement with observed periods and stability strips
- amplitudes theoretically not well understood
- major progress due to new opacities (include Fe-ionization, which is important for hotter stars)

5.1.4 Cepheids and RR Lyr stars

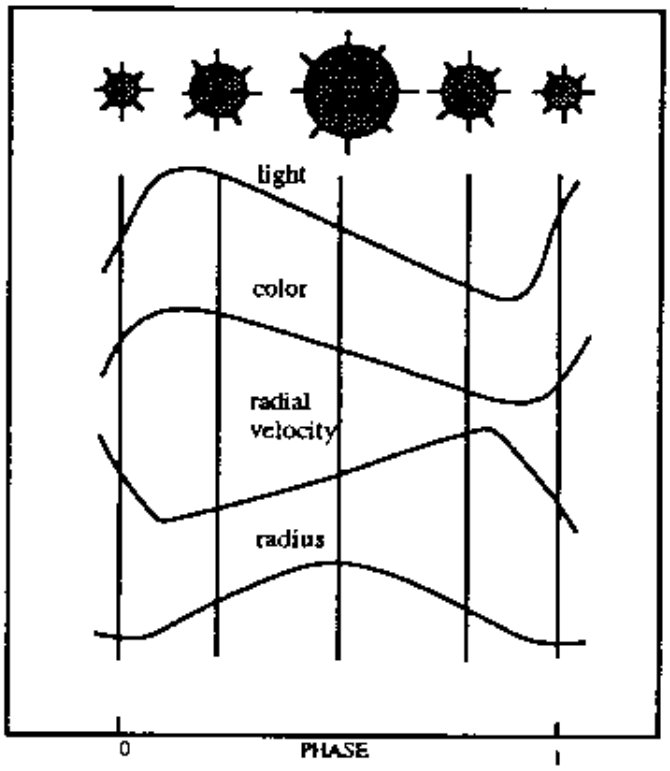

Variations in light, colour, radial velocity and radius for Cepheids (from dLD)

Cepheids (after δ Cephei) are the most important pulsating stars. Their pulsation periods are in the range of 5-10 days and the brightness amplitudes lie between 0.2 and 2 magnitudes. They have been identified to be Pop. I intermediate-mass stars in core-helium burning loops, driven by the κ-mechanism.

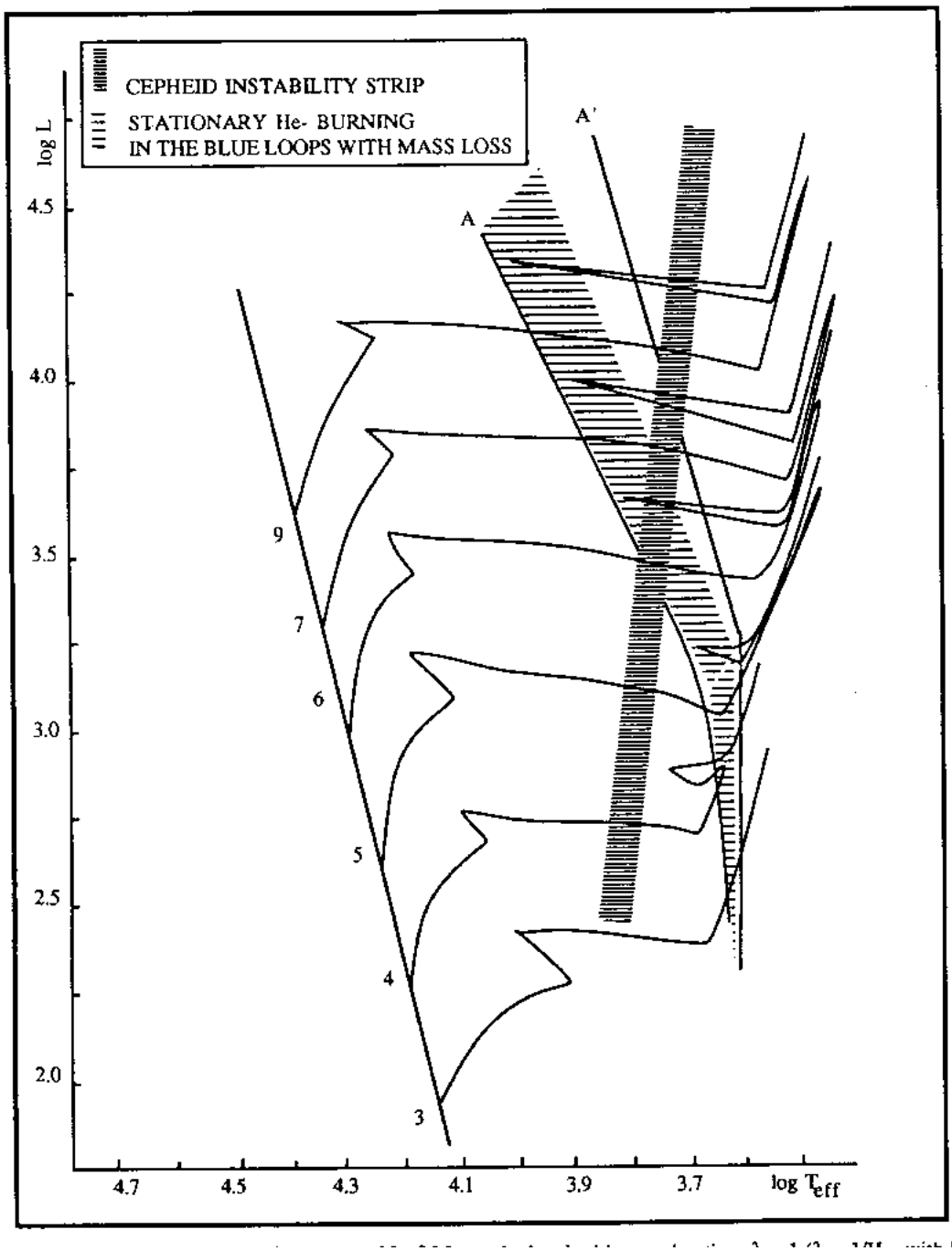

The instability strip crossing evolutionary paths of intermediate stars (from dLD)

For Cepheids, very early a period-luminosity relation has been found by Henrietta S. Leavitt. This implies that if the period is known, which is easy, the absolute brightness can be derived. From the apparent one, the distance can be infered. Presently, one of the *Hubble Space Telescope* Key Projects is looking for Cepheids in clusters of galaxies to determine their distance and finally the Hubble constant H_0. Since Cepheids are intrisically bright, they can be observed at large distances.
However, the use of this relation has a long history of errors due to unrecognized dependencies: there are different types of Cepheids and the metal dependence is not well-known. It is still a focus of active research to keep the errors as small as necessary.

The most recent relation for galactic Cepheids is using HIPPARCOS parallaxes (Feast & Catchpole 1997):

$$\langle M_V \rangle = -2.82 \log \Pi - 1.43 \tag{5.2}$$

(Π in days).

RR Lyr stars are the Pop II equivalent of Cepheids. They are found in globular clusters and serve as distance indicators. Again, the uncertainties in the period-luminosity relations are still too high (in particular, the calibration of the zero-point is uncertain; there are no nearby RR Lyr stars). Periods are between 0.2 and 1 day, and amplitudes of order 0.2 mag. Sources for errors are the existence of fundamental and first overtone pulsators, and the fact that the stars are in different evolutionary phases, crossing the instability strip from either side on their looping paths. In practice a relation between mean brightness and metallicity is used. The one we prefer is that of Walker:

$$M_V(RR) = 0.15[Fe/H] + 0.73, \tag{5.3}$$

which translates into a relation for RR Lyr stars on the zero-age HB (where core helium burning just has started)

$$M_V(RR) = 0.20[Fe/H] + 0.93, \tag{5.4}$$

From our theoretical model, we derive, for comparison

$$M_V(RR) = 0.21[Fe/H] + 0.91, \tag{5.5}$$

5.2 Helium stars

Stars with an extremly low hydrogen abundance in the photosphere $X < 10^{-4} X_\odot$ are called *helium stars* (except for those, of course, which also lack He).
They appear as

- Wolf-Rayet stars: massive stars near the MS
- extreme He-stars (EHe): hot stars on post-AGB tracks; low mass
- R CrB stars: presumably the predecessors of the EHe stars; $T_{\rm eff} \approx 5000 \cdots 12000$ K; $M \approx 0.8 M_\odot$ carbon rich; deep brightness declines
- Hydrogen-deficient carbon stars (HdC): even cooler than the R CrBs, but no declines
- He-rich central stars of planetary nebulae: post-AGB stars
- He-rich White Dwarfs (DB)
- subdwarf-O stars (sdO): located on the extreme blue HB; low mass ($\approx 0.4 M_\odot$)
- type I supernovae

Only for the WR-stars it is rather clear that heavy mass loss has stripped off the H-envelope and let us see into the former core. For all other stars, the origin of the H-deficiency is unclear. Speculations are

- core He-flash explosions, which lead to a loss of the envelope
- strong winds on the AGB
- special superwind at the end of the AGB
- final thermal pulse during post-AGB evolution using up the thin H-envelope
- binary mergers: in binary systems, mass transfer is easy; it is therefore easy to strip a star off his H-envelope; later the two stars have to merge, however

5.3 Abundance anomalies

5.3.1 Short overview

The relative abundances of the metals as known from the Sun is a reference for all stars. Every deviation from it is considered as an anomaly. There are a few exceptions: the total metal abundance and the abundances of the so-called α-elements (which are those of the α-capture chain starting with oxygen: O, Ne, Mg, Si, Ca, ...). These are overabundant relative to the solar metal distribution, whenever the material a star has been made of, experienced pollution by supernovae of type II, but not type I (example: the globular cluster stars). It appears now that there are two generic metal mixtures: the solar one (SN II+I signature) and the α-enhanced one).
In a strict sense, helium stars are anomalous as well, because their paucity in hydrogen is no normal consequence of stellar evolution. On a less drastic scale we also find stars with helium over- and hydrogen-underabundance of factors of 2.
An incomplete list of anomalies:

- helium abundance $Y \approx .40$ in OB-stars
- nitrogen overabundance in OBN-stars
- carbon underabundance in Red Giants
- O-under- and Na & Al-overabundances in Red Giants

- Ap stars: He, Mn, Hg, and other elements anomal (MS stars of spectral types B–F ($20000 \cdots 8000$ K)
- Ba-stars: G-type stars with Ba and other s-process elements enhanced

... and one of explanations:

- ordinary 1st dredge-up: explains C-underabundances and reduced $^{12}C/^{13}C$ isotope ratios (CNO-cylce signature)
- diffusion in stellar winds and magnetic fields (Ap stars)
- pollution by AGB-companions (Ba stars)
- rapid rotation causing partial or almost complete mixing of the whole star (OB helium rich stars; N-overabundance in massive stars)
- over- and undershooting from convective layers (CN-anomalies)
- turbulent diffusion induced by differential rotation (Red Giant anomlies)

In the following I will concentrate on the last point as an example.

5.3.2 Abundance anomalies in globular cluster Red Giants

In many GCs, bright Red Giants have been investigated for their metal contents. Although the stars of one cluster overall have a very narrow range of total metallicity, star-to-star variations have been found. They are:

1. C is underabundant (up to factor 1/30)
2. $^{12}C/^{13}C$ is underabundant (up to factor 1/10)
3. Na is anti-correlated with O, which can be over- and underabundant (up to factors 3)
4. Mg is underabundant and Al anti-correlates with it
5. and more ...

It has been shown that *all* these anomalies arise from H-burning in the CNO- and equivalent cycles operating at higher (sometimes much higher) T such as the NeNa- and MgAl-cycles. There are two competing scenarios to explain them: the *primordial* one claiming that the initial molecular cloud already had the observed anomalies, and the *deep-mixing* scenario claiming that the star produced them itself in the H-shell and that turbulent diffusion, caused by internal differential rotation, mixed them to the convective envelope where they are immediately transported to the surface.
Both scenarios have arguments in favor: for the deep-mixing scenario the main argument is that C gets the more underabundant the brighter the star is. The anomaly is therefore coupled to evolution. Standard stellar evolution in fact predicts this (due to the 1st dredge-up), but to a lesser extend and at higher luminosities than observed. The primordial scenario is favored by the fact that some anomalies appear to start already at the turn-off, where no deep convection has set in and diffusive mixing is difficult to obtain. Second, at least MgAl-cycle anomalies require shell temperatures never reached in RGB-stars. They could be reached in AGB-stars.

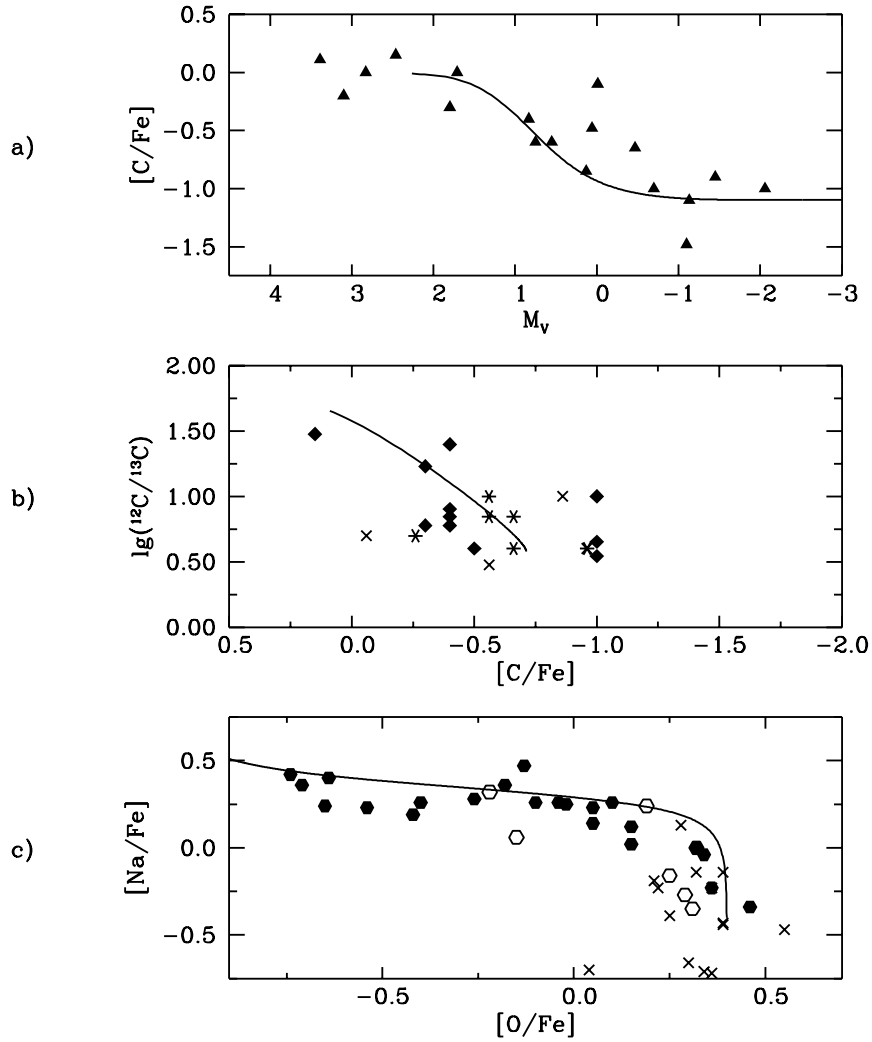

Abundance anomalies in GC RGB stars: (a) C-anomaly in M92; (b) C-isotope anomaly in M4, M22 and halo stars; (c) Na-O anti-correlaton in M3, M13 and field stars. The lines are theoretical solutions of the deep-mixing scenario (from Denissenkov & Weiss, A&A 308, 773 (1996))

This figure shows some success of the deep-mixing scenario. However, the deficits are that for different anomalies, different parameters (penetration depth and diffusive speed) for the turbulent diffusion are needed and that the MgAl-anomaly can not be explained. Presently, we are working on a combined scenario, where some anomalies are created in AGB-stars (by the same effect) and others in the RGB-stars originating from material polluted by these AGB-winds.
But maybe the situation is even more complicated ...

5.3.3 Concluding thought

Stellar evolution theory has had great success in the past. In principle, we know exactly, how stars live and operate, even in the interiors, where we cannot observe them directly. The fast-growing field of spectroscopy will confront us with more and more detailed data that challange our understanding, as the known anomalies already do. The inclusion of more physical effects – such as diffusion and rotation – will be necessary, not only for accurate solar models but for all kinds of stars.
One should always remember that almost all fields in astrophysics rely on the results of stellar evolution. One should not think that we understand stars enough to forget this!

Chapter 6

Appendix: Thermodynamical Relations

The first law of thermodynamics is

$$\mathrm{d}q = \mathrm{d}u + P\mathrm{d}(1/\rho).$$

Assume an *equation of state* (EOS) of the form $\rho = \rho(P,T)$ and $u = u(\rho,T)$ i.e. ignore the dependence on composition.
Definitions:

$$v := 1/\rho \tag{6.1}$$

$$\alpha := \left(\frac{\partial \ln \rho}{\partial \ln P}\right)_T, \qquad \delta := \left(\frac{\partial \ln \rho}{\partial \ln T}\right)_P \tag{6.2}$$

$$\rightarrow \frac{\mathrm{d}\rho}{\rho} = \alpha\frac{\mathrm{d}P}{P} - \delta\frac{\mathrm{d}T}{T} \tag{6.3}$$

$$c_P := \left(\frac{\mathrm{d}q}{\mathrm{d}T}\right)_P = \left(\frac{\mathrm{d}u}{\mathrm{d}T}\right)_P + P\left(\frac{\mathrm{d}v}{\mathrm{d}T}\right)_P \tag{6.4}$$

$$c_v := \left(\frac{\mathrm{d}q}{\mathrm{d}T}\right)_v = \left(\frac{\mathrm{d}u}{\mathrm{d}T}\right)_v \tag{6.5}$$

$$\mathrm{d}u = \left(\frac{\mathrm{d}u}{\mathrm{d}v}\right)_T \mathrm{d}v + \left(\frac{\mathrm{d}u}{\mathrm{d}T}\right)_v \mathrm{d}T \tag{6.6}$$

$$\rightarrow \mathrm{d}s = \frac{\mathrm{d}q}{T} = \frac{1}{T}\left[\left(\frac{\partial u}{\partial v}\right)_T + P\right]\mathrm{d}v + \frac{1}{T}\left(\frac{\partial u}{\partial T}\right)_v \mathrm{d}T \tag{6.7}$$

$$\left(\frac{\partial u}{\partial v}\right)_T = T\left(\frac{\partial P}{\partial T}\right)_v - P \tag{6.8}$$

The last equatin is obtained, when differentiating (7) twice, first w.r.t. ∂T and ∂v and then in reversed order and using the fact that s is a complete form.
From (6) we get (with $u = u(P,T)$)

$$\frac{\mathrm{d}u}{\mathrm{d}T} = \left(\frac{\partial u}{\partial T}\right)_v + \left(\frac{\partial u}{\partial v}\right)_T \frac{\mathrm{d}v}{\mathrm{d}T} \tag{6.9}$$

$$\rightarrow \left(\frac{\partial u}{\partial T}\right)_P = \left(\frac{\partial u}{\partial T}\right)_v + \left(\frac{\partial u}{\partial v}\right)_T \left(\frac{\partial v}{\partial T}\right)_P \tag{6.10}$$

$$= \left(\frac{\partial u}{\partial T}\right)_v + \left(\frac{\partial v}{\partial T}\right)_P \left[T\left(\frac{\partial P}{\partial T}\right)_v - P\right] \tag{6.11}$$

where (8) was used. From (4), (5) and (11) we get

$$c_P - c_v = \left(\frac{\partial v}{\partial T}\right)_P \left(\frac{\partial P}{\partial T}\right)_v T$$

but

$$\left(\frac{\partial P}{\partial T}\right)_v = \frac{P\delta}{T\alpha}$$

and thus

$$c_P - v_v = \frac{P\delta^2}{\rho T\alpha} \tag{6.12}$$

which for an ideal gas reduces to

$$c_P - c_v = \mathcal{R}/\mu$$

Write

$$\begin{aligned}
\mathrm{d}q &= \mathrm{d}u + P\mathrm{d}v = \left(\frac{\partial u}{\partial T}\right)_v \mathrm{d}T + \left[\left(\frac{\partial u}{\partial v}\right)_T + P\right]\mathrm{d}v && (6.13)\\
&= \left(\frac{\partial u}{\partial T}\right)_v \mathrm{d}T + T\left(\frac{\partial P}{\partial T}\right)_v \mathrm{d}v && (6.14)\\
&= c_v\mathrm{d}T - \frac{T}{\rho}\left(\frac{\partial P}{\partial T}\right)_v \frac{\mathrm{d}rho}{}\rho && (6.15)\\
&= c_v\mathrm{d}T - \frac{P\delta}{\rho\alpha}\frac{\mathrm{d}rho}{\rho} && (6.16)\\
&= c_v\mathrm{d}T - \frac{P\delta}{\rho\alpha}\left(\alpha\frac{\mathrm{d}P}{P} - \delta\frac{\mathrm{d}T}{T}\right) = \left(c_v + \frac{P\delta^2}{\rho\alpha T}\right)\mathrm{d}T - \frac{\delta}{\rho}\mathrm{d}P && (6.17)\\
&= c_P\mathrm{d}T - \frac{\delta}{\rho}\mathrm{d}P && (6.18)
\end{aligned}$$

where (5), (9) and (12) were used. The final expression will be used in the structure equation for energy generation.
Define the *adiabatic temperature gradient*

$$\begin{aligned}
\nabla_{\mathrm{ad}} &:= \left(\frac{\partial \ln T}{\partial \ln P}\right)_s && (6.19)\\
&= \frac{P\delta}{\rho c_P T} && (6.20)
\end{aligned}$$

which results from $0 = \mathrm{d}q$ for adiabatic changes.